12-2000

The Viscoelastic Behavior of Pigmented Latex Coating Films

Katharina Prall

THE VISCOELASTIC BEHAVIOR OF PIGMENTED LATEX COATING FILMS

BY

Katharina Maria Prall

Dipl.-Ing.

Technische Universitat Graz

Austria, 1996

A THESIS

Submitted in Partial Fulfillment of the
Requirements for the Degree of
Doctor of Philosophy
(in Chemical Engineering)

The Graduate School

University of Maine

December, 2000

Advisory Committee:

Pierre F. LePoutre, Ph.D.	Professor of Chemical Engineering, Advisor
Stephen M. Shaler, Ph.D.	Professor of Wood Science & Forest Engineering, Cooperating Professor of Chemical Engineering, Advisor
Douglas W. Bousfield, Ph.D.	Professor of Chemical Engineering
John C. Hassler, Ph.D.	Professor of Chemical Engineering
Peter C. Hayes, Ph.D.	Research Scientist, BASF, Charlotte, North Carolina

THE VISCOELASTIC BEHAVIOR OF PIGMENTED LATEX COATING FILMS

By Katharina Maria Prall

Thesis Advisors:
Dr. Stephen Shaler
Dr. Pierre Lepoutre

An Abstract of the Thesis Presented
in Partial Fulfillment of the Requirements for the
Degree of Doctor of Philosophy
(in Chemical Engineering)
December, 2000

The mechanical properties of paper coatings are essential for use performance of coated paper (e.g. calendering, printing degradation during printing operations, pick). This study investigates the microscopic and macroscopic mechanisms that determine the viscoelastic behavior of pigmented latex coating films.

Pigmented coating layers were prepared with different microstructures. This was achieved by using different pigment types and shapes (polystyrene plastic pigment – spheres, precipitated calcium carbonate – rhombs, clay – plates), and changing pigment volume concentration (PVC). Two styrene-butadiene latices with different degree of carboxylation (acidic level 0.3% and 4.5%) were evaluated to determine effect of adhesion. The viscoelastic material response of the coating films (film thickness between 25μm to 35μm) was determined by dynamic mechanical thermal analysis in tensile mode.

Changes in viscoelastic response over entire pigment volume concentration range was found to be distinct for the three different pigment systems. Storage and loss modulus were strongly related to the thermal softening of the coating latex. Reinforcement through pigment was found to

be depending on pigment volume concentration, pigment type as well as temperature/frequency range. Above latex glass transition region the coatings showed for all pigments with increasing pigmentation an increase in storage modulus depending on the storage modulus of the pure pigment ($E_{clay}>E_{CaCO3}>E_{plastic\ pigment}$). Below glass transition region calcium carbonate pigment showed an increase in storage modulus, leveling off at 70%PVC. Clay pigment coatings performed a maximum in storage modulus at 50%PVC. For polystyrene plastic pigment coatings the storage modulus decreased with increasing pigment volume concentration. For clay a depression behavior was observed coinciding with the latex glass transition region. For 90%PVC the depression behavior was reversible, whereas for lower pigment volume concentrations the behavior was irreversible resulting in a common transition for repeated scans. The maximum in tan Delta (damping factor) decreased for all pigments with increasing pigmentation. Glass transition temperatures determined by dynamic mechanical thermal analysis were consistently higher than measured by differential scanning calorimetry. Master curves were calculated with time-temperature-superposition and William-Landel-Ferry-theory. Tensile tests were performed in an Environmental Scanning Electron Microscope. A LWC-base-paper was coated and then analyzed to observe the influence of the coating layer.

ACKNOWLEDGEMENTS

The author expresses her deepest gratitude to her advisors Prof. LePoutre and Prof. Shaler for their excellent guidance, patience and endless enthusiasm throughout her studies. Special thanks to the committee members Prof. Bousfield, Prof. Hassler and Dr. Hayes for their help and valuable discussions.

This research was funded by the industrial sponsors of the Paper Surface Science Program at the University of Maine.

A final word of appreciation goes to the authors family for their love and support

TABLE OF CONTENTS

LIST OF TABLES

LIST OF FIGURES

1 Introduction

Industrial coatings are applied onto substrates to improve optical, physical and mechanical properties. In the paint industry, surface protection, optics, appearance and aesthetics are typically the most important parameters. Paper is coated in order to improve printability and optical characteristics. Paper coatings have to undergo further processing steps after application (e.g. calendering, printing, converting), and adequate mechanical properties of paper coatings are essential for good end-use performances.

The objective of this study was to investigate microscopic and macroscopic factors/mechanisms that determine the mechanical properties of pigmented latex coating films. Mechanical properties of porous pigmented coatings in particular offer a number of challenges. The properties of filled polymer systems have been investigated to a large extent, but the mechanical properties for porous coatings are less understood.

A typical pigmented coating consists of [Braun 1993]:

1) a polymeric film forming binder,
2) a pigment providing the character of coating, and
3) a solvent, often water.

Coatings are composite materials with mechanical properties that depend, in a complex manner, on the mechanical properties of the polymeric binder, the pigment type, shape and size distribution and on interphase phenomena governing the transfer of stresses.

Paint coatings are usually formulated at low pigment volume concentrations for durability. At such PVC levels the coating can be considered as a two-phase system. Paper coatings contain only a low level of binder, they are formulated well above the critical pigment volume concentration,

where air voids are introduces into the system. Paper coatings are therefore a three-phase and properties are also determined by the porous structure of the coating. The structure of such coatings depends not only on coating components, but also on processing parameters during coating process: Method of application (rod, blade), drying conditions (air, IR, contact) and converting process (calendering). Furthermore the properties of the base sheet are influencing, too. Binder migration, building an interphase region of coating and basesheet are important. Additional coatings as well as paper do show inhomogeneities due to morphological variations. Consequently, the coated paper product can be considered as a laminate of layers of different moduli and extensibility, including layers that are complex interphases, and all layers show viscoelastic behavior due to the presence of polymeric materials (cellulose, binders).

Knowledge of the structure of a paper coating, i.e. the spatial arrangement of pigment particles and binder, the interactions between pigment and binder and its relationship to mechanical performance are essential factors for the control of product quality and are a necessity in developing and designing an optimal product.

2 Definitions and Literature Review

2.1 Mechanics of Material

2.1 .1 Stress

Stress describes the intensity forces acting inside a body, and is defined as force F per unit area A. The external surface forces are in equilibrium with the internal body forces [Timoshenko and Goodier 1970].

$$\sigma = \lim_{\Delta A \to 0} \frac{\Delta F}{\Delta A} = \frac{dF}{dA} \qquad \textit{Equation 1}$$

2.1.2 Deformation and Strain

The shape of a solid is deformed when it is subjected to loads. Strain describes the local deformation of line elements (normal strain) or angles between line elements (shear strain). Displacement describes the movement of a point or line element during the deformation process with reference to a fixed coordinate system.

Consider a small element of an elastic body undergoing a deformation, where u, v, w are the components of displacement of point 0, parallel to coordinate axes x, y, z, respectively.

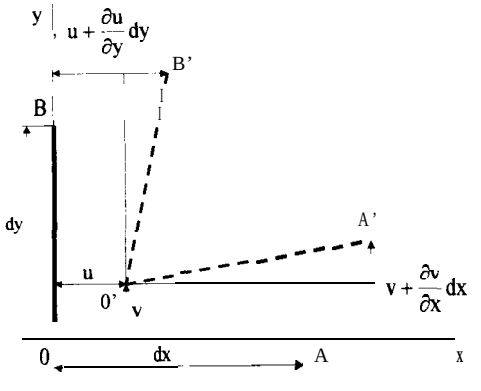

Figure I Deformation of an elastic body, Timoshenko and Goodier (1970).

Small displacement strains can then be defined as

Normal strains:

$$\varepsilon_x = \frac{\partial u}{\partial x} \quad , \qquad \varepsilon_y = \frac{\partial v}{\partial y} \quad , \qquad \varepsilon_z = \frac{\partial w}{\partial z} \qquad \textit{Equation 2}$$

Shearing strains:

$$\gamma_{xy} = \frac{\partial u}{\partial y} + \frac{\partial v}{\partial x} \quad , \qquad \gamma_{xz} = \frac{\partial u}{\partial z} + \frac{\partial w}{\partial x} \quad , \qquad \gamma_{yz} = \frac{\partial v}{\partial z} + \frac{\partial w}{\partial y} \qquad \textit{Equation 3}$$

With these six quantities, elongation and distortion angle in any direction can be calculated.

2.1.3 Elasticity, Hooke's Law

The simplest model of a deformable solid body is the idealized elastic theory. Several further assumptions are often made:

- Homogeneous material (properties are the same at each point),
- Isotropic material (properties are the same in each direction), and
- Deformations are infinitesimal and elastic.

In *Hooke's* Law the stress σ is proportional to strain ε by Young's modulus E. For the uniaxial case this is represented as:

$$\sigma = E\varepsilon \qquad \textit{Equation 4}$$

A mechanical model describing elastic deformation would be an ideal spring.

2.1.4 Viscosity, Newtonian Fluid

For a Newtonian Fluid, stress σ is proportional to the strain rate $\frac{d\varepsilon}{dt}$ multiplied by the material's viscosity η.

$$\sigma = \eta \frac{d\varepsilon}{dt} \qquad \textit{Equation 5}$$

A mechanical model describing viscous deformation would be a **dashpot**.

2.2 Viscoelasticity

Viscoelastic materials in general show a behavior intermediate between a perfect elastic solid and a viscous liquid **[Flügge** 1967, Ferry 1980, Findley, Lai and Onaran **1989]**. The response to application of force depends on the time scale of deformation (stress or strain rate) as well as temperature.

$$\sigma = \sigma(\varepsilon, t) \qquad \textit{Equation 6}$$

The viscoelastic constitutive relations can be determined through dynamic measurements. Consider a material subjected to an oscillating load of small amplitude. A sinusoidal stress σ will produce a sinusoidal strain ε, and vice versa. However, because of the viscous component of the deformation, a phase shift will be observed between stress and strain (Figure 2).

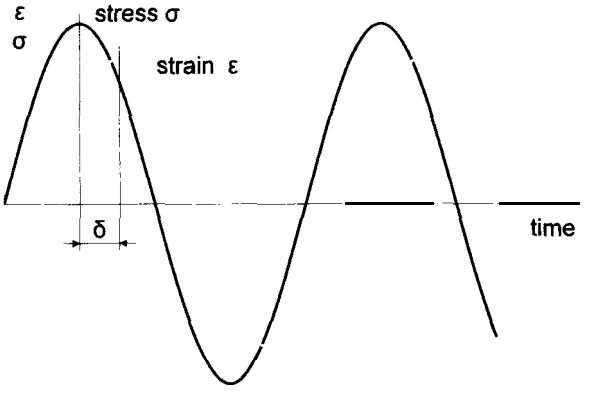

Oscillating stress σ and strain ε and phase lag δ.

The storage modulus is the modulus in-phase with stress and strain, representing the elastically stored energy, which is fully recoverable in the system. The loss modulus is out of phase, and is associated with the dissipation of energy as heat during the cycles of deformation.

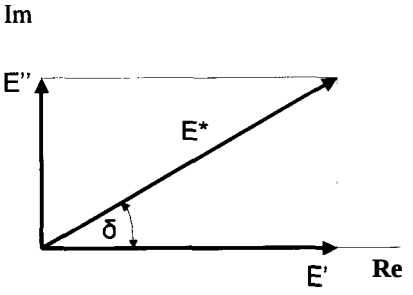

Storage, loss modulus and complex modulus shown as vectors.

The loss factor or damping factor tan 6 is a measure of the lag between applied stress and the strain response (Figure 2) and can be defined as the ratio of loss modulus to storage modulus (Equation 7).

$$\tan\delta = \frac{E''}{E'} = \frac{Loss\ \ Modulus}{Storage\ \ Modulus} \qquad \text{Equation 7}$$

Viscoelastic responses can also be divided into a linear response regime, where the Boltzmann superposition principle may be applied, and a nonlinear regime. The Boltzmann superposition principle predicts that two applied stresses act independently and the resulted strains add linearly [Aklonis and MacKnight 1983]. Most analyses are based on linear viscoelastic material behavior.

2.2.1 Dynamic Mechanical Thermal Analysis

A dynamic mechanical thermal analysis consists in measuring the strain of a material subjected to a dynamic changing force, usually sinusoidal, and as a function of temperature. It gives information about bulk properties directly affecting the material performance. Furthermore, it supplies information about major transitions as well as secondary and tertiary transitions of the

material. In the transition zones, the loss factor tan Delta goes through a pronounced maximum as a function of frequency or temperature.

The viscoelastic response of latex based pigmented coatings is important for the performance of coated paper. The viscoelastic material function of coating films is preferably determined on free coating films detached from their substrate – as in that case the defined material properties are determined – although thin, brittle specimens might be difficult to handle. Most viscoelastic measurements of paper coatings reported in the literature were therefore performed on coating composites, using polyimide [Parpaillon et a/. 1985, Kan et a/. 1996, Rigdahl et al. 1997], or paper [Joyce, Hagen, and de Ruvo 1997 , Engstrom and Lind 1995] as a substrate.

2.2.2 Mechanical Models of Viscoelastic Behavior

Models of linear viscoelastic behavior are comprised of combinations of linear springs and linear viscous dashpots. Inertia effects are neglected in such models. The two basic models are Maxwell and Voigt element.

- The *Maxwell* element is a series combination of elastic and viscous element.

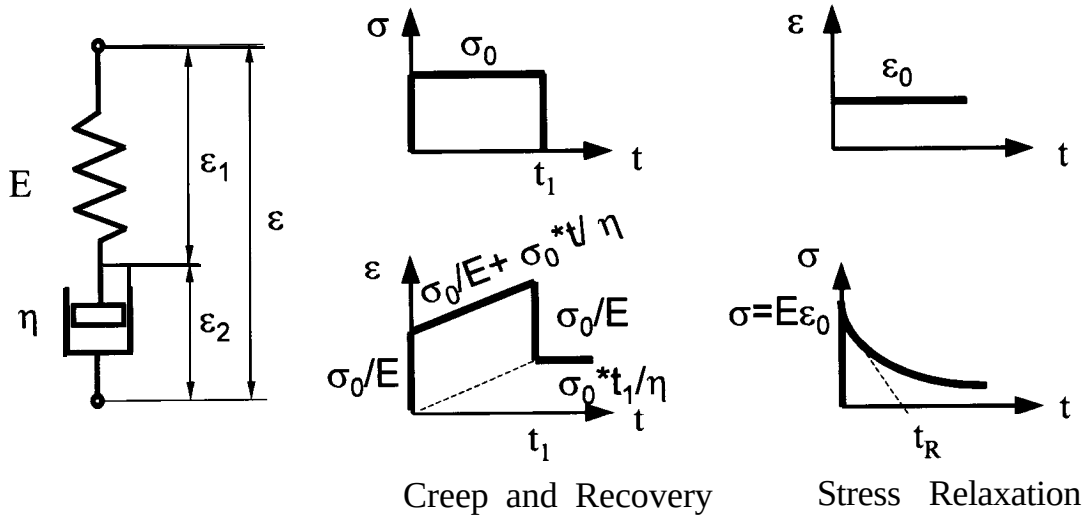

Figure 4 Behavior of a Maxwell element.

The total strain ε is the summation of the individual strain of spring ε_1 and dashpot ε_2.

$$\varepsilon = \varepsilon_1 + \varepsilon_2$$ Equation 8

Also the strain rate $\frac{d\varepsilon}{dt}$ is additive.

$$\frac{d\varepsilon}{dt} = \frac{1}{E}\frac{da}{dt} + \frac{\sigma}{\eta}$$ *Equation 9*

The governing differential equation (Equation 9) can be solved for applied stress or strain through application of the appropriate boundary condition.

- The *Voigt or Kelvin element* is a parallel combination of elastic and viscous element.

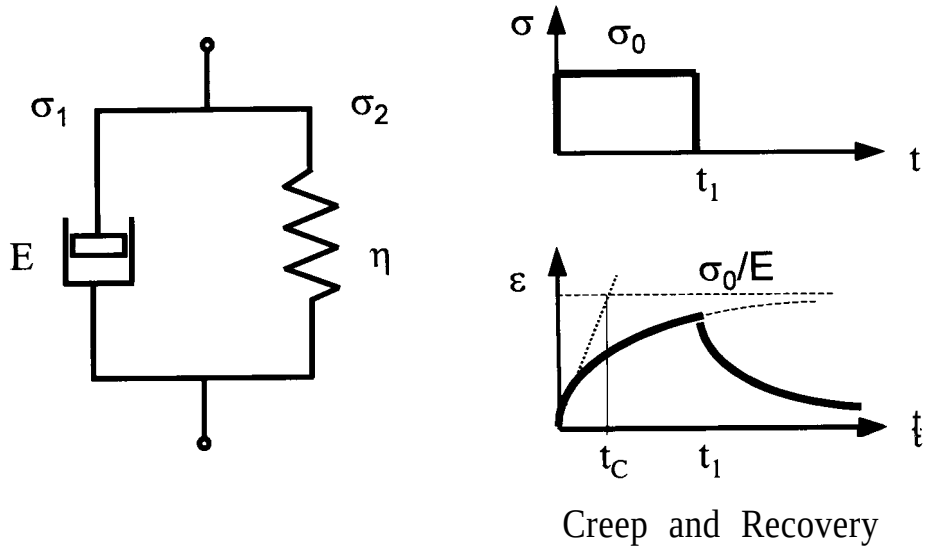

Figure 5 Behavior of a Voigt / Kelvin element.

The strain rate on each element must be equal, therefore the stresses are additive.

$$\sigma = \sigma_1 + \sigma_2$$ *Equation 10*

$$\sigma = E\varepsilon + \eta\frac{d\varepsilon}{dt}$$ *Equation 11*

For constant stress (creep experiment), the linear differential equation can be solved exactly. The Voigt equation cannot be solved for stress-relaxation (constant strain), because the dashpot element cannot be deformed instantaneously.

Linear viscoelastic behavior implies that at any time the response is directly proportional to the value of the initiating signal. The linear theory of viscoelasticity can be expressed with linear differential equations, where the coefficients of the differentials are constant material parameters. The general differential equation for linear viscoelasticity is as follows [Barnes, Hutton and Walters 1989]:

$$\left(1+\alpha_1\frac{\partial}{\partial t}+\alpha_2\frac{\partial^2}{\partial t^2}+\ldots+\alpha_n\frac{\partial^n}{\partial t^n}\right)\sigma=\left(\beta_0+\beta_1\frac{\partial}{\partial t}+\beta_2\frac{\partial^2}{\partial t^2}+\ldots+\beta_m\frac{\partial^m}{\partial t^m}\right)\varepsilon \qquad \textit{Equation 12}$$

where $n=m$, or $n=m-1$

Expansion of the general governing constitutions model (Equation 12) for various coefficients results in several commonly occurring relationships.

Table I Differential equations for viscoelastic models.

-parameter models:		
Hooke's elasticity (linear solid behavior):	$\beta_0 \quad (\beta_0 = E)$	$\sigma = \beta_0 \varepsilon$
Newtonian viscous fluid:	$\beta_1 \quad (\beta_1 = \eta)$	$\sigma = \beta_1 \frac{\partial \varepsilon}{\partial t}$
!-parameter models:		
Voigt / Kelvin element:	$\beta_0, \beta_1 \quad (\beta_0 = E, \quad \beta_1 = \eta)$	$\sigma = \beta_0 \varepsilon + \beta_1 \frac{\partial \varepsilon}{\partial t}$
Maxwell element:	$\alpha_1, \beta_1 \quad (\alpha_1 = \frac{\eta}{E}, \ \beta_1 = \eta)$	$\sigma + \alpha_1 \frac{\partial \sigma}{\partial t} = \beta_1 \frac{\partial \varepsilon}{\partial t}$
3-parameter model:		
Standard solid:	$\alpha_1, \beta_0, \beta_1$	$\sigma + \alpha_1 \frac{\partial \sigma}{\partial t} = \beta_0 \varepsilon + \beta_1 \frac{\partial \varepsilon}{\partial t}$
	where $\alpha_1 = \frac{\eta_2}{E_1 + E_2}$, $\beta_1 = \frac{E_1 E_2}{E_1 + E_2}$, and $\beta_2 = \frac{E_1 \eta_2}{E_1 + E_2}$	
4-parameter model:		
Burger's model:	$\alpha_1, \alpha_2, \beta_1, \beta_2$	$\sigma + \alpha_1 \frac{\partial \sigma}{\partial t} + \alpha_2 \frac{\partial^2 \sigma}{\partial t^2} = \beta_1 \frac{\partial \varepsilon}{\partial t} + \beta_2 \frac{\partial^2 \varepsilon}{\partial t^2}$
	where $\alpha_1 = \frac{\eta_1}{E_1} + \frac{\eta_1}{E_2} + \frac{\eta_2}{E_2}$, $\alpha_2 = \frac{\eta_1 \eta_2}{E_1 E_2}$, $\beta_1 = \eta_1$, and $\beta_2 = \frac{\eta_1 \eta_2}{E_2}$	

More complex material response can be mimicked with higher order (n>4) expansions of Equation 12. The main usefulness of the mechanical models is to facilitate the definition of parameters that characterize the time dependence of viscoelastic response. However, this approach requires the determination of additional material constants and often does not extrapolate well to long-term (creep) performance.

The differential equations of Table 1 can be solved for a simple stress state by applying Laplace transformation. The results for complex modulus, consisting of storage and loss modulus for dynamic sinusoidal input are shown in Table 2, where ω represents the angular frequency.

Table 2 Complex modulus for 2- and I-parameter viscoelastic models.

Complex Modulus:	$E^* = E'+iE''$	
2-parameter models:		
	Storage Modulus $E'(o)$	Loss Modulus $E''(\omega)$
Kelvin element:	R	$\eta\omega$
Maxwell element:	$\dfrac{\dfrac{\eta^2\omega^2}{R}}{1+\dfrac{\eta^2\omega^2}{R^2}}$	$\dfrac{\eta\omega}{1+\dfrac{\eta^2\omega^2}{R^2}}$
4-parameter model:		
	Storage Modulus $E'(o)$	Loss Modulus $E''(o)$
Burger's model:	$\dfrac{\alpha_1\beta_1\omega^2 - \beta_2\omega^2(1-\alpha_2\omega^2)}{\alpha_1^2\omega^2+(1-\alpha_2\omega^2)^2}$	$\dfrac{\alpha_1\beta_2\omega^3-\beta_1\omega(1-\alpha_2\omega^2)}{\alpha_1^2\omega^2+(1-\alpha_2\omega^2)^2}$

2.2.3 Time-Temperature Superposition

The principle of time temperature superposition enables the prediction of a material's behavior for different time scales beyond those easily obtained experimental [Ferry 1980, Aklonis and MacKnight 1983]. Time-temperature superposition is based on linear viscoelastic theory. The time-temperature superposition states that the modulus measured at a particular temperature T and real time t corresponds to the same value of modulus in the master curve at the reference temperature T_r and reference-scale time coordinate t_r (Equation 13). The time dependence is

determined by evaluating the material's behavior over a short time period at different temperatures The reference time is related to the real time by the shift factor a_T (Equation 14).

$$E(T,t) = E(T_r,t_r) \qquad \text{Equation 13}$$

$$a_T(T) = \frac{t}{t_r} \qquad \text{Equation 14}$$

The shift factor a_T is given by the Williams-Landel-Ferry equation (Equation 15), where C_1 and C_2 represent the Universal Constants, C_1=17.44, C_2 =51.6, and T_g the glass transition temperature of the material. The function log a_T as a function of reference temperature is shown in Figure 6.

$$\log a_T(T) = \frac{-C_1(T-T_g)}{C_2+T-T_g} \qquad \textit{Equation 15}$$

The constants C, and C_2, originally thought to be universal constants, have been shown to vary from polymer to polymer and additionally depend on the way of measurement and in which region or viscoelastic zone they were determined [Mark 1996]. Mark also reported C_1 and C_2 constants for various polymer systems.

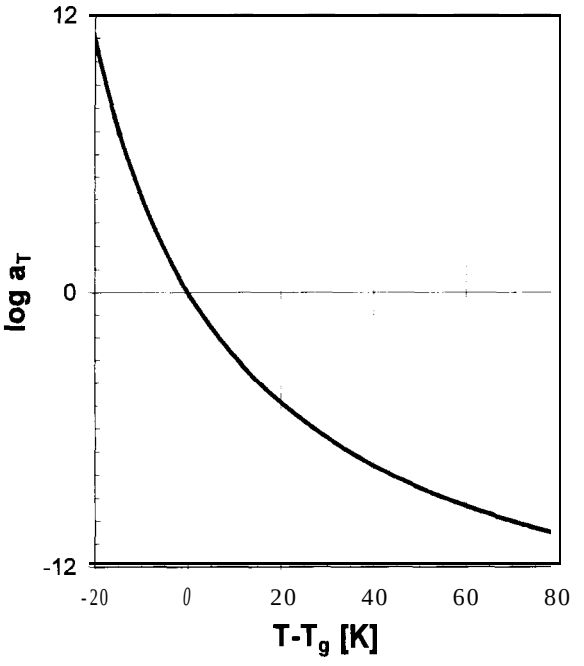

Figure 6 WLF-equation with universal constants.

The time-dependent characteristics of the dynamic moduli of viscoelastic materials are strongly related to their internal structure and environmental conditions [Findley et al. 1989].

The dynamic nature of calendering or printing processes imposes short duration events on coatings and coated paper. With dynamic mechanical thermal analysis and time-temperature superposition it is possible to predict the materials behavior for those short impacts.

2.3 Composites

2.3.1 Definition of Composites

A composite consists of two or more distinct materials, assembled to combine specific characteristics and properties [Agarwal 1979, Tsai and Hahn 1980]. The discontinuous phase is usually, but not always, harder and stronger than the continuous phase and is called the *reinforcement* or *reinforcing material,* whereas the continuous phase, which transfers loads

between particles, is referred to as the ***matrix.*** The properties of composites are influenced by the properties of their constituent materials, their distributions, and the interactions among them. Fillers are widely used to improve the mechanical properties of the matrix material, such as, fracture resistance, stiffness, toughness, and temperature performance.

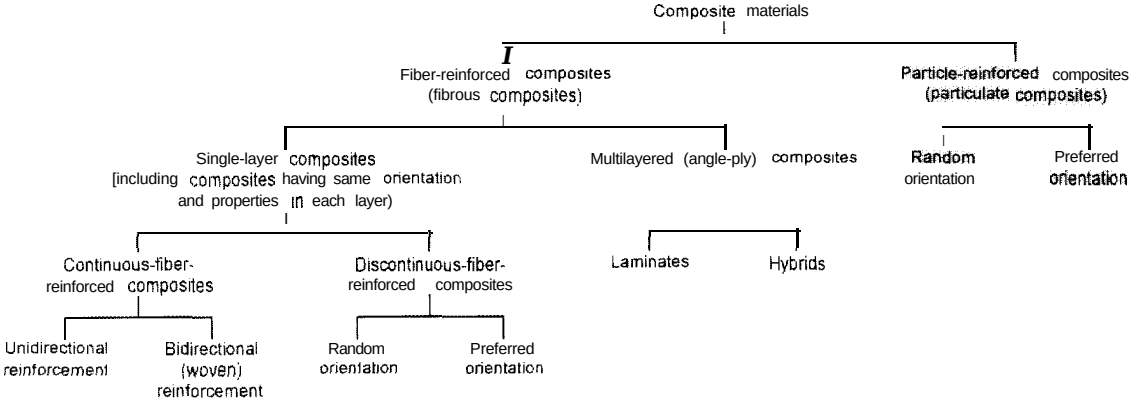

Figure 7 *Classification* ***scheme*** *of* ***composite materials.***

Pigmented coatings can be considered as particle-reinforced polymer composites with random orientation of the particles, or with preferred orientation of the particles in the plane of the coating in case of the anisometric particles, such as plate-like clay. Paper coatings additionally contain air voids. A coated paper itself can be considered as a multilayered hybrid composite of at least three different layers:

- The base paper, a fibrous composite with preferred in-plane orientation, which can contain fillers.
- The interphase, where penetration of the coating into the base paper occurs.
- And on top a layer of pigmented coating. The coating can be a single layer, or can consist of as many as three different layers (triple coating).

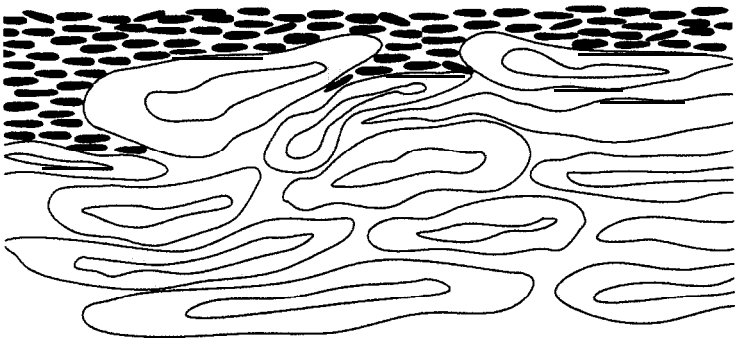

Figure 8 Structure of coatedpaper

2.3.2 Pigment Volume Concentration

The coating composition can be described in several different ways. Weight fractions are commonly used in industrial processes describing the components' relative proportions.

$$W_B = \frac{M_B}{M_B + M_P} \quad , \quad W_P = \frac{M_P}{M_B + M_P} \qquad \text{Equation 16}$$

W_B, W_P . . . . . weight fraction of binder and pigment

M_B, M_P . . . . . mass of binder and pigment

For paper coating formulations, the binder to pigment ratio is typically expressed in *park per hundred (pph)*. The *pph binder* is the amount of binder in grams per hundred grams of pigment.

$$pph\ binder = \frac{M_B}{M_P} * 100 \qquad \left[\frac{g\ binder}{100\ g\ pigment}\right] \qquad \text{Equation 17}$$

The use of weight fraction ignores the fact that different components have different densities, and therefore different volumes. For analytical purposes, volume fractions are thus used.

The *Pigment Volume Concentration (PVC)* is the ratio of volume of the pigments, to the total volume of the solid components in the coating. While the different densities of the components are taken into consideration, the volume contribution of air voids is not.

$$PVC = \frac{V_P}{V_P + V_B} = \frac{\frac{M_P}{\rho_P}}{\frac{M_B}{\rho_P} + \frac{M_B}{\rho_B}}$$ *Equation 18*

V_B, V_P . . . . . volume of binder and pigment

ρ_B, ρ_P . . . . . density of binder and pigment

2.3.3 Critical Pigment Volume Concentration

The terminology of *Critical Pigment Volume Concentration (CPVC)* was first introduced by Asbeck and van Loo in 1949, describing a fundamental physical transition point in a pigment-binder system at which the appearance and behavior of paint films change considerably.

"The critical pigment volume concentration is the point at which just sufficient binder is present to fill completely the voids left between particles in a pigment-binder system. It represents the densest degree of packing of the pigment particles commensurate with the degree of dispersion in the system." [Asbeck and van Loo 1949]. This definition indicated that above the CPVC porosity arises in the coating layer, and implied that CPVC measurement methods would be best based on film porosity. Furthermore, the presence of aggregates or agglomerates influences the CPVC, where the packing of pigment particles is in general not a unique property of the pigmentation.

In paint research it is common to characterize the CPVC by a number of methods, [Stieg 1973, Bierwagen and Rich 1983]. Different experimental methods were reviewed to determine CPVC (Table 3), and also methods were shown how to predict CPVC for latex coatings [Bierwagen 1972].

Table 3 Influence of P VC on different properties as summarized by Stieg (1973).

	Below CPVC; as the PVC falls	At the CPVC	Above CPVC; as the PVC rises
Gloss	⇧	Minimum	
Hiding power per unit of pigment	⇧	Minimum	⇧
Penetration	⇧	Minimum	⇧
Sheen uniformity	⇩	Maximum	
Angular sheen			⇧
Viscosity	⇩		⇧
Flexibility	⇧		
Washability	⇧		
Porosity			⇧
Color uniformity		Maximum	⇩
Film density		Maximum	

CPVC was found to be not only a pigment related effect (particle shape, size distribution, packing characteristics and surface chemistry), but **also** a polymer related effect [Lepoutre and Rezanowich 1977, Bierwagen and Rich 1983]. del Rio and Rudin (1996) investigated the effect of latex particle size and CPVC by optical methods, giving an exponential relationship between CPVC and latex particle size.

Pigmented coatings at low pigment volume concentration (<CPVC) are filled polymeric systems (Figure 9), building an impervious coating. Those coatings consist of two phases where the mechanical and chemical characteristics are dominated by the matrix properties [Braun 1993, Lepoutre and Hiraharu 1989].

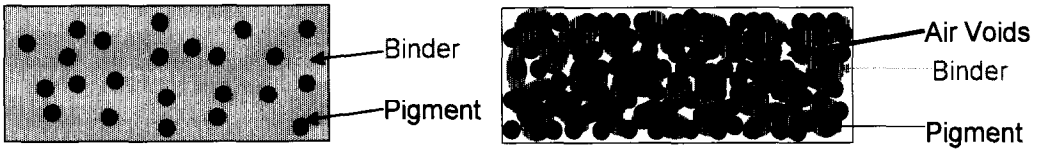

Below CPVC, 2 phase coating:
pigment + binder,
binder is continuous phase

Above CPVC, 3 phase coating:
pigment + binder + air,

*Figure 9 Schematic ofpigmented coatings below and **above** the critical pigment volume concentration*

With increasing pigment volume concentration, critical pigment volume concentration will be reached. All properties change rapidly around the critical pigment volume concentration as seen in Figure 10 and Figure 11. The change in properties occurs for various properties at different pigment volume concentrations, as the properties are influenced differently depending on agglomeration/dispersion effects, as well as by coalescence and mechanism of film formation in latex coatings upon drying.

Above the CPVC there is no longer enough binder present to completely fill the voids between pigment particles. Air is included into the matrix. The presence of air voids results in a coating consisting of three phases – binder, pigment and air. Floyd and Holsworth (1992) described the inclusion of air voids as a "phase inversion". The air void structure impacts different properties to a different degree. The thickness and total volume of the film will be greater than it would be indicated by the sum of pigment and binder volume. The presence of air increases the reflectance, gloss and opacity of the film above the levels observed at the CPVC because pigment/binder interfaces are replaced by pigment/air interfaces, which increases the average refractive index difference between pigment and medium. These optical effects are immediately apparent and therefore the PVC of their appearance shows excellent correlation with the CPVC. [Bierwagen and Hay 1975, Bierwagen 1992].

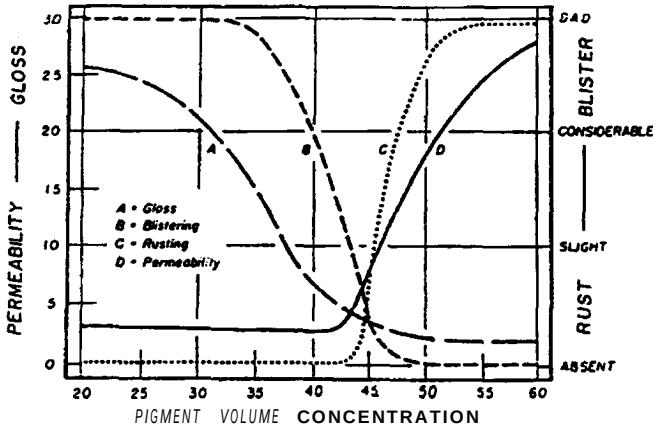

Figure IO Typical curves change in gloss, blistering, rusting andpermeability of a paint film as a function ofpigment volume concentration, by Asbeck and van Loo, (1949).

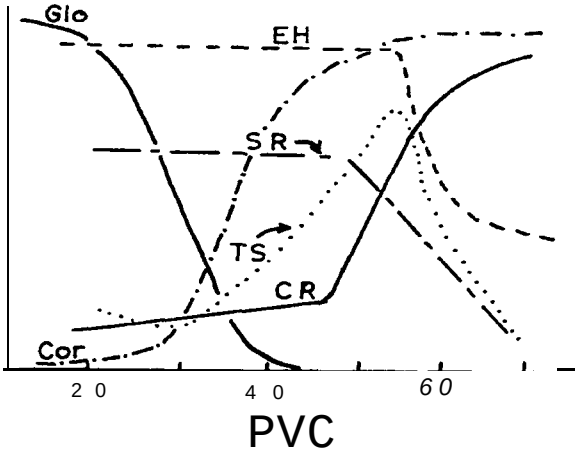

Figure I I Typical curves of gloss, enamel holdout, scrub resistance, tensile strength, contrast ratio and corrosion for an acrylic emulsion based paint pigmented with calcium carbonate versus pigment volume concentration, by Schaller (1968), Floyd and Holsworth (1992).

Schaake, Heijkant and Huisman (1988) described a "real" CPVC defined as the pigment volume concentration at which porosity starts and above which a coating layer is porous. This "real CPVC" was measured on magnetic coatings by mercury porosimetry and compared with results obtained from tensile tests, gloss, abrasion, magnetic moment, and oil absorption. It was found, that a first inflection points in the plots of the logarithm of the Young's modulus and the magnetic moment versus the pigment concentration coincided well with the "real CPVC". Furthermore, it was stated, the widely supported point of view [Stieg 1973, Bierwagen and Rich 1983] that the CPVC of a pigment system is only determined by the physical nature of the pigmentation - its average particle size, shape and particle size distribution, whether corrected or not for an adsorbed polymer layer - is too idealistic and not reality. It is more correct to state that a given pigmented system has a certain CPVC, which depends on pigmentation, formulation, preparation and application conditions.

2.3.4 Particle Packing in Latex Paints

Nolan and Kavanagh (1995) showed different models for random state packing of spherical and nonspherical particles. In a further step they predicted particle packing in acrylic latex paints, and

were able to determine from the simulation the CPVC for a simple latex-pigment system. Particle size distribution of the pigment (TiO_2, and $CaCO_3$) and latex particle size distribution and the deformation or softness of the latex had to be known. The predicted values for CPVC were in good agreement with experimental results on gloss and transmission.

2.3.5 Pigments

Pigments are the discontinuous, particulate phase of the coating composite. The major pigment used in paper coatings is clay [Hagmeyer 1997]. Clay is an aluminum silicate with a layered structure ($Al_2O_3*2SiO_2*2H_2O$). It has a plate-like particle shape and a particle size distribution. Another widely used paper coating pigment is calcium carbonate ($CaCO_3$). The structure of ground calcium carbonate is isometric, and has a size distribution. Precipitated calcium carbonate, a so-called engineered pigment is increasing in use, designed with specially shaped forms. Polymeric pigments are becoming of grater commercial importance. They are also used in paper coatings in combination with conventional inorganic pigments. Such synthetic pigments are typically made of polystyrene. The particles are non-film-forming at ordinary temperatures and stay more or less discrete under the conditions of application, drying and finishing. The pigments can be monodisperse or polydisperse. Monodisperse pigments with uniform sphere diameter are useful for model evaluations.

2.3.6 Binders

The binder has the ability to coalesce into a coherent film, which is capable of bonding the pigment particles to themselves and to the paper substrate, providing the coating with the mechanical strength that is required in subsequent printing and converting operations.

In paper coatings the level of binder is kept at a minimum for economical reason. The volume of binder is much less than the interparticle volume so that paper coatings are porous and permeable composites.

Binders used for paper coatings can be separated into two groups, natural binders such as starch and proteins, and synthetic polymers. Latices are synthetic binders and primarily used in paper coating formulations to yield improved coating strength, sheet gloss, ink gloss and printability. When used as binders, the latices – generally based on styrene/butadiene, vinyl acetate or acrylic polymers – are formulated so that they form a film under normal drying conditions.

Styrene-butadiene (S/B) latex is a milky white suspension of finely distributed spherical copolymer particles in water. Depending on the S/B ratio, copolymers with different glass transition temperatures can be produced resulting in soft or hard polymers.

2.3.6.1 Glass Transition Temperature (T,)

Below the glass transition temperature a plastic or elastomeric polymer is a supercooled liquid and behaves like a rigid solid. Above this temperature, the behavior of a thermoplastic material is soft rubbery and will depend on its level of crystallinity. A noncrystalline (amorphous) polymer will have a large decrease in modulus at the glass transition temperature [Mark 1993, Harper 1996]. During the temperature interval of the glass transition region many properties of the polymer change. For the mechanical properties a significant decrease is observed.

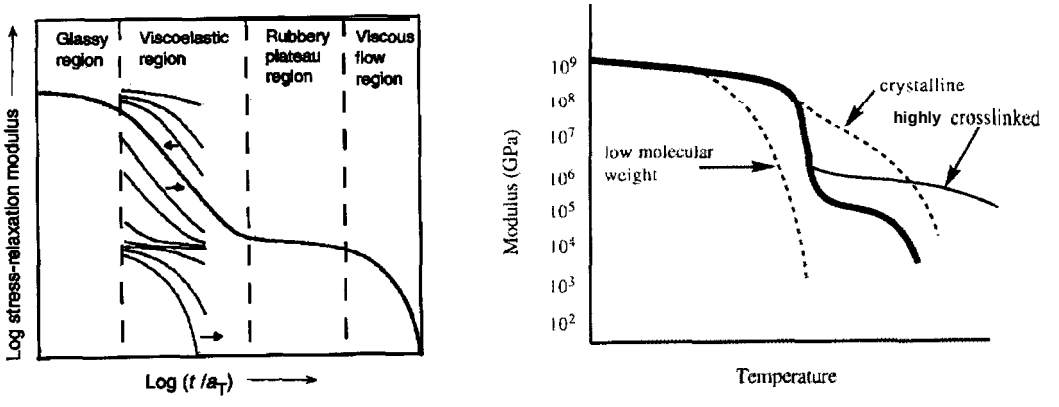

Figure 12 Behavior of storage modulus as a function of time and temperature [Fried 1995].

The **glass** transition temperature is defined as the temperature region in which the polymer changes from hard and glassy condition to the rubbery or amorphous condition.

2.3.6.2 Minimum Film Formation Temperature (MFFT)

"When a latex dispersion is applied on a substrate and evaporation is allowed to proceed, a continuous, homogeneous film is formed under appropriate conditions. This is called film formation." [Keddie 1997].

The minimum film formation temperature is defined as the lowest possible temperature at which film formation can occur as determined by visual observation of cracking or whitening [ASTM D-2354-68]. In general the MFFT is above the glass transition temperature of the polymer, and correlates very well with the T,.

It has been shown that for clay-latex coatings dried below the MFFT and subsequently heated above the MFFT, that the optical properties are enhanced. Dry sintering of particles increased the average size of microvoids without significantly affecting the total void content [Lepoutre and Alince 1981].

2.3.7 Mechanical Properties of Composites

The mechanical properties of a composite material depend on the properties of its constituents and their distribution, as well **as** on physical and chemical interactions. Properties of composites can be determined through experimental measurements. However, there exist many different mathematical models to predict mechanical properties. In the models here presented, it is assumed that the materials have linear elastic and isotropic behavior, and that the reinforcement material is homogeneously distributed throughout the matrix. Further, perfect adhesion at the

interface between the two phases is assumed. These assumptions are not always appropriate in actual composites. Such micromechanical models are quite accurate for many material systems [Agarwal and Broutman 1980] and may offer insight into the effect of compositional changes on performance.

2.3.7.1 Rule of Mixtures

The simplest model is the *Rule* of Mixtures, giving a linear relationship between the moduli of the two constituent. The elastic modulus of the coating, E_C, is the summation of the elastic moduli of the components, E_P and E_B, multiplied by their volume fraction, V_P and V_B. For the rule of mixture a state of plane strain is assumed in the system.

$$E_C = E_P \frac{V_P}{V_P + V_B} + E_B \frac{V_B}{V_P + V_B} \qquad \text{Equation 19}$$

E_C ..... Elastic modulus of the coating (composite)

E_P ..... Elastic modulus of pigment (reinforcement material, filler)

E_B ..... Elastic modulus of binder (continuous matrix)

V_P ..... Volume of pigment

V_B ..... Volume of binder

The Rule of Mixture accurately predicts the stress-strain behavior of unidirectional composites subjected to longitudinal loads [Agarwal and Broutman 1980], and has been successfully applied to glass- or ceramic-fiber-reinforced thermosetting plastics.

2.3.7.2 Transverse Rule of Mixtures

The *Transverse* Rule *of* Mixtures describes a hyperbolic relation between the moduli of the two components and assumes a state of plane stress in the system.

$$\frac{1}{E_C} = \frac{1}{E_P}\frac{V_P}{V_P + V_B} + \frac{1}{E_B}\frac{V_B}{V_P + V_B} \qquad \textit{Equation 20}$$

The reciprocal of the coating modulus E_C equals the sum of the reciprocal moduli of the components, E_P and E_B, multiplied by their volume fraction, V_P and V_B.

These two models are the two extremes, with either assuming plain strain (Rule of Mixture), or plain stress (Transverse Rule of Mixture). Other micromechanical models typically predict behaviors within these two limiting borders.

2.3.7.3 Halpin Tsai Equation

A more generalized and commonly used equation is the Halpin-Tsai equation (1969), which is derived from the Rule of Mixtures.

$$E_C = E_B \frac{1 + \xi\eta \dfrac{V_P}{V_P + V_B}}{1 - \eta \dfrac{V_B}{V_P + V_B}} \qquad \textit{Equation 21}$$

$$\eta = \frac{\dfrac{E_P}{E_B} - 1}{\dfrac{E_P}{E_B} + \xi} \qquad \textit{Equation 22}$$

$\xi = 2$ for particles with circular or square cross section

$\xi = 2\frac{a}{b}$ for particles with rectangular cross section

The shape parameter ξ is a measure of reinforcement and depends on the fiber geometry, packing geometry, and loading conditions. It is suggested that for spherical particles the shape parameter ξ is constant; therefore the equations for plain stress and plain strain are the same. Figure 13 shows the comparison of elastic moduli derived from the different models. Halpin and Tsai (1969) have demonstrated the applicability of these equations.

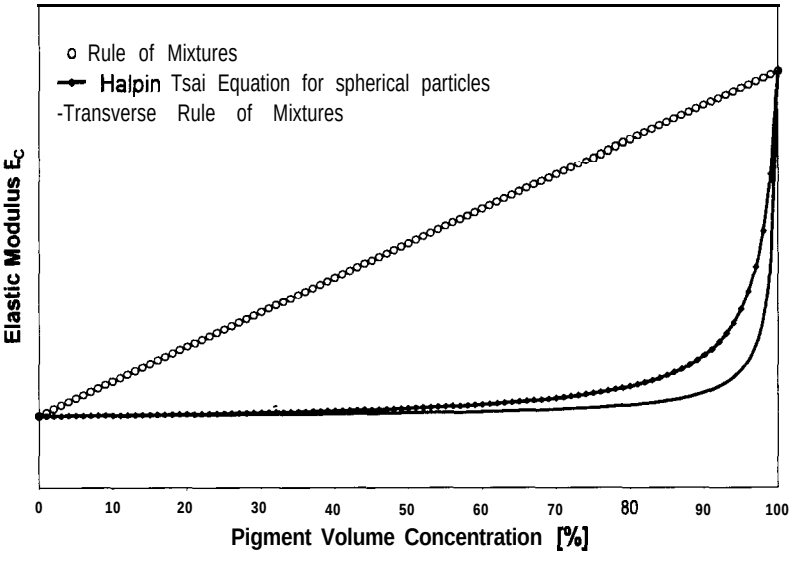

Figure 13 Comparison of Rule of Mixture, Transverse Rule of Mixtures and Halpin-Tsai equation

2.4 Filled Polymers, Paint Films, Paper Coatings – A Review

Much research concerning the mechanical properties of filled polymers has been reported. However, most has concentrated in the low pigment volume concentration range. Influence of pigmentation on optical properties of paint films and paper coatings are investigated sufficient.

The porous nature of paper coatings is known to have a very strong influence on its optical, and mechanical properties. Mechanical behaviors of paper coatings as a thin film have been investigated only to a limited extent in the literature.

2.4.1 Optical Properties

Optical properties are a function of the properties at the interfaces. The magnitude of the difference in refractive index across an interface determines, in part, the light-scattering efficiency. Other factors include the size of the scattering species relative to the light wavelength. Lepoutre 1989].. Air voids included in the film act as additional scattering centers, improving the "dry hiding" in paint films [Anwari et *al.* 1991]. In a given system, the light scattering coefficient was found to be linearly proportional to coating porosity [Lepoutre et al. 1977]. Gloss is the ratio of specularly reflected light to incident light. For optically smooth surfaces, gloss varies with refractive index and angle of incidence according to Fresnel's law. Gloss is a function of roughness, an increasing roughness degrades gloss [Braun 1993]. del Rio and Rudin (1996) showed for a TiO_2 paints with different latices (particle size ranging from 200nm to 1200nm) the development for gloss for different incidence angles. A minimum in gloss was found at the critical pigment volume concentration. However the CPVC values were found to be different for different incident angles, depending on surface roughness. An incident angle of 85" was found to correlate best with the CPVC.

2.4.2 Microstructure, Adhesion

Harding and Berg (1997) investigated filled polymer composites with fillers possessing different surface energies to analyze the dependence of mechanical properties on the inter-facial strength of filler and matrix. A high purity silica quartz sand with spheroidal particles was used and treated with three different organofunctional silane coupling agents to vary coverage. The matrix polymers were thermoplastic polymers, poly(methyl methacrylate) (PMMA) and poly(vinyl butyral)

(PVB). Inverse gas chromatography was used to estimate the energetic and Lewis acid-base nature of filler and matrix surface. Surface energy was also measured with dynamic contact angle method. Mechanical tests were performed on a beam deflection tester following ASTM 7900. The elastic bending modulus and maximum yield stress were determined. The fracture interfaces were characterized with a scanning electron microscope. It could be seen that PMMA composites failed all cohesively within the matrix, unaffected by the filler surface treatment. PVB composites failed at the interface although with filler surface modification significant changes were observed on stress-strain behavior where the elastic-bending moduli stayed constant. Therefore, the level of adhesion at low strain levels does not affect the elastic-bending modulus, as the interface was not failing. Differences in inter-facial chemistry were not reflected in the composite mechanical properties.

In filled systems the binder adheres to the filler initially, reinforcing the system. Tensile tests are performed. When the applied stress approaches the yield stress the particle/matrix interfaces are delaminated, adhesive bonds between binder and particles break and vacuoles form around the solid particles. The stress-strain curves show precisely the elongation at which adhesive failure begins, and the adhesive strength can be determined [Touissant 1973/74]. Tensile tests of poly(vinyl chloride) filled with ground calcium carbonate were carried out with different particle size distribution (2µm and 8µm) by Nakamura, Fukuoka and Ilda (1998). With scanning electron microscopy the delamination in the particle/matrix interfaces could be seen clearly.

Several adhesion theories have been proposed, trying to explain how bonds are formed [Wu 1982 and Lepoutre 1994]. Thermodynamic adhesion refers to equilibrium inter-facial forces or energies associated with reversible processes, such as ideal adhesive strength, work of adhesion, and heat of wetting. *Chemical* adhesion refers to adhesion involving chemical bonding at the interface. Mechanical adhesion arises from microscopic mechanical interlocking of structural elements. *Electrostatic adhesion* takes place at any boundary between two oppositely charged surfaces. For polymers the *Diffusion* theory was developed, proposing an interdiffusion

of chain segments between two polymeric materials. A transition region is formed and there is no longer a clear interface between the materials. In the Weak-Boundary theory the formation of a strong joint is prevented by weaker boundary layers formed near the interface. The Adsorption theory considers that the adhesive adsorbs on the adherent, ensuring an intimate contact and intermolecular force of attraction can operate.

Lepoutre (1994) analyzed which adhesion phenomena mainly can be examined in coated paper. The requirements for adhesion in coated paper are, the formation of an interface or interphase, the establishment of strong intermolecular bonds across the interface, and the reinforcement of weak boundary layers. In the interface or interphase, stresses are transferred and distributed. For coated paper two theories that complement each other can be applied, the adsorption theory, predicting bond formation, and the weak boundary layer theory, predicting bond failure. Dickson (1997) investigated the importance of mechanical interlocking between coating and basesheet.

lnoue and Lepoutre (1992) determined the effects of pigment particle size, particle shape, and surface chemistry on the cohesion of pigmented coatings based on clay, calcium carbonate, and polystyrene latex using sodium carboxymethylcellulose as a binder. The critical binder content (CBC) – the minimum binder level required to form a coherent film – was characterized by an abrasion test. The cohesive strength in z-direction was evaluated by a delamination test. Surface characterization was measured with inverse gas chromatography. For the examined pigments an increase in cohesion was shown with increasing particle size. Clay coatings were found more resistant to in-plane stresses, where $CaCO_3$ showed higher strength in out-of-plane stresses, in other words particle shape affected the stress concentration and dissipation. Particle size distribution affected the packing density and therefore the void fraction. The strength of bonds at the polymer-solid interface depended largely on molecular interactions, particular acid-base interactions.

2.4.3 Mechanical Properties

The influence of fillers on mechanical properties was explored for filled polymers and paint films when the pigment volume concentration is below CPVC.

For a filled polymer system, glass beads in isotactic polypropylene, the stress-strain behavior and failure mechanism was analyzed by Sjörgen and Berglund (1997). An increase in content of glass beads resulted in a decrease of strain to failure, Poisson's ratio, and an increase of Young's elastic modulus. It was seen that an increase in bead diameter lead to a decrease in strain to failure, where Young modulus and Poisson ratio remained unaffected.

If the filler forms agglomerates, it can act as crack initiation sites. The ultimate strength will depend on the strength of the interphase. This in turn is dependent on the polymer-polymer and filler-polymer compatibility, which can be controlled by chemical modification of the filled system. The microstructure of mixtures of polypropylene/polystyrene and barium sulfate adding maleic anhydride-grafted polypropylene (PP-g-MAH) or styrene-maleic anhydride copolymer (SMA), was investigated by Hammer and Maurer (1998). Analysis was performed in the solid and melt state with a dynamic mechanical analyzer and a scanning electron microscope. The microstructure in a polypropylene/polystyrene/ $BaSO_4$ filled blend could be controlled by addition of PP-g-MAH or SMA. It was found that the filler was occluded at the interface of the polymer phases in the pure filled blend. An addition of $BaSO_4$ resulted in a substantial decrease in the phase domain size.

Toussaint (1973, 1974) and Zosel (1980) reviewed the mechanical properties of different paint films (below CPVC). In general they found that the tensile strength of isolated pigmented films increased with pigment volume concentration as compared with that of an unpigmented film, reaching a maximum value at CPVC. For values higher than the CPVC the tensile strength diminished. The ultimate strain was found to decrease continuously with the PVC. The reinforcing effect was more or less pronounced, depending on the binder/solids system involved, but in every

case the changes in property were approximately proportional to the PVC. Young's modulus, torsion modulus and damping factor increased proportional with the pigment volume concentration. The magnitude of change depended on several factors, such as size, morphology and chemical nature of the particles, surface treatment, polymer physical state, and humidity. The influence of the PVC on glass transition temperature was reviewed, and different results, often contradicting, were seen. That was explained by different types of interactions (hydrodynamic, physical adsorption, chemisorption) taking place between pigment and polymer. If the T_g is accurately measured, its value could be a measure for the modifications of the properties of the polymer phase as the result of the incorporation of a second phase.

2.4.4 Paper Coatings

Paper coatings are applied as an aqueous suspension of a pigment and a binder in soluble or particulate form. The aqueous phase is then removed by drainage into the sheet and by evaporation. At the end of this process a structure has formed. The structure of paper coatings containing kaolin and calcium carbonate has been studied and reviewed in depth by Lepoutre (1989).

Lepoutre (1990) discussed pigmented coating considered as a high performance composite, which has to balance optical, mechanical, and fluid transport properties. The structure of paper coatings was examined and relationships between surface and bulk structural parameters and end-use properties discussed. Pigment shape is an important factor determining coating structure. Cross section examination in a scanning electron microscope showed well-ordered arrangements of clay platelets with interparticle bonding of the film forming latex binder. Sketches such as Figure 14 have been suggested to represent the binder-pigment arrangement.

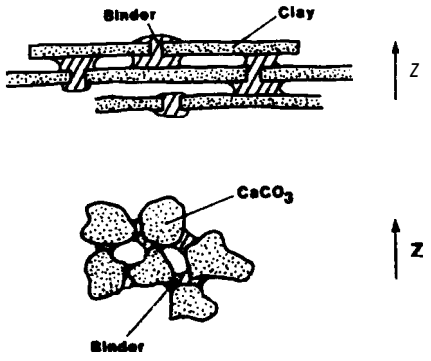

***Figure 14 Sketches** of **clay and calcium carbonate coatings** [from **Parpaillon et al.** 1985].*

Size distributions of particles influence the bulk structure. A narrow distribution results in a bulky structure where a polydisperse pigment packs with a higher density. Brightness and opacity are a function of the coatings' light scattering ability. The light scattering coefficient was found to be linear proportional to coating porosity.

The mechanical properties of pigmented coating films are sensitive to changes in the properties of the binders, the type and morphology of the pigments, and the extent of pigment coverage by the binder [Parpaillon et *a/.* 1985 and Lepoutre 1989]. The pigment volume concentration of paper coatings is typically formulated above the critical pigment volume concentration, where the latex polymer forms a discontinuous film, and a porous structure results.

Parpaillon et *al.* (1985) measured the mechanical properties of clay-based pigmented coating films containing different carboxylated-styrene-butadiene latex binders. They observed an increase in the in-plane tensile strength, in elongation at rupture and in the tensile modulus (stiffness) with increasing binder content. Films based on mixtures of clay and increasing calcium carbonate resulted in a decrease of tensile strength, elongation at rupture and stiffness. Results obtained by Electron Spectroscopy for Chemical Analysis (ESCA) suggests that clay and calcium carbonate interact in different ways with the styrene butadiene, the binder coverage of calcium carbonate being more extensive than that observed for clay.

Raman (1997) was studying the effect of pigment volume concentration on the bulk mechanical properties of free films consisting of styrene butadiene latex with polystyrene pigments. At low pigment volume concentration (PVC <40%), it was found that an increasing pigment concentration leads to better strength of the coating, the experimental results following very well with the model of Halpin Tsai. At high pigment volume concentrations (PVC>70%), tensile strength decreased with increasing pigment concentration, as the amount of binder being present in the film was not enough to provide good bonding between the pigment particles.

Okomori, Enomae, and Onabe (1999) compared Clark stiffness (i.e. bending resistance when a paper strip bends due to its own weight) and pure bending stiffness (i.e. paper strip is bent with the same curvature along the whole span). Coated paper was considered as a two-layer composite. The Young's modulus of the coating layer was determined both theoretically and empirically. The effect of starch and plastic pigment on Young's modulus was examined. Increasing starch ratio increased Young's modulus. Using plastic pigments with smaller particle diameter resulted in higher Young's modulus. Double coatings with coatings of different color formulations were evaluated to improve stiffness of the coated paper.

Lepoutre and Hiraharu (1989) were investigating the effect of the porous structure of coating on its mechanical strength in the transverse direction. The strength of material decreases when voids are introduced, as these are not load bearing. Clay coatings have at the same binder level a lower cohesive strength than calcium carbonate coatings. This is due to the different failure mechanism that results from the different pigment shape, and the higher void fraction.

Perhaps the most significant influence on mechanical properties however, is the glass transition temperature of the binder. Storage and loss modulus of the coating layers were found to be strongly related to the thermal softening of the coating latex. Performing dynamic mechanical analysis, Parpaillon et al. (1985) observed that an incorporation of pigments into the binder

resulted in an increase of glass transition temperature. This was interpreted as a result of a decrease in segmental mobility of the polymer molecules due to the presence of the clay particles, and interaction between pigments and binder. Hagen, Salmen, and de Ruvo (1993) showed that the glass transition temperature of a latex polymer increased with increasing volume fraction of filler at high filler contents due to filler-matrix interactions. Mechanical damping was also observed to decrease with increasing filler content in the coating. Comparing glass transition temperatures determined by mechanical thermal analysis and glass transition temperatures obtained from thermodynamic measurements (e.g. differential scanning calorimetry), mechanical measurements consistently exhibited higher values [Hill 1987].

Kan et a/. (1996, 1997) determined the viscoelastic properties of paper coatings by dynamic mechanical spectroscopy, predicting the effect of calandering on gloss, based on the elastic modulus of coating. With the used latices (carboxylated styrene butadiene latex) it was found for clay coatings and clay/plastic pigment (90/10) coatings that an increase in the volume fraction of binder increased the storage modulus of the coating in the regime below the glass-transition temperature and reduced the modulus in the regime above the glass-transition temperature.

Rigdahl et al. (1997) determined the influence of the morphology of heterogeneous latex particles on the mechanical properties of latex films and on the function of the latices as binders in porous structures, such as coating layers. A two-stage polymerization process and polystyrene with three different molecular weights were used to prepare heterogeneous carboxylated styrene-butadiene latices. A kaolin clay pigment was used and dynamic mechanical properties of the coating suspensions were measured. Coatings were drawn down on polyester film. Light scattering coefficient and gloss were determined. It was found that a higher modulus (determined by the morphology of the latex film) in the rubbery region was associated with coating layers with higher porosity, greater light scattering ability, and higher coating gloss. This was interpreted as the result of retarded shrinking of the coating layers during drying.

Yamaguchi et a/. (1993) and Ishikawa, Yamashita, and Tsuji (1995) observed changes in storage modulus with temperature for thick layers (150μm and 300μm) of clay/calcium carbonate coating samples. The observed change in storage modulus was described by three transition zones. They posited that with increasing temperature the coating structure changes and an orientation of the clay particles takes place.

Most dynamic mechanical thermal analysis was performed using torsional pendulum instruments (Zosel 1980, Parpaillon et a/. 1985, and Kan et a/. 1996, 1997) and polyimide films as coating substrates. Ishikawa et *al.* (1995) and Yamaguchi et a/. (1995) performed three point bending tests on relatively thick coating layers. Hagen et a/. (1993), Engstrom and Lind (1995), and Joyce et al. (1997) performed three point bending on coated paper samples.

Dynamic mechanical thermal analysis in tensile mode on thin free coating samples has not been reported in the literature.

2.4.5 Coated Paper

Poor surface strength can lead to problems when paper is subjected to converting operations Evanoff, Gerlach, and Lyne (1983]. The three basic types of surface failure of a coated paper were described as base-stock failure, failure in the coating-substrate interface, and failure in the coating layer. For failure in the coating layer the internal bonding, provided by the binder, between the pigment particles determines the overall strength.

Engstrom and Rigdahl (1992) reviewed some literature about surface strength of coated paper, the failure mechanism and mechanical properties. Failure also may be initiated by surface defects in the coated surface. The variation in the mechanical properties of the coating with changes in its formulation is discussed; and further basic concepts on the micro-mechanical behavior of coated papers are proposed.

Joyce, Hagen, and de Ruvo (1997) evaluated the dynamic mechanical properties of lightweight-coated paper with a 50:50 clay/calcium carbonate coating. Paper thickness increased due to absorption of water from the coating. The amount of water absorbed depended on the immobilization solids of the coating. The distribution of coatings across the thickness was studied with osmium tetroxide stained samples in an environmental scanning electron microscope equipped with an electron dispersive X-ray analysis measurement system. The results confirmed that the base sheet absorbed coating. The influence of coating penetration on bending stiffness was determined below and above the glass transition temperature.

Engström and Lind (1995) investigated how the bending stiffness of coated material is affected by the interaction between the coating color and the base paper and by the type of pigment. Based on their experiments a model was developed to calculate the bending stiffness. The results showed that both the coating thickness and the water picked up by the base paper during coating process determined bending stiffness. Coating thickness increased the stiffness, while the water decreased it. Approximately $5 g/m^2$ of the coating penetrated into the base paper, so the coated paper was modeled as a three-layer structure, coating – interphase – base paper. Coatings based on clay or gypsum showed a higher bending stiffness than coatings based on calcium carbonate. For calendered papers, the experimental and calculated bending stiffness showed a good agreement. For uncalendered papers, the calculated bending stiffness was higher than the experimentally measured values.

2.4.6 Models for Coated Paper Composites

Cox (1952) did one of the first studies of elasticity and strength of paper and other fibrous materials, analyzing the effect of orientation of the fibers on stiffness and strength. For a planar matrix it was shown that all possible types of elastic behavior might be represented by composition of sets of parallel fibers in appropriate ratios. The means of transfer of load from fiber to fiber were considered and it was concluded that the effect of short fibers might be represented

merely by use of a reduced value for their modulus of elasticity. The results of the analysis were applied to samples of resin bonded fibrous filled materials and moderately good agreement with experimental results was found.

Benabdi and Roche (1997) determined theoretical and experimentally the Young's modulus of coating materials when applied to substrates (epoxy adhesive layer applied to a titanium plate). Tests were performed using a three-point flexure tester. Residual stresses were generated during sample preparation, giving a significant radius of curvature to the bi-material strip only in longitudinal direction. Therefore the curved beam theory was used for calculation. The system was considered as a plate (width to thickness ratio >5). Flexure stiffness was calculated as a function of initial radius of curvature, radius of curvature during flexure test, Young's modulus of the materials and geometrical characteristics of the two layers. These equations then were used to calculate the Young's modulus of the coating material using various models (Stoney, Roll, and Inoue). It was observed that for the model proposed by Benabdi and Roche the Young's modulus of the coating was independent of experimental parameters, for other model equations the Young modulus depended on experimental data.

Suhling (1990) was reviewing existing continuum models for the mechanical response of paper and paper composites. The two current modeling techniques are based on hydrogen bond and fiber network. Due to the preferred fiber orientation of paper in plane, paper is considered anisotropic and therefore it is modeled as an orthotropic solid material. The behavior of paper is highly nonlinear and strongly influenced by environmental conditions. In the micromechanical approach, paper was considered to be heterogeneous in nature and the interactions between the micro-scale constituents were examined in detail. In the macromechanical approach, the material was assumed homogeneous and the effects of the micro-scale constituents are detected as averaged apparent properties.

Hagen et *al.* (1993) presented an analysis of clay-based coatings on paper using laminate theory. The coated paper was treated as a three-ply laminate. The estimated values of the mechanical damping for the laminated structure and experimental results were compared. The theoretical values were slightly lower than the experimental data but the dependence on filler content was observed to be consistent with measured values. It was shown that penetration of coating components into the paper formed an interaction zone with mechanical properties different from those of the other layers.

3 Objectives and Approach

3.1 Objective

The objective of this study was to investigate microscopic and macroscopic factors that determine viscoelastic mechanical properties of pigmented latex coating films, and to establish relationships between structure, composition and performance of pigmented latex coatings.

3.2 Approach

In order to determine the influence of the pigment shape, pigmentation level and adhesion on mechanical properties and coating structures coatings with different microstructures were prepared by varying pigment types, binder carboxylation degree and pigment volume concentration. A wide range of pigment volume concentrations was examined to fully illustrate trends and major transitions in performance, i.e. above and below critical pigment volume concentration. Three commonly used coating pigments were tested. The pigment categories included two mineral pigments, clay, representing a plate like structure, calcium carbonate having a prismatic structure, and an organic polystyrene plastic pigment with monodispersed spherical particles. The pigment types not only have a different pigment shape, but also exhibit different surface energies (Table 4). This changes the wettability (Berg 1993) and hence binder coverage.

The particles show different packing abilities. During the coating process, clay particles are orienting parallel to the surface, building a composite with preferred orientation. Calcium carbonate coatings and polystyrene coatings have no preferred orientation. Composites with preferred orientation are expected to have higher mechanical properties in the orientation of the pigments.

Table 4 Surface energies ofpigments

Pigment Material	Surface Energies [mJ/m^2]			
	Dispersive γ^d	Polar γ^p	Total γ	References
Polystyrene	41.4	0.6	32.8	Mark (1996)
Clay	28.3	40.8	69.1	Al-Turaif and Lepoutre (2000)
Calcium Carbonate	70			Lundqvist (1996).

The mechanical properties of coatings are to a large degree determined by the properties of the binders. The binder properties depend among others very much on their glass transition temperature. Binders with a glass transition of around 0°C were used in order to be able to prepare coatings at room temperature and guarantee film formation. A difference in carboxylation level of binder was selected to alter adhesion of the coating between pigments and binder. The two latices were prepared to have the same particle size and glass transition temperature, while latex I had a normal high carboxylation degree and latex II showed a minimum on carboxylation degree. For the latex with normal high carboxylation degree, high adhesion phenomena were expected. For the latex with a minimum of carboxylation degree, very low or no adhesion phenomena were expected.

The pigmented latex coatings were considered as a composite material. The composite properties were approached in two ways, macroscopic and microscopic. Bulk properties of the coatings were measured including film thickness, grammage, void fraction and gloss. Macroscopic mechanical properties were determined. Static tests were performed with a conventional tensile tester to obtain Young's modulus. Dynamic mechanical thermal analysis was performed over a wide range of temperature (i.e. below glass transition temperature of the binder, and above glass transition temperature of the polystyrene plastic pigment). Storage and loss moduli as a function of temperature were obtained, as well as tan Delta indicating the glass transition temperature of the materials. Performing frequency tests at different temperature levels,

and by applying time-temperature superposition and William-Landel-Ferry equation, the time dependent material behavior was investigated.

Microscopic stress-strain behavior and its relation to pigment concentration, distribution, and agglomeration were evaluated by conducting mechanical tests within an environmental scanning electron microscope. A tensile stage **was** used to obtain images at different elongation levels. The displacement of particles and corresponding field-strain maps were generated with an image analysis program.

In a further step coatings with 90PVC were applied to LWC-paper, and dynamic mechanical thermal analysis was performed.

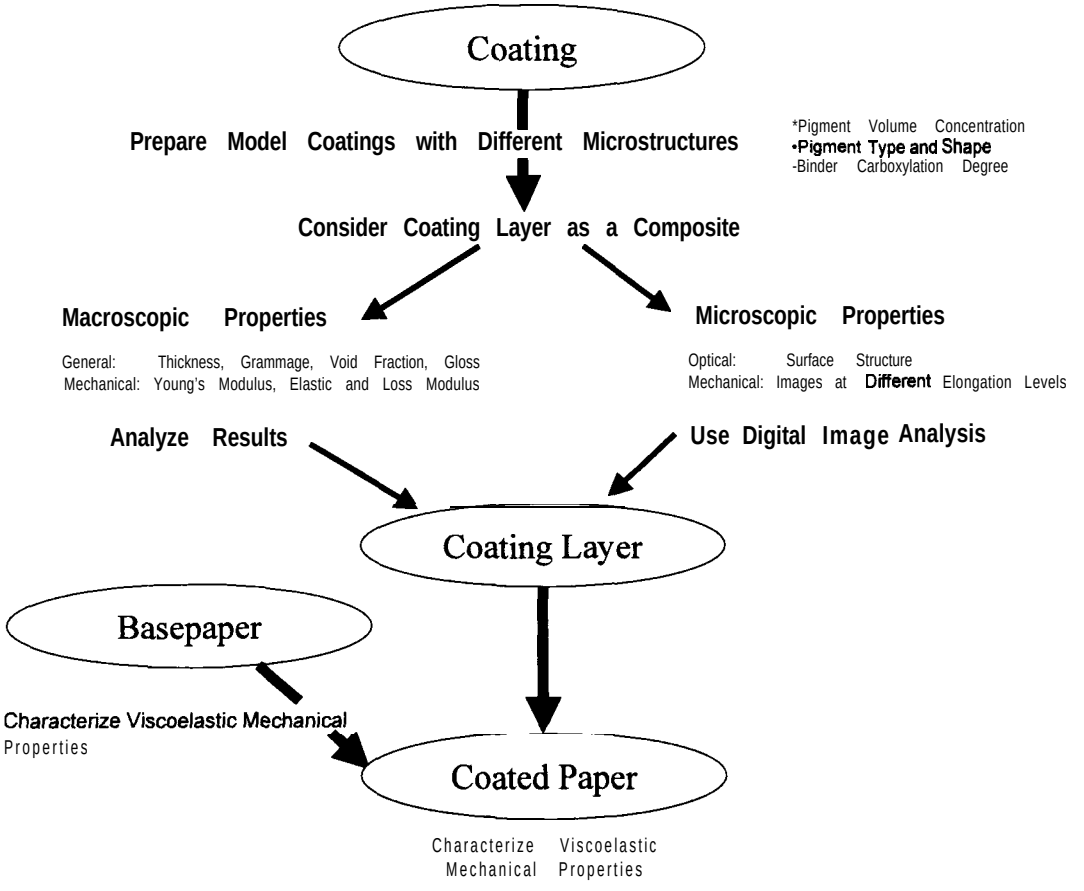

Figure 15 Chart of approach

4 Experimental Methods

In the following section the materials used are described. The procedures for specimen preparation are described in detail. The films of the pigmented latex coatings were analyzed and tested to characterize their properties and structure. Specific test methods used are explained.

4.1 Materials

4.1 .l Pigments

Three commercial grade pigment types with different shapes and properties were used. The polystyrene plastic pigment (PP 722HS) was an organic spherical pigment with a monodisperse distribution, a particle diameter of 0.5µm, and a density of 1 .05g/cm^3. The clay (Astraplate) was a platelike mineral pigment with a density of 2.62g/cm^3, and 84% of the particles were smaller then 2µm. The precipitated calcium carbonate (Albaglos S) had a prismatic particle shape with rhombohedral crystal structure, a polydispersity factor of 1.44 and a density of 2.71g/m^3. The different pigments are illustrated in Figure 16 to Figure 18. The companies supplying the pigments are listed in Table 5.

Table 5 Trade names and suppliers for pigment types

Pigment Material	Name	Supplier
Polystyrene Plastic Pigment	PP 722HS	DOW, Midland, MI 48674, USA
Clay	Astraplate	IMERYS, Sandersville, GA 31082, USA
Calcium Carbonate	Albaglos S	Specialty Minerals, Bethlehem, PA 18017, USA

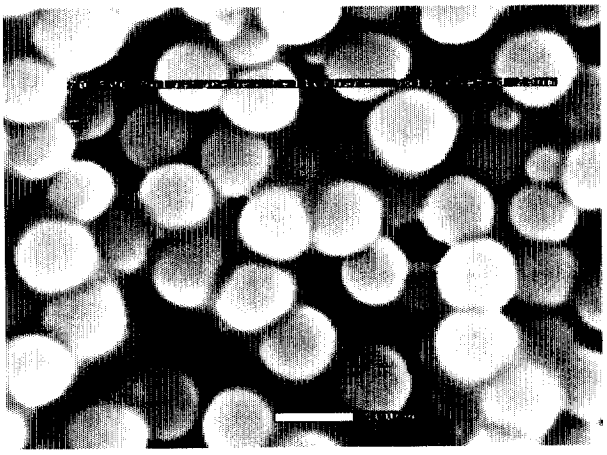

Figure 16 Polystyrene plastic pigment, PP 722 HS (DOW), 70% Pigment volume concentration, latex I, coated on cellophane as substrate, scale bar 0.5μm, coating sputter coated with 20nm gold, accelerating voltage 20kV, working distance 7.6mm, chamber pressure 2.5Torr, ESD

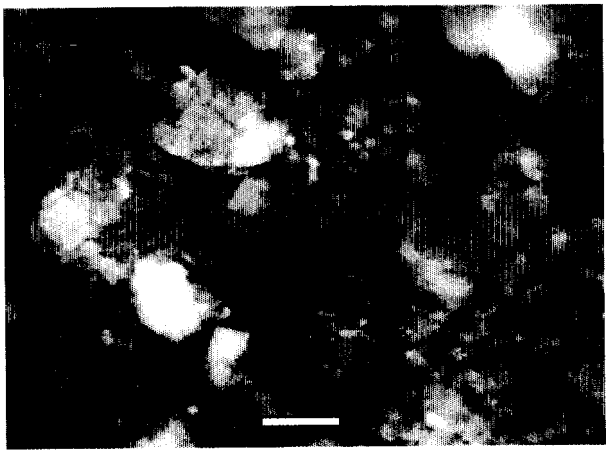

Figure 17 Clay, Astraplate (IMERYS), scale bar 2μm, accelerating voltage 18kV, working distance 8.4mm, chamberpressure 3.5Torr, ESD

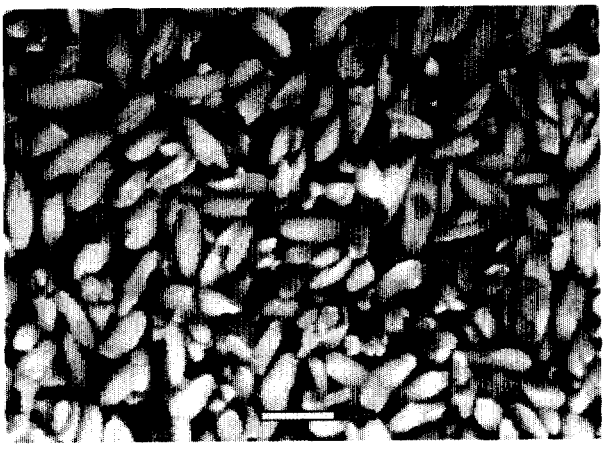

Figure 18 Precipitated calcium carbonate, Albaglos S (Specialty Minerals), scale bar 1μm, accelerating voltage 18kV, working distance 6.2mm, chamber pressure 3.5Torr, ESD

4.1.2 Latices

Two experimental latices (denoted latex I and II) were provided by the BASF-company (Charlotte, NC 28273, USA). Both latices were produced to have the same particle size and glass transition temperature (see Table 6) while experimental latex I had a higher carboxylation degree then latex II. The difference in carboxylation level of binder was selected to alter adhesion of the coating between pigments and binder. For latex I with high carboxylation degree (acidic level 4.5%) , high adhesion phenomena were expected. For latex II with a minimum of carboxylation degree (acidic level 0.3%), very low or no adhesion phenomena were expected.

Table 6 Characteristics of selected experimental latices

a)	Acidic Level	Particle Size	Glass Transition Temperature (mid point DSC-plot)
Experimental Latex I	4.5 %	155 nm	0.6 °C
Experimental Latex II	0.3 %	158 nm	1.0 °C

a) Source: Personnel communication Dr. Peter Hayes, BASF, Charlotte, NC

4.2 Preparation of Coating Dispersion

The coating colors were prepared in a conventional manner from dry pigment and dispersed pigment solutions. The clay pigment was received in dry form. A slurry was prepared at 67% solids by weight, the pH was adjusted to 8.5 using NaOH. Calcium carbonate pigment and plastic pigments were obtained in slurry form. Table 7 shows the solid contents of the different components.

Solid contents ofpigment slurries and latices

	Solid Content [%]
Clay, Astraplate	67.0
PCC, Albaglos S	71.3
Plastic Pigment, PP 722 HS	50.1
Experimental Latex I	50.9
Experimental Latex II	38.0

Binder was subsequently added to the pigment suspensions to generate a range of PVC levels. The initial solids contents of the coating suspensions containing mineral pigments were adjusted to be between 60 to 65-weight%. Plastic pigment coatings were formulated at an initial solids content of 50-weight% for latex I. For coatings prepared with latex II the solids content resulting from mixing the two components – pigment slurry and binder – was used. The relation between pigment volume concentration and weight fraction (based on Equation 18) was calculated for different pigments and summarized in Table 8.

Table 8 *Pigment volume concentrations versus weight fractions*

Density [g/cm^3]				
Binder	Polystyrene Plastic Pigment	Clay Astraplate	$CaCO_3$ Albaglos S	TiO_2
1.00	1.05	2.62	2.71	4.00
Pigment Volume Concentration [%]	Weight Fraction of Binder "pph" [g Latex/100g Pigment]			
90	10.58	4.24	4.10	2.78
80	23.81	9.54	9.23	6.25
70	40.82	16.36	15.81	10.71
60	63.49	25.45	24.60	16.67
50	95.24	38.17	36.90	25.00
40	142.86	57.25	55.35	37.50
30	222.22	89.06	86.10	58.33
20	380.95	152.67	147.60	100.00
10	857.14	343.51	332.10	225.00

4.3 Free Film Preparation Methods

Properties of films are preferably determined on free films, to exclude any influence of a substrate. There exist different methods to prepare free films. The procedures how to obtain free films are limited described in the literature. Yaseen and Ashton (1977) differentiated three types of methods to prepare free films of organic coatings:

- Mercury or metallic surfaces are used as a base substrate that can be amalgamated with mercury (ASTM D 823).
- Water-soluble or water-sensitive materials are used as a substrate:
  e.g. photographic paper-gelatin (method by DBR/NRC laboratory, see Harris, J. (1956) Official Digest. 28(372): 230), methyl cellulose, or cellophane
- Substrates possessing low surface tension
  silicone release agents, polytetrafluoroethylene, PE-coated aluminum foil, PE-foil

It is important that the method of preparation affects the film properties as little as possible. Yaseen and Ashton (1977) analyzed the influence of preparation method on the physical properties (water absorption, water vapor permeation and mechanical properties), and found that mechanical properties were not affected by the method of free film preparation for phenolic varnishes and unpigmented alkyd resins. However, water absorption and permeability of these films depended on the preparation method.

To prepare free coating films alternative methods were evaluated. Coating films below CPVC could be separated from different substrates without too many difficulties. Coatings at high pigment volume concentration were brittle, i.e. the thin films broke easily. In general the films were delicate to handle.

Coating on Mylar@ resulted in a very uniform surface, but thin coating layers could not be peeled off after drying for coating thickness below 500µm. Attempts to isolate films cast on aluminum foil were unsuccessful since adhesion between aluminum foil and coating was too high to peel off the coating layer. Polyethylene-coated aluminum foil was a satisfactory substrate for preparing thin coatings with pigment volume concentration below the critical pigment volume concentration. However, coatings with high pigment volume concentrations were too brittle to be peeled from PE-coated aluminum. The same response occurred when preparing coatings on pure polyethylene foil. Attempts to coat on Teflon@ were not successful due to rapid dewetting of the coating before consolidation could take place. This is due to low surface energy of Teflon".

4.3.1 Cellophane as a Substrate

Cellophane foil was determined to be a good alternative as a base substrate. The material's hydrophilic behavior is similar to that of paper. Different types of cellophane - uncoated and PVdC-lacquered cellophane foil, as well as different grammages -were obtained from UBC (UBC Cellophane Ltd., Bath Road, Bridgewater, Somerset TA6 4PA, UK). The pigmented coatings could not be removed from the PVdC-lacquered cellophane foil. The use of uncoated cellophane foil (300P) with a grammage of 30g/m^2 resulted in excessive curl during the coating and drying process, producing a non-planar film. The cellophane 300P showed with air humidity a strong swelling and shrinking behavior. Immersing the cellophane in water resulted for the length direction in swelling of ca. 2% and shrinkage in cross direction of ca. 10%.

Coating on uncoated cellophane foil, 600P, with a grammage of 60g/m^2 resulted in uniform, flat films with thickness down to 10 µm. This substrate was used to prepare coating films with polystyrene plastic pigment and latex I.

Coatings were drawn down on 60g/m^2 cellophane (600P) using a draw down coater (KCC 303 Control Coater, RK Print-Coat Instruments Ltd., Royston, UK) with wire wound rods. The optimal

size of the cellophane was determined with 8cm in width and 9cm in length. A lager sample size increased curling during the coating process and drying. The coatings then were dried at room temperature and oven cured at 80°C for one minute. For the tensile tests the coated cellophane was cut into sample size, 10mm parallel strips. This coated strips were dipped into water, and the coating could be released from the cellophane due to the effect that cellophane swells by contact with water. Each strip then had to be re-dried under a heating lamp. The dry strips were stored before testing onto a flat Teflon@ surface to smoothen and avoid sticking. This method was rather time consuming, and the reject rate was high (tear by peeling coating from cellophane, curling and sticking together during re-drying, tear by peeling off from Teflon@,...). Additionally it was not known if the contact with water would influence mechanical properties of the investigated coatings. Exploratory tensile tests of films prepared on cellophane and polyester (Figure 30) indicated a lower modulus resulted for the cellophane prepared films. Presumably the use of water to release the coating, and re-drying impacted the mechanical behavior.

4.3.2 Polyester Foil as a Substrate

Another method, based on low surface energy of the substrate was investigated. Therefore different types of polyester films were examined. It was seen that thickness of the substrate is important. From polyester film substrates with thickness above 20µm the coating could not be separated without being damaged. Different polyester films from Dupont® (Melinexe and Mylar@) showed good abilities to remove the coating. The film Melinex® 442/48gauge showed best abilities to release thin coating films. Melinexe HS2/48gauge and Melinex® 800/48gauge were other possible options (48gauge = 12µm).

The best performance separating coating layers over the whole PVC range was observed with another commercial product, a polyester film called “Look! Roasting *film*”, supplied by Terinex Ltd. England, Hammond Road, Elms Estate, Bedford MK41 OND, UK. The polyester film had a thickness of ~13µm. The prepared free coating films showed a constant quality in flatness and

evenness. Therefore this film (Look! Roasting *film*, Terinex Ltd.) was the final solution to the problem of generating thin free films over the PVC range of 0%-90%.

The coating films were prepared by gap application (60µm wet gap size) on a draw down coater (KCC 303 Control Coater, RK Print-Coat Instruments Ltd.) on the film from Terinex Ltd. Coated sample size was 18cm in width, and 30cm to 35cm in length. A minimum of three films was prepared for each pigment volume concentration level. Samples were dried at room temperature over night and oven cured for 1 minute at 80°C. The average final coating film thickness ranged from 25µm to 35µm. Pure latex films and pigment films were prepared with higher thickness (latex: 165µm, pigment: 500µm). The coating films were released from the substrate by peeling the substrate off. A typical sample size for a free coating film would be 10cm in width and 15cm in length. The coating films then were cut into suitable sample size with razor blades (for tensile tests: 10mm width, 70mm length, dynamic mechanical thermal analysis: 5mm width, 35mm length, environmental scanning electron microscope: 5mm width, 70mm length).

4.4 Characterization Techniques of Coating Properties

4.4.1 Coating Weight

The coat weight or grammage of coating is the weight of dry coating per unit area, expressed in g/m^2. Measurements were performed on three samples 5cmX5cm, coated on polyester film (TAPPI Test Methods T410 om-98).

4.4.2 Thickness

Thickness of the coatings applied on the polyester foil was measured on three samples 5cmX5cm (TAPPI Test Methods T-500-98). With grammage and film thickness apparent density was calculated.

$$Density = \frac{Grammage}{Thickness}\left[\frac{g}{m^3}\right] \qquad \textit{Equation 23}$$

Film sample size for mechanical testing, including width and thickness, was measured with a micrometer (Mytutoyo Nr. 293, O-25mm ±0.001 mm, measurement force 5-l ON, Japan).

4.4.3 Void Fraction Measured by Oil Absorption

The porous nature of coatings, especially above the CPVC, is an important component of the coating enhancing optical properties, such as light scattering and opacity. However, more porous coatings show a more brittle behavior. One method to measure porosity is by replacing the air in the voids with oil [Lepoutre and Rezanowich 1977].

Void fraction is the ratio of the volume of air included into the coating to the total volume of the solid components of the coating (Equation 24). The air is replaced by silicone oil (100% Poly(dimethylsiloxane), CAS# 63148-62-9). The difference in weight between voids filled with air and oil is measured, converted into volume fraction by density of coating and silicon oil and the void fraction is calculated. The density of the coating can be determined from the components densities (Table 9). In this calculation total permeability is assumed, and blind voids within the coating matrix are neglected

$$Void\ Fraction = \frac{\frac{M_{Oil}}{\rho_{Oil}}}{\frac{M_{Oil}}{\rho_{Oil}} + \frac{M_{Coating}}{\rho_{Coating}}} \qquad \left[\frac{vol}{vol}\right] \qquad \textit{Equation 24}$$

Table 9 Densities of coating components and silicon oil

Component	Density [g/m^3]
Silicon oil	0.96
Polystyrene plastic pigment (DOW PP 722 HS)	1.05
$CaCO_3$ (Albaglos S)	2.71
Clay (Astraplate)	2.62
Experimental latex I and II	1.00

On three samples with a size of 5cmX5cm the mass of coating was determined, then silicone oil was applied and allowed to soak until the oil fully penetrated. The excess of silicone oil was wiped off. The amount of penetrated oil was determined by weighing and void fraction was calculated.

4.4.4 Gloss

Gloss is the ability of a coating to reflect light specularly and is a partial measure of the surface quality and shiny appearance of coated paper. It was measured at 75" with a Hunter Lab Model D48 on the three samples coated on the polyester film, 5 measurement per sheet (TAPPI Test Methods T480 om-92).

4.4.5 Static Measurements of Mechanical Properties - Tensile Tests

Tensile tests were performed on a conventional mechanical tester, (INSTRON Model No. 5564, Figure 19) to determine elastic modulus, strength and extension to failure. The free coating films were conditioned under 23°C and 50%R.H. for at least 24 hours. The samples were cut into parallel strips (width: 10mm, length: 70mm). The gauge length in the Instron tensile tester was 25mm. Sample thickness was measured with a caliper as described before. For the polystyrene plastic pigment coatings with latex I a minimum of 12 samples were tested for the different pigment volume concentrations.

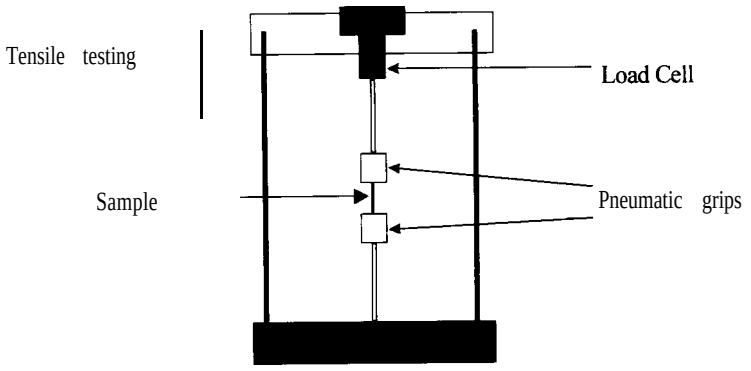

Figure 19 Schematic of a tensile tester [Raman 1997]

A commonly used specimen geometry for tensile tests is a dog-bone shaped specimens (Figure 20). This option to cut dog-bone shaped samples was discarded, as it was not possible to get clean cutting edges with the existing devices and cutting tools.

Figure 20 Dog-bone shaped test specimen

Using parallel strips for tensile test resulted in frequent breaks at the grips. In that case strength of material and strain to failure are not represented absolutely, the determined values are below the material ultimate values.

Tensile tests were performed with a constant crosshead movement rate, ranging from lmm/min to 40mm/min depending on pigment volume concentration. A 100N load cell was used (INSTRON Load Cell Type 2525-807). The cell sensitivity can be seen in Table 10:

Table IO Sensitivity of 1OON load cell (INSTRON, type 2525)

± 0.4% of readings down to 1/10 of capacity
± 0.5% of readings down to 1/100 of capacity
± 1 .O% of readings down to 11250 of capacity

4.4.6 Dynamic Mechanical Thermal Properties

Dynamic mechanical analysis enables simultaneous measurement of elastic and viscous behavior by determining the response of a specimen to periodic deformations or stresses, at varying temperatures. The instrument used (DMTA IV from Rheometrics Scientific, Piscataway, NJ 08854, USA) is a forced resonance analyzer, with linear vertical displacement transducers to determine the probe position. Tests were performed in tensile mode (Figure 21). The test dimensions were 5mm in width with a gauge length of 10mm (total specimen length was 30mm).

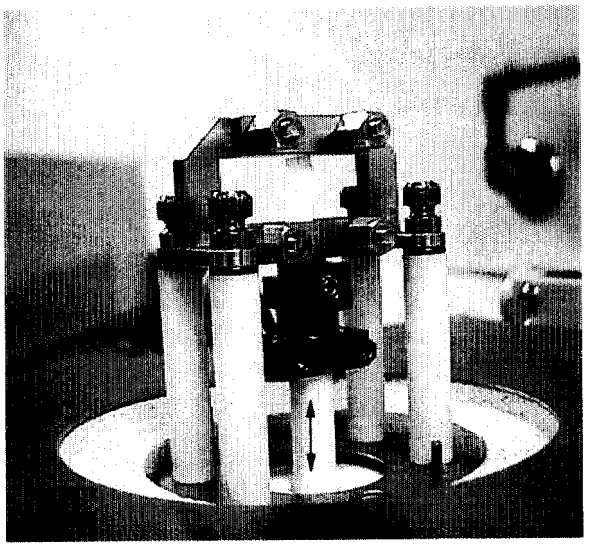

Figure 21 Tensile stage of Dynamic Mechanical Thermal Analyzer, DMTA IV from Rheometrics Scientific

Since the testing mode was tensile, a static tensile strain larger then the cyclic strain amplitude has to be superimposed in order to prevent buckling during a periodic cycle. Therefore, some degree of stress relaxation takes place in viscoelastic materials in addition to the oscillating deformation (Figure 22). The static force for all measurements was chosen to be 20% larger then the force necessary for the applied oscillating strain amplitude. All tests were performed in strain-controlled mode.

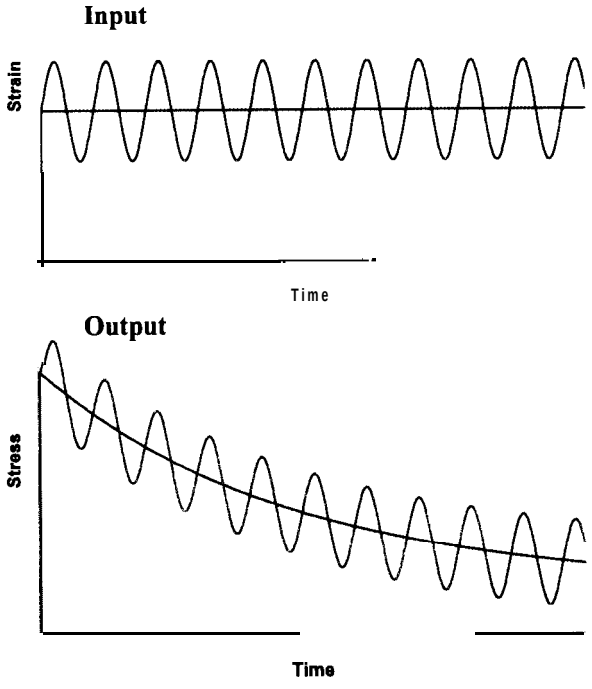

Stress relaxation for oscillating strain

Several factors may influence the results of dynamic mechanical analysis, for example mechanical inertia, thermal lag, scanning rate, specimen size, position in the analyzer, and clamping effects. Since different analyzers often have different sample chamber geometry, factors such as the heat conductivity of the specimen, the sample clamping arrangement, and the environment may become important for temperature accuracy [Hagen et *al.* 1994].

Clamping pressure was selected to be $8*10^{-2}$Nm. A higher clamping pressure increased breakage during testing, clamping pressure below $4*10^{-2}$Nm did not provide sufficient grip, as evidenced by material slippage.

The experiments performed can be grouped as dynamic stress-strain curves, temperature-time studies and frequency studies. The linear viscoelastic region of the pigmented coatings was determined by strain scans, where the strain amplitude increased proportionally with the increase of applied static force. The obtained results were used to select the initial static force and strain amplitudes for all subsequent experiments. High pigment volume concentration samples exhibited a linear viscoelastic behavior, whereas samples below the critical pigment volume concentration did not show a linear viscoelastic behavior in the tested strain range. To minimize the error due to nonlinear material response, the applied load and strain ranges were selected in the lower range of measurable response. For all tests the initial static force was 0.01N (Figure 23). For frequency scans a strain amplitude of 0.00255% was chosen, which is the minimum strain amplitude to be measured by the instrument. For temperature scans, the strain amplitude was set to 0.05%, with the exception of pure pigment samples, which were tested at a strain amplitude of 0.01%.

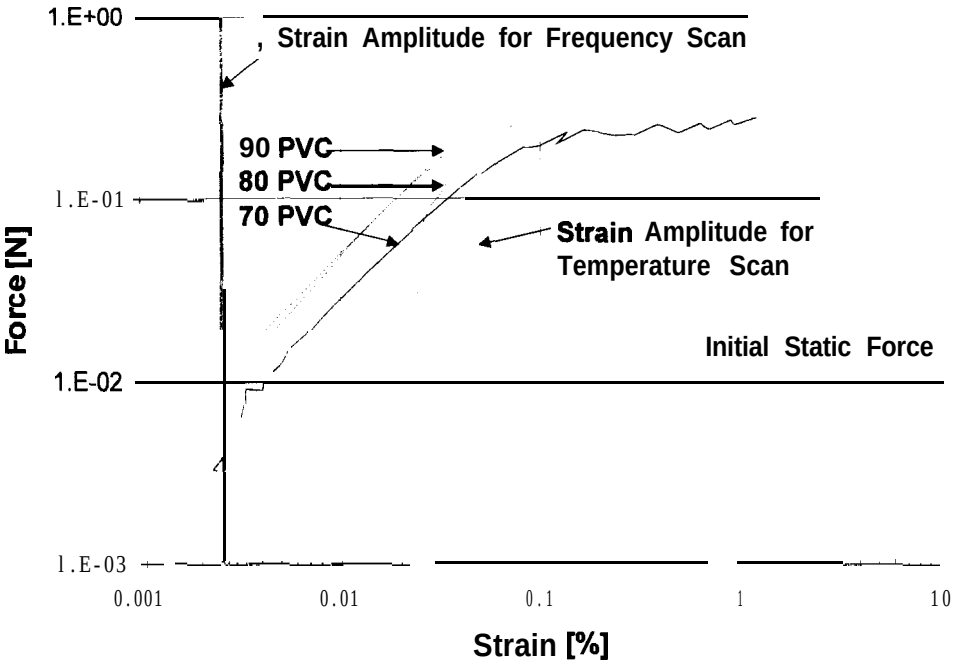

Figure 23 Strain scans performed on $CaCO_3$ and latex I coatings at 90%. 80% and 70% pigment volume concentration; the measurement parameters, initial static force, and strain amplitudes for temperature andfrequency scans are indicated

Temperature scans were performed in the range of -50°C (well below the glass transition temperature of the latex polymer), to +150°C (above the glass transition temperature of the polystyrene plastic pigment), using a heating rate of 1°C/min. A sinusoidal varying strain with amplitude of ±0.05%, or ±0.01% was applied at a frequency of 1 Hz. A minimum of at least two samples was tested for each pigmentation level.

The dynamic nature of the calendering or printing processes imposes short duration events on coatings and coated paper. The behavior for such short time scales can be predicted by applying time-temperature superposition (Equation 13 to 15, page 10). Frequency scans were performed from 0.1 Hz up to 100Hz, while temperature levels reached from -15°C up to 80°C in intervals of 5°C. This resulted in a final time scale from 10^{-12}Hz to 10^{9} Hz (using Universal Constants for the Williams-Landel-Ferry Theory). The master curves were calculated at a reference temperature of

0°C. From each pigmentation level were two master curves determined. The glass transition temperature of the latex, determined by dynamic scanning calorimetry, was used for calculating the shift factor. For the coatings with polystyrene pigment, the glass transition temperature of the pigment was neglected based on the assumption that for the tested temperature levels the pigment does not undergo any structure changes and behaves as rigid spheres.

4.4.7 Micro Structural Analysis – Surface Analysis

The sample surface morphology and microscopic mechanical properties were investigated with an Environmental Scanning Electron Microscope (ESEM) Model E-3 from Philips ElectroScan. A basic diagram of the ESEM is shown in Figure 24. The advantage of using an ESEM is that samples can be observed at different pressures, and samples can be viewed in their natural state. No complicated specimen preparation such as dehydration or conductive coating is necessary. This was essential for imaging the samples within the tensile stage. For surface analysis the samples partly were sputter coated with a 20nm gold layer for imaging to enhances the image quality. The sputter coater was a Hummer VI-A from Anatech Ltd., Alexandria, VA.

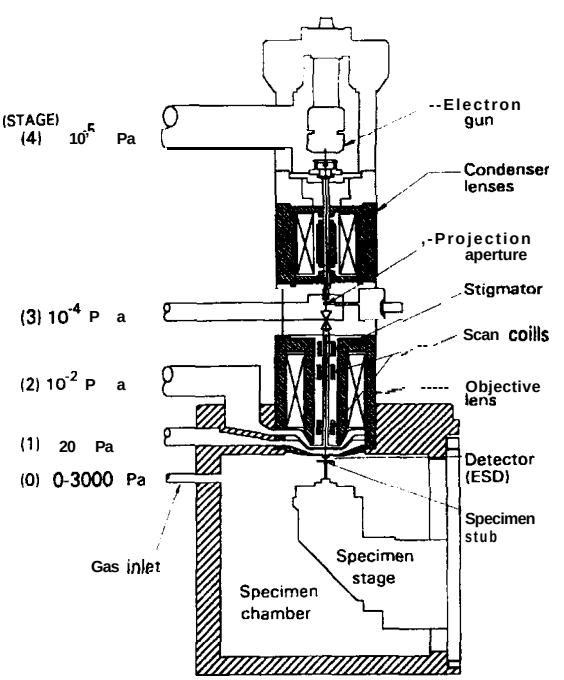

Figure 24 Schematic diagram of Electroscan ESEM [Danilatos, 1980]

All images were obtained with a secondary electron detector (ESD). In a secondary electron detector the secondary electrons – inelastically scattered electrons with low energies typically under 50eV – are collected. The gathered image gives information about surface topography.

4.4.8 Micro Structural Analysis – Strain Mapping

For tensile testing in the Environmental Scanning Electron Microscope a micro-mechanical tensile stage was used (Figure 25). The stage was originally provided by ElectroScan and subsequently modified by Shaler et *al*. (1995). The stage had a dual crosshead movement in order to keep the area of interest centered on the viewing monitor while load was applied.

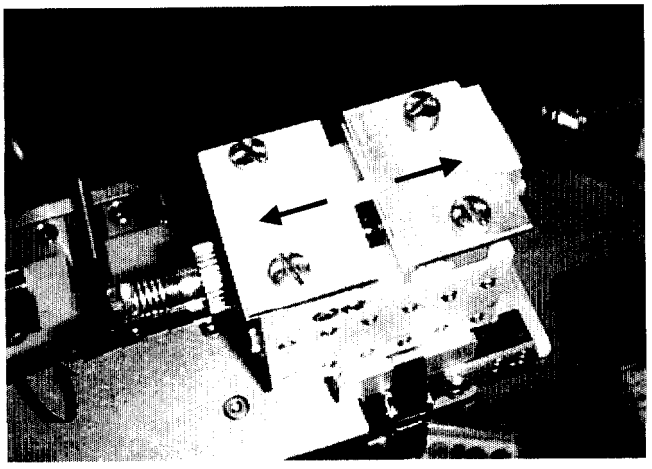

Figure 25 Microtensile stage for Environmental Scanning Electron Microscope

The samples had 5mm in width, and 40mm length. The gauge length was 5mm; the elongation rate in the tensile stage was constant with 1µm/s. Micrographs were taken at increasing elongation rates (every 10s). An image analysis program "Sherlock" was used to trace displacement of pigment particles.

5 Physical Properties

The effect of pigment volume concentration on the physical properties was determined by measurements of gloss, void fraction and determination of density.

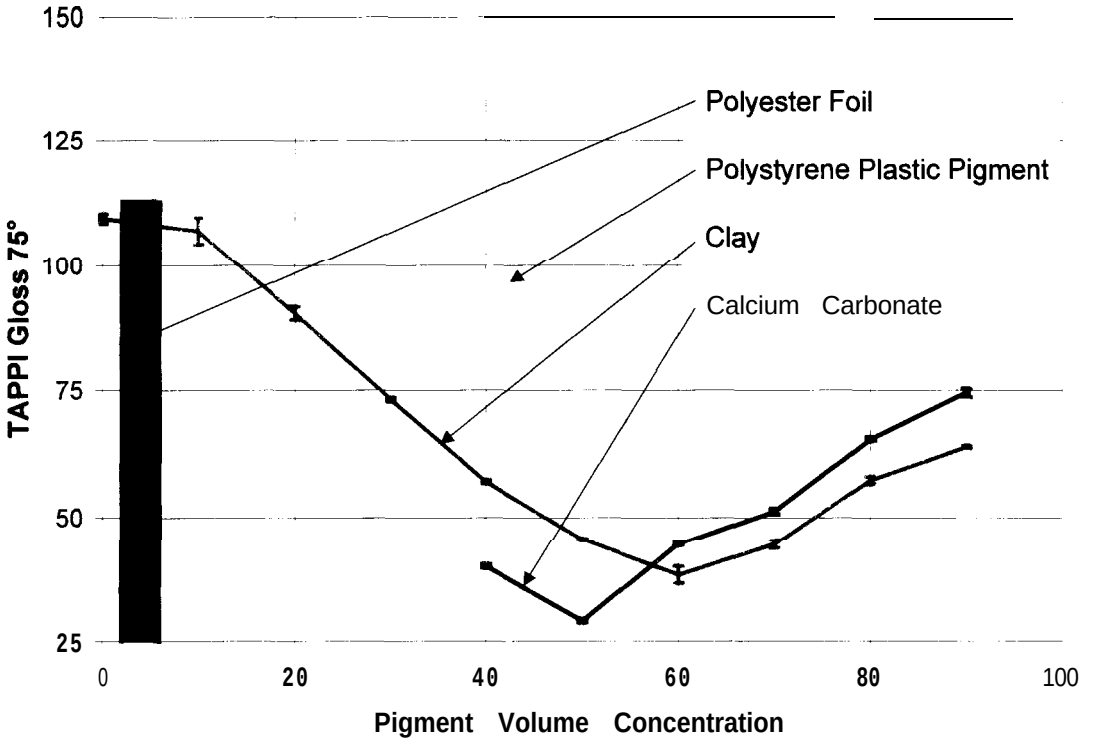

***Figure 26** Influence of **pigment volume concentration on** gloss for **the three different pigment types, polystyrene plastic pigment,** clay, **and calcium carbonate with experimental latex I; samples** coated on polyester film*

Figure 26 shows the change in gloss over the pigment volume concentration range for the three different pigment types. The gloss of the polyester film **was** measured slightly higher than the gloss observed for the pure latex film coated on polyester. For polystyrene pigment, the gloss with 10% pigment volume concentration was much higher than for the pure latex film. Below the critical pigment volume concentration the gloss **was** highest with plastic pigment. Gloss

decreased for all three pigments with increasing pigmentation level, and gloss reached a minimum, which indicated the critical pigment volume concentration for the three different pigments. For the calcium carbonate the minimum was seen at around 50% PVC, for clay around 60% PVC, and for the polystyrene plastic pigment the minimum occurred around 70%PVC. Above the critical pigment volume concentration the increase in gloss occurred with calcium carbonate more rapid.

Table 11 Comparison of gloss for the two different latices and clay pigment

PVC [%]	Clay, Latex I	Clay, Latex II
90	64.0 ±0.23	62.7 ±0.37
80	57.5 ±0.78	57.6 ±0.43
70	44.7 ±0.87	48.0 ±0.46

For 90% PVC, the clay pigment and latex I showed a slightly higher gloss. For 80% PVC, latex I and II showed equal gloss values, where at 70% PVC the clay-coating with latex II had a gloss three points higher (Table 11).

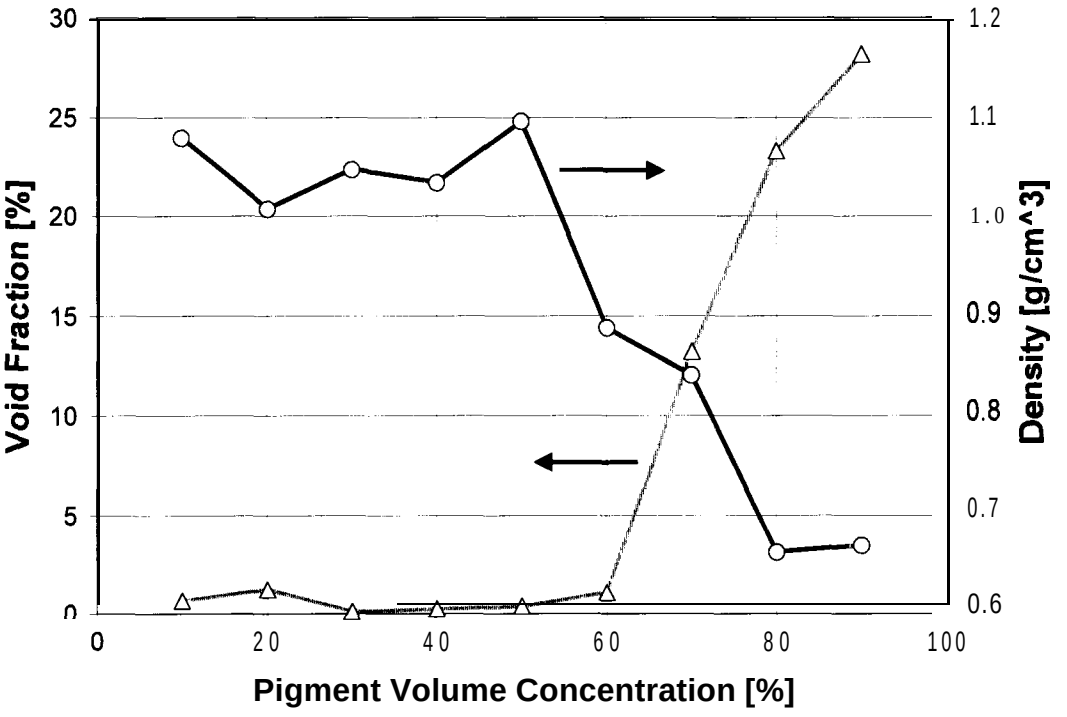

Figure 27 Void fraction and density of polystyrene plastic pigment and latex I coatings with increase in pigment volume concentration

Permeability and void fraction increased with increasing pigment volume concentration. Density showed the opposite behavior of the void fraction. The region of rapid change was designated to indicate the critical pigment volume concentration (Figure 27).

6 Macroscopic Mechanical Properties – Static Measurements

Static mechanical tests were performed on polystyrene plastic pigment coatings prepared with latex I. The influence of film preparation technique was investigated by comparing coatings with 40% PVC (below the CPVC) and 60% PVC (above CPVC) prepared on the two different substrates, cellophane and polyester foil. The influence of the pigmentation level on Young's modulus was determined. The materials' viscoelastic behavior was examined by testing 40% PVC coatings at varying deformation speeds (1 Omm/min and 15mm/min).

The stress-strain curves for the range from 20% to 90% pigment volume concentration are presented in Figure 28. The absolute values for stress and strain to failure are not representative values due to the fact that most samples broke at the grips. But a general trend still can be estimated from the diagrams. Tensile strength increased with increasing pigment volume concentration, reaching a maximum around 50% to 60% PVC, the critical pigment volume concentration region, and decreasing then rapidly. The strain to failure exhibited a decrease with increasing pigment volume concentration (Figure 28 and Figure 29). This has been observed before, and is well established in the literature [Schaller 1968, Raman 1997].

Different crosshead rates were used in order to keep measurement time within 1 minute. An increase in strain rate increases elastic modulus of viscoelastic materials. The deformation speeds ranged from 1 mm/min to 40mm/min.

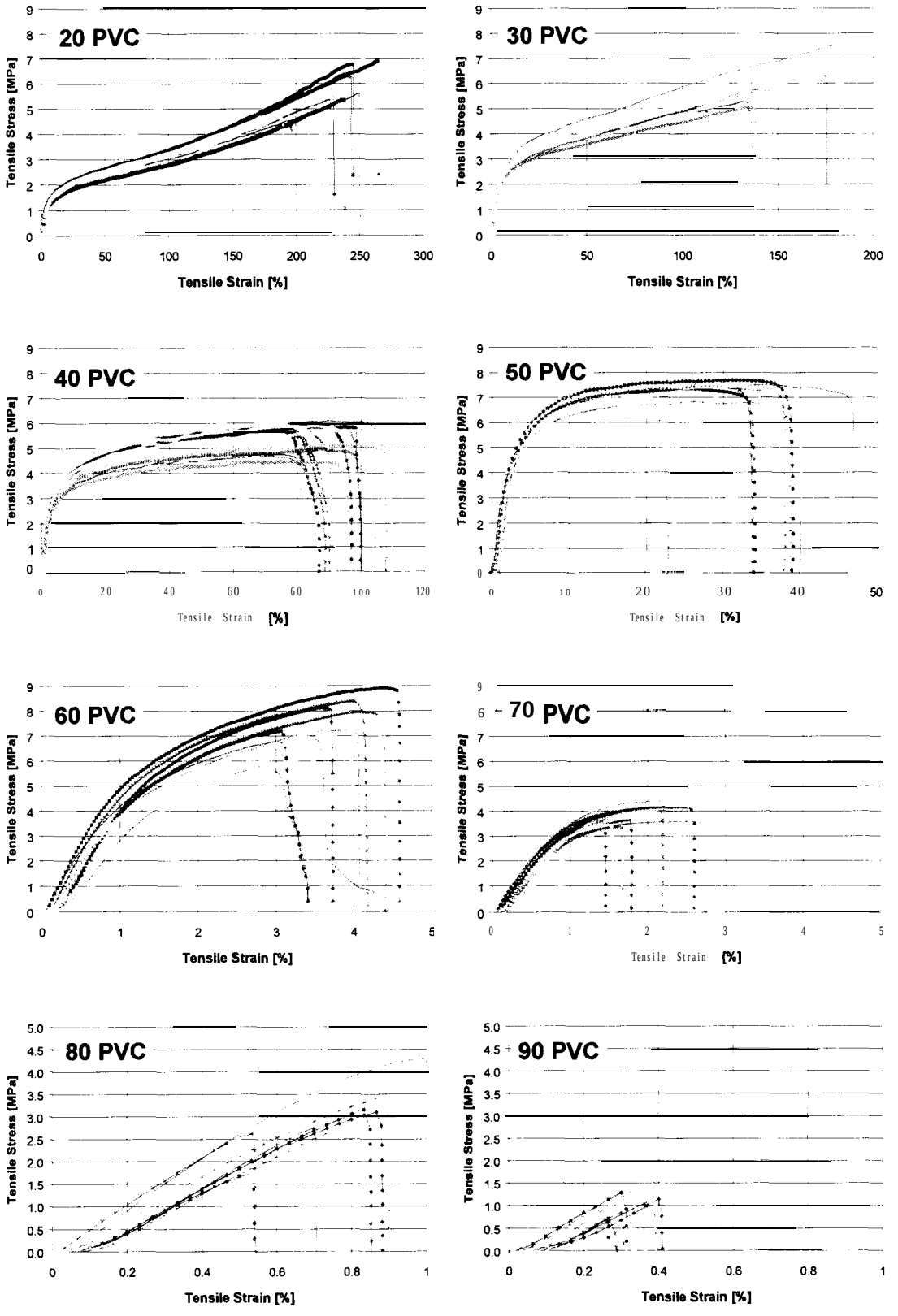

Figure 28 Stress-strain diagrams for coatings with polystyrene plastic pigment and latex I

The Young's modulus increased with increasing pigment volume concentration (Table 12 and Figure 30). Around the critical pigment volume concentration, a rapid increase in the elastic modulus was observed. Above the critical pigment volume concentration the elastic modulus leveled off. Experimental scatter occurred due to inhomogeneity of the films, and is not high for mechanical testing. Different crosshead rates were used for different pigment volume concentration levels. The use of a single crosshead rate for all tests would have created an even larger disparity in elastic modulus with change in pigment volume concentration.

Table 12 ***Young's modulus for coatings with polystyrene plastic pigment and latex I at different pigment volume concentrations, varying crosshead speed.***

Pigment Volume Concentration [%]	Testing Speed [mm/min]	Elastic Modulus [MPa]	Coefficient of Variation [%] (Number of tested samples)
90	1	496	8.1 (13)
80	1	534	12.4 (15)
70	1	445	8.8 (15)
60	1	468	14.4 (14)
50	15	122	13.3 (15)
40	15	26	23.2 (19)
30	40	8	12.8 (14)
20	40	4	11.9 (12)

Comparing the influence of film preparation methods with cellophane and polyester foil on the mechanical properties showed lower storage moduli for the samples prepared with cellophane (Figure 30). This might be due to the influence of the water used to separate the coatings from the cellophane. Stresses due to swelling are implied onto the coatings. The strain was observed to be slightly higher for samples prepared on cellophane (Figure 29).

Yaseen and Ashton (1977) compared different film preparation possibilities and found no significant influence on mechanical properties. But performance of permeability and absorption of phenolic varnishes and unpigmented alkyd resins depended on film preparation mode.

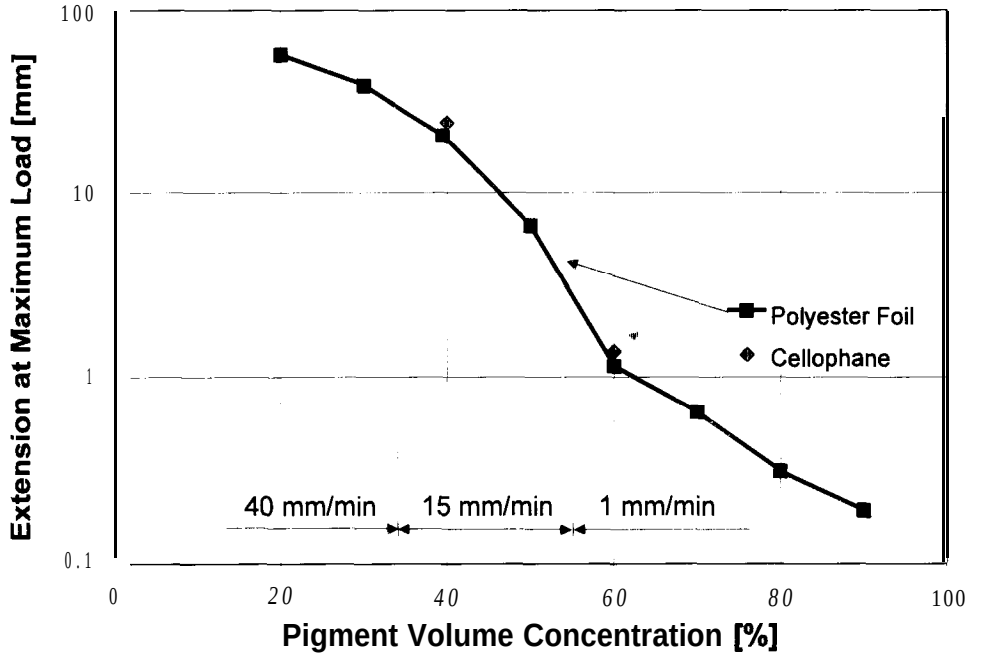

Figure 29 Change of the extension at maximum load with increasing pigment volume concentration for plastic pigment and experimental latex I, both preparation methods: cellophane and polyester foil

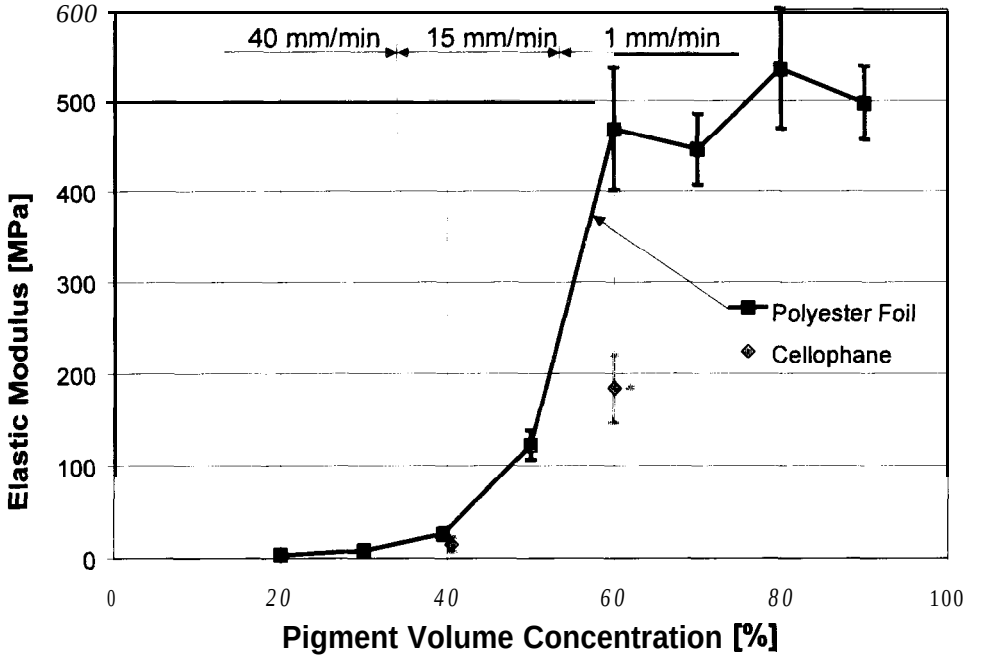

Figure 30 Change of elastic modulus with pigment volume concentration for plastic pigment and experimental latex I, presenting both preparation method: cellophane and polyester foil

The viscoelastic behavior of the coating is demonstrated on a 40% PVC polystyrene plastic pigment and latex I coating (Figure 31). The tensile tests were performed with two different crosshead speeds, 10mm/min and 15mm/min. The increase in testing speed resulted in a lower strain to failure, a higher Young modulus and a higher tensile strength.

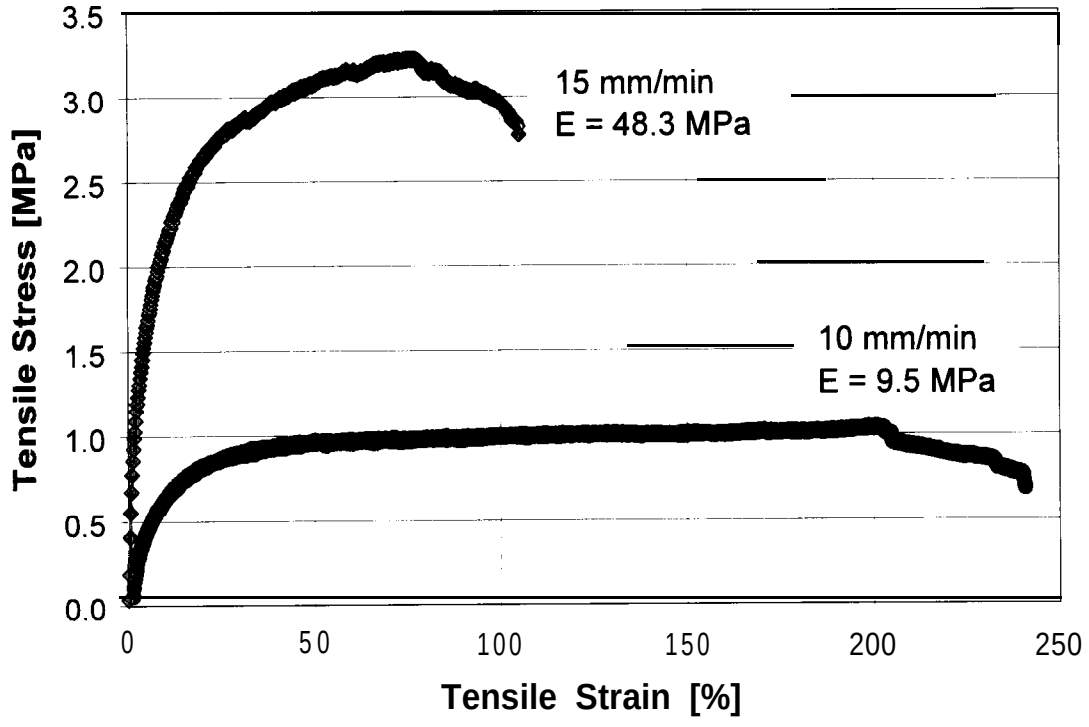

Figure 31 ***Influence of crosshead speed (10mm/min and 15mm/min) on material behavior for a polystyrene plastic pigment coating with latex I at 40% pigment volume concentration***

Over the pigment volume concentration range, three different regions have to be differentiated and analyzed: below CPVC, CPVC region, and above CPVC. Below the CPVC region the coatings behave as a filled polymeric system. The incorporation of a rigid pigment in the binder matrix improves mechanical properties. Tensile stress and elastic modulus increase with increasing pigment volume concentration, strain to failure decreases. The Rule of Mixtures gives good estimations in this region.

As the pigment volume concentration is increased it reaches the CPVC region. Properties change rapidly, The tensile strength reaches a maximum; the elastic modulus shows a rapid increase.

Above the CPVC region, as the pigment volume concentration increases, the amount of binder available to keep the pigments together is decreasing, and the bonding between the pigment particles is diminishing. Due to the porous structure the tensile strain is reducing and mechanical strength is decreasing. The elastic modulus had reached a maximum at CPVC and did not exhibit any significant change with increasing PVC.

The highly viscoelastic behavior observed, led to further investigations with a dynamic mechanical thermal analyzer, and time-temperature dependent behavior of the pigmented coatings could be obtained.

7 Viscoelastic Properties by Dynamic Mechanical Thermal Analysis

During the static tests a strong viscoelastic material behavior was observed. Dynamic mechanical thermal experiments in tensile mode were conducted to describe the material behavior over a wide range of temperature and time.

7.1 Effect of PVC on Different Pigment Types

The time and temperature dependencies of storage modulus (E') and loss modulus (E") for coatings with varying pigment volume concentration were obtained for coatings with calcium carbonate (Figure 32), polystyrene plastic pigment (latex I: Figure 39 and latex II: Figure 62) and clay (latex I: Figure 50 and latex II: Figure 64). The introduction of rigid particles, the pigments, into a soft matrix, the binder, is typically associated with an increase in modulus (Agarwal and Broutman 1980). It is well known that for viscoelastic materials the storage modulus diminishes rapidly during glass transition region. Therefore, the influence of pigmentation on the

a) moduli in glassy state,

b) moduli during glass transition, and

c) moduli in rubbery state,

was analyzed for the different pigments. Master curves describing the time behavior of viscoelastic coatings were calculated from frequency scans by applying time-temperature superposition and WLF-theory according to Equations 13 to 15. That enables the prediction of a material's behavior for different time scales beyond those easily experimental attainable.

7.1.1 Effect of Pigment Volume Concentration for Calcium Carbonate Pigment and Latex I – Temperature Dependency

Coatings containing the calcium carbonate pigment (Figure 32) performed over a wide PVC range in a typical viscoelastic manner. At low temperatures, the storage modulus was constant with temperature, during glass transition region the storage modulus decreases, where loss modulus reaches a maximum. Introducing calcium carbonate pigment into the binder matrix resulted for all pigment volume concentrations over the measured temperature range in higher storage moduli then for the pure latex sample.

Below the latex glass transition temperature, storage modulus showed a glassy behavior and no dependence of temperature. The storage modulus increased from ca. 2GPa (pure latex) to ca. 7GPa (80% pigment volume concentration). The differences seen in Figure 32 between coatings formulated at 70%, 80%, and 90% pigment volume concentration were not significant in this temperature range, repeated measurements exhibited values within the range of 6GPa to 7GPa for those pigment volume concentrations.

Within the glass transition region (0°C to 25°C), the storage modulus decreased rapidly, the elastic behavior becomes dominated by viscous behavior. An increase in pigmentation level resulted in a suppression of softening behavior (Figure 32 to Figure 34). It is also important to know if and how the glass transition temperature is modified by incorporation of a pigment. The peaks in loss modulus and tan Delta were reached at higher temperatures with increasing pigmentation levels until 70% PVC, above 70% PVC the temperature decreased again (Figure 33 and Figure 34). Therefore, a maximum in glass transition temperature of the coatings determined by dynamic mechanical thermal analysis was reached at 70% PVC. Touissant stated in 1973/1974, that if the glass transition temperature of the polymer lies below ambient temperature, an increase in pigment volume concentration will be observed due to restricted segment mobility

of the latex, or in the opposite case of a glass transition temperature above ambient temperature, a decrease will be observed.

Above glass transition temperature the coating behavior changed with increasing pigment volume concentration from rubbery to glassy behavior. A significant separation between the different pigment volume concentration levels was observed (90% PVC ~4GPa, 80% PVC ~3GPa, 70% PVC -2GPa. 60% PVC ~1GPa, 50% PVC ~0.7GPa).

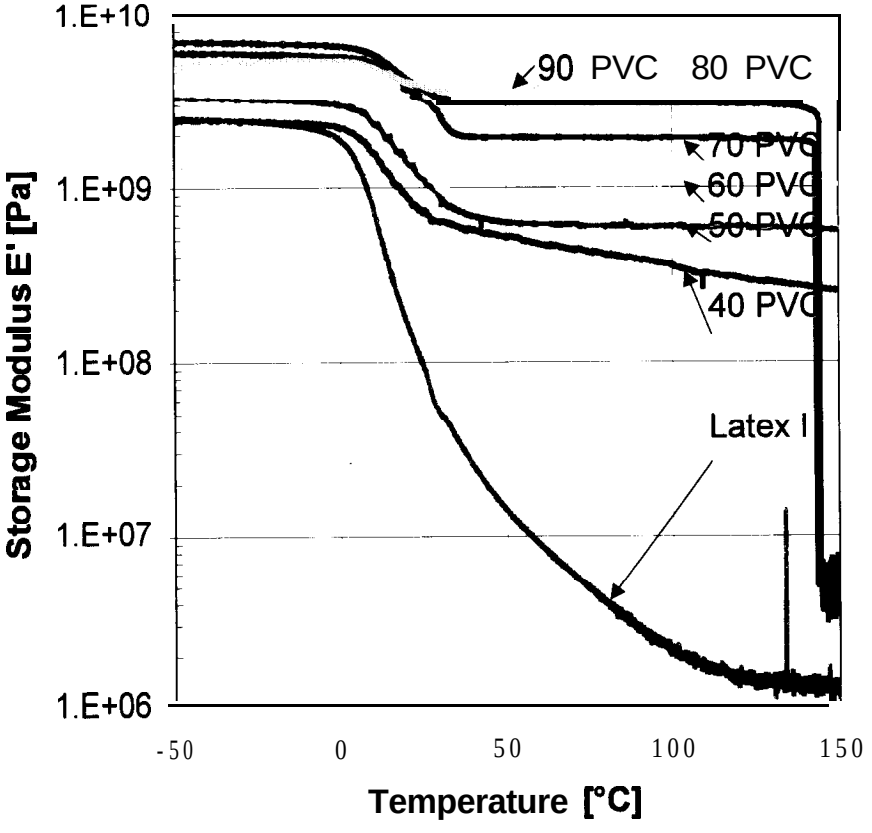

Figure 32 Storage modulus versus temperature for latex I and calcium carbonate coatings at different pigment volume concentrations.

For pigment volume concentrations above 60% pigment volume concentration, a failure or sudden drop occurred in storage modulus at temperatures around 145°C (70% PVC, 80% PVC) and 155°C (90% PVC). This might be a result of latex flow at higher temperatures.

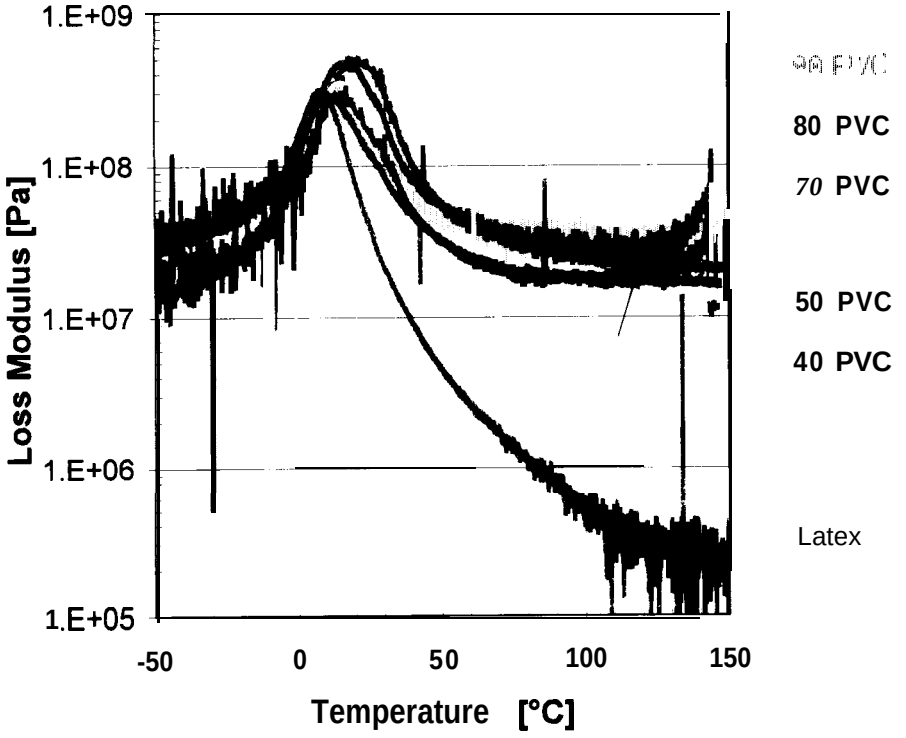

Figure 33 Loss modulus versus temperature for latex I and calcium carbonate coatings at different pigment volume concentrations.

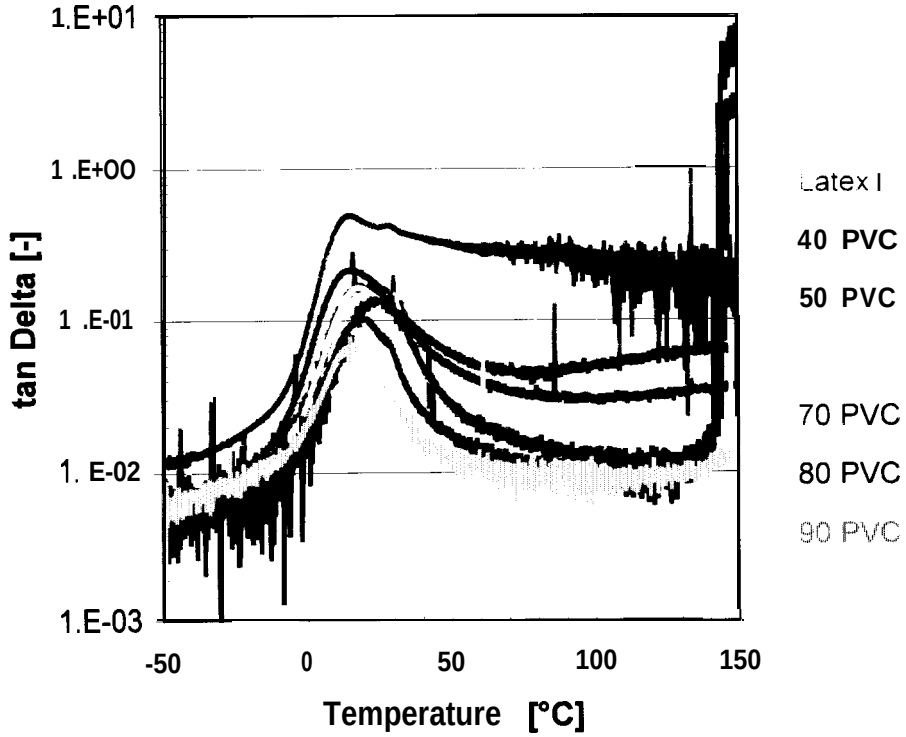

Figure 34 tan Delta versus temperature for latex I and calcium carbonate coatings at different pigment volume concentrations

Attempts to evaluate pure calcium carbonate samples by dynamical tensile tests were unsuccessful due to the brittle nature of the samples. Performing a facile extrapolation, the storage modulus of pure calcium carbonate was estimated to be approximately 8GPa, loss modulus to be approximately 70MPa, and both independent of temperature in the chosen range of -50°C to +150°C.

The applicability of classical composite theories was investigated in order to illustrate to what extent a prediction of the composite behavior is possible knowing the mechanical properties of the pure components, pigment and latex. The actual measured material behavior was compared to Rule of Mixture (Equation 19), Transverse Rule of Mixture (Equation 20) and Halpin-Tsai equation for spherical particles (Equation 21 and Equation 22). As input for the equations, the moduli of pigment and matrix are required at the specified temperature level, as well as the corresponding respective volume fractions. The curves were calculated at four different temperature levels (-20°C, 0°C, 20°C and 80°C), for storage modulus, loss modulus, tan Delta and complex modulus (only for polystyrene plastic pigment coatings and clay coatings).

Figure 36 and Figure 37 show the comparison between average of moduli and tan Delta values obtained from experiments (2 to 8 measurements) and those calculated by the different composite theories, using the estimated values for storage and loss modulus for calcium carbonate (E'=8GPa, E"=70MPa). Over the whole temperature range, the experimental obtained values never followed only one of the different rules over the pigment volume concentrations. For the storage modulus a change in mixture behavior with temperature was observed. Experimental values at -20°C were below the Transverse Rule of Mixture, at 0°C the Transverse Rule of Mixture predicted the storage modulus quite well. With increase in temperature the mixture behavior of storage modulus was measured within the limits of Halpin-Tsai Equation and Rule of Mixture.

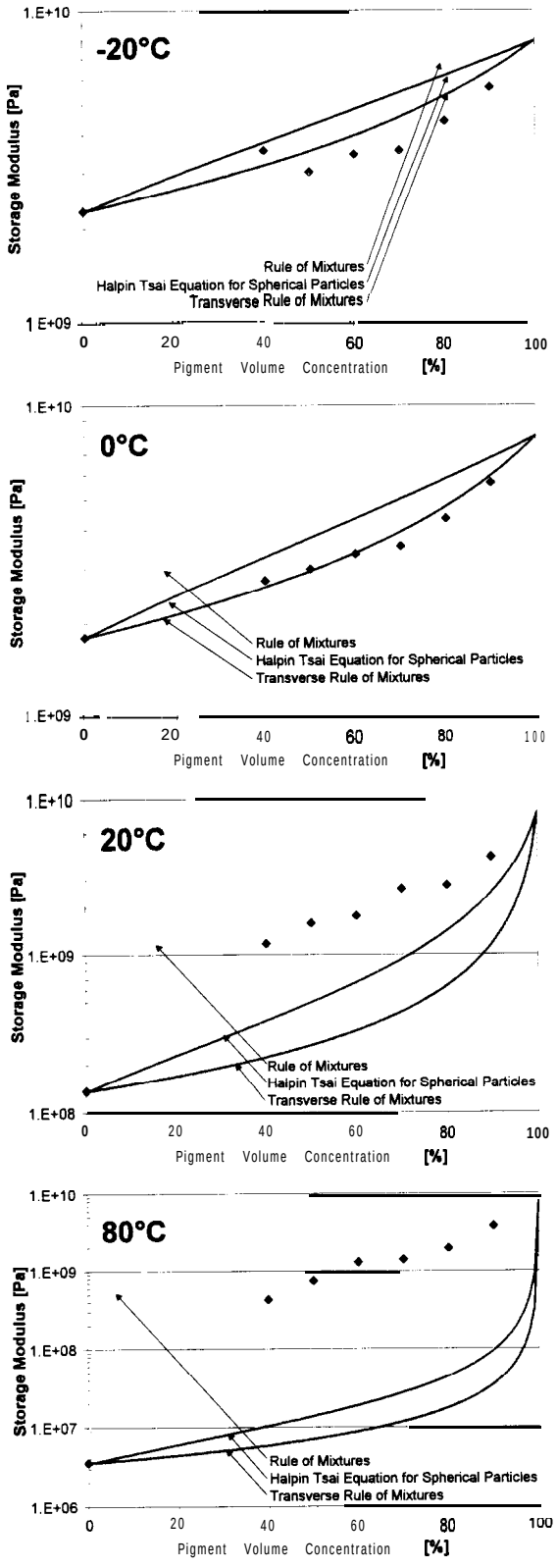

Figure 35 Comparison Rule** of **Mixtures,** Halpin **Tsai Equation** for **spherical particles, and Transverse Rule** of **Mixtures** for **storage** for **coatings with latex I and calcium carbonate at** different **temperature levels (0 = experimental values)

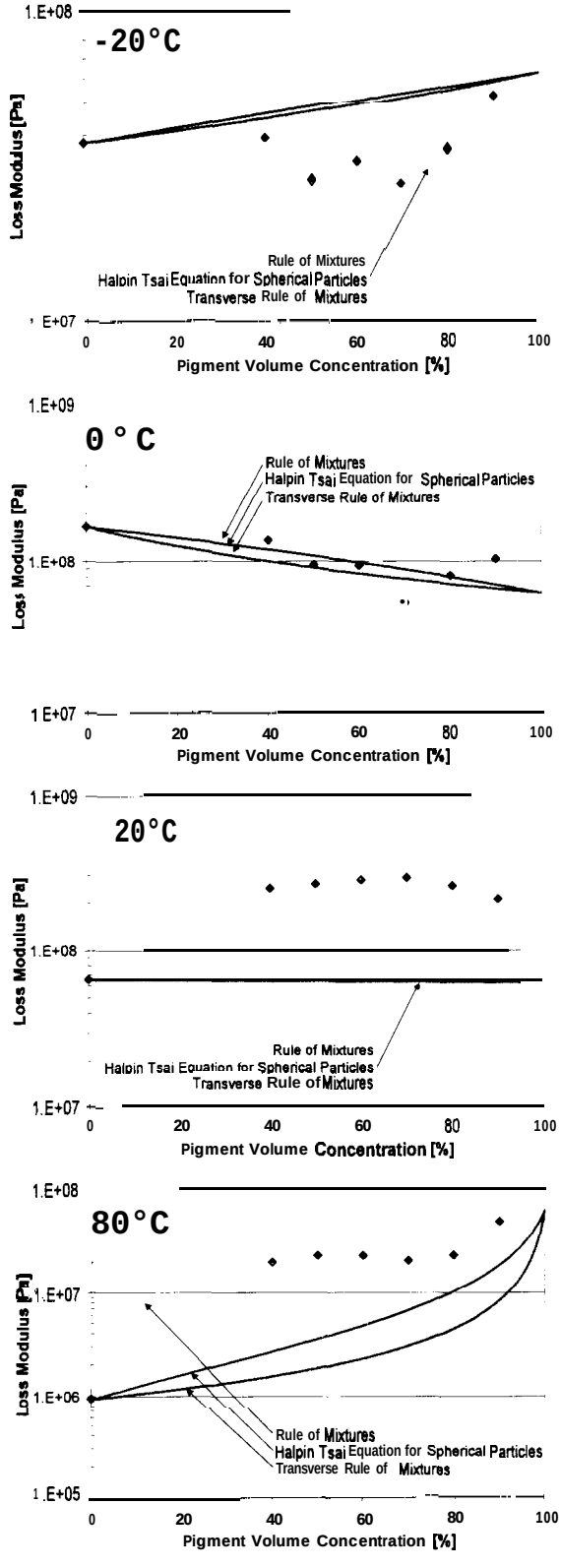

Figure 36 Comparison Rule of Mixtures, Halpin Tsai Equation for spherical particles, and Transverse Rule of Mixtures loss moduli for coatings with latex I and calcium carbonate at different temperature levels (0 = experimental values)

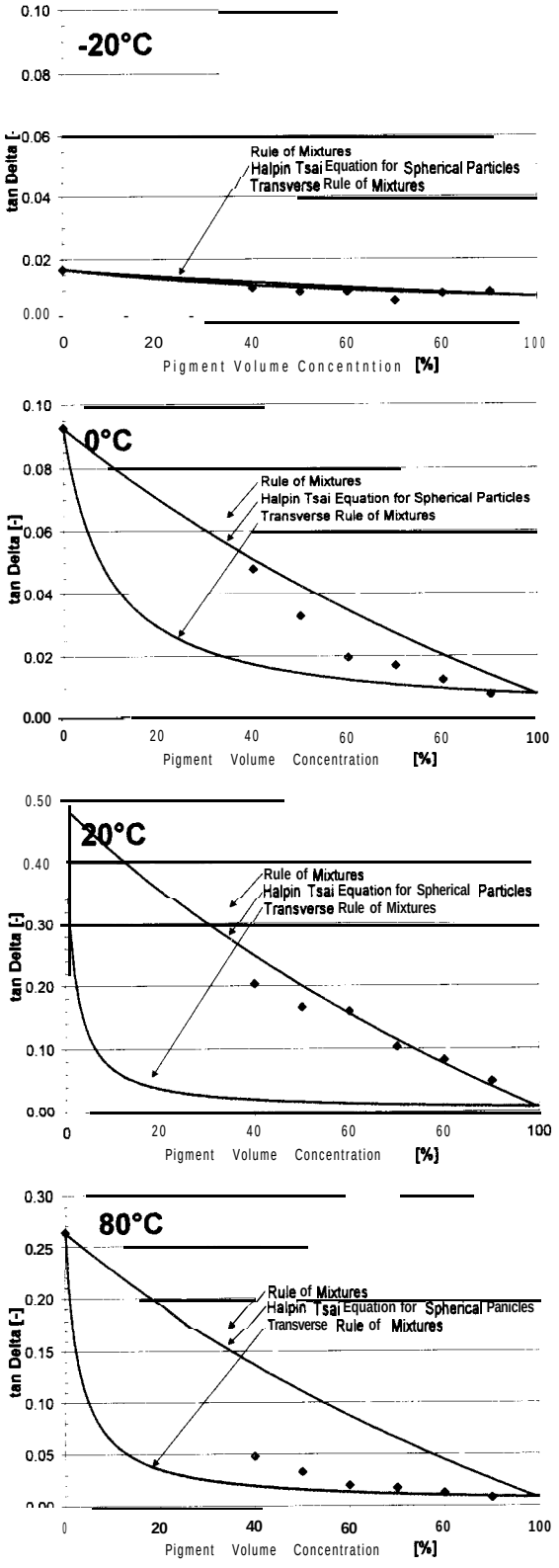

Figure 37 Comparison Rule** of **Mixtures,** Halpin **Tsai Equation** for **spherical particles, and Transverse Rule** of **Mixtures** for **tan Delta** for **coatings with latex I and calcium carbonate at** different **temperature levels (0 = experimental values)

The different composite theories did not give good predictions for the loss modulus below glass transition temperature. Around the glass transition region (0°C and 20°C) the assumed loss modulus of calcium carbonate was close or smaller then the loss modulus of the latex at the equivalent temperatures. For 0°C, prediction was possible, where for 20°C the measured loss moduli were completely out of range. For higher temperatures, at 80°C, the Rule of Mixtures was a relatively good predictor for the loss modulus.

For tan Delta, the Transverse Rule, and Rule of Mixtures built an lower and upper boundary, and tan Delta was measured over the whole temperature range within those limits (Figure 37). For 20°C the Halpin-Tsai equation showed a good prediction for tan Delta, for 80°C the Transverse Rule of mixtures fitted well in the high PVC range.

7.1.2 Effect of Pigment Volume Concentration for Calcium Carbonate Pigment and Latex I – Time Dependency

The master curves shown in Figure 38 are calculated at 0°C, by applying time-temperature superposition, WLF-theory and using the Universal Constants. Each frequency scan is represented by three points, the median of 20 values, in order to reduce the amount of data.

At frequencies above 1 Hz, the storage moduli of calcium carbonate coatings were independent of frequency (strain rates) irrespective of pigment volume concentration. This essentially elastic behavior showed material's storage moduli ranging from 1.5GPa (pure latex I) to 5GPa (90% PVC). For coatings with 90% pigment volume concentration, the storage modulus was nearly independent for the frequency range from 10^{-9}Hz to 10^{+9}Hz. For pigment volume concentrations below 90% PVC, with increasing frequency (strain rate) major changes in storage modulus occurred at frequencies of 10^{-6}Hz to 1Hz. This frequency range corresponded with the transition region observed around the glass transition temperature of the latex. Below the

frequency of 10^{-4}Hz the behavior of latex changed to a highly viscous character (high dependency of strain rate). The addition of pigment reduced the rate of change in storage modulus and frequency (strain rate) dependence changed. With higher pigmentation level the storage modulus showed an increasing elastic behavior in the frequency range from 10^{-9}Hz to 10^{-6}Hz. In summary, an increase in pigment volume concentration resulted in and predicted an increase of storage modulus for long-term as well as short-term behavior.

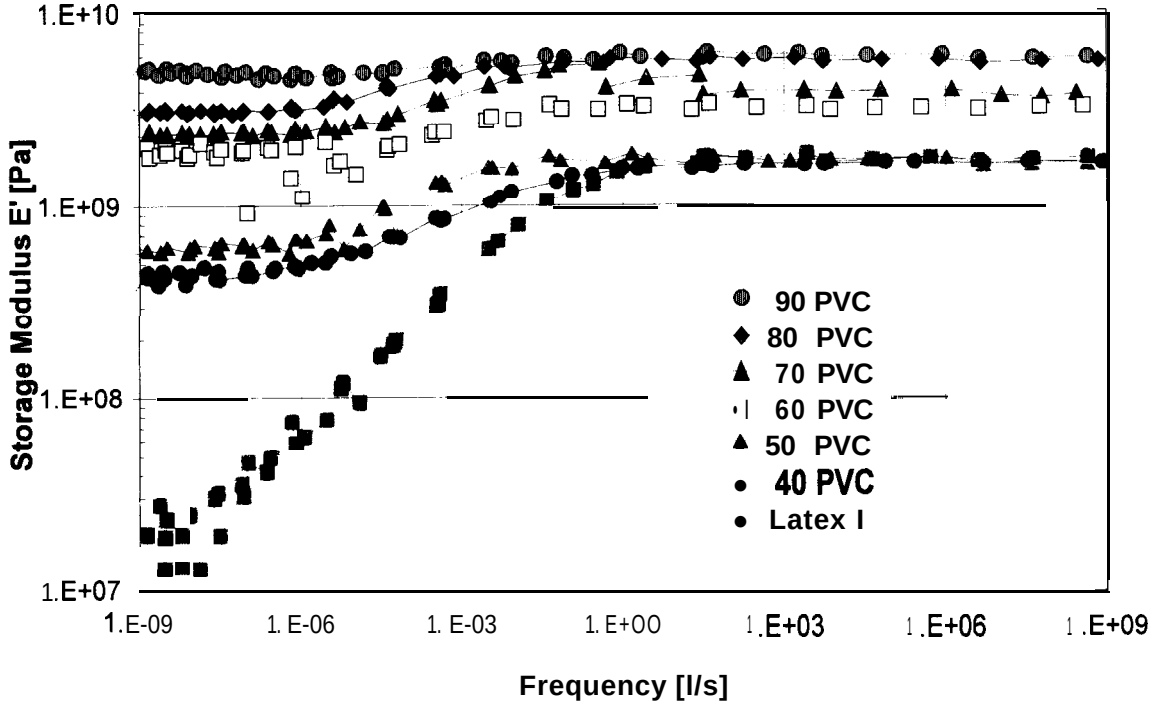

Figure 38 Master curves of storage modulus calculated at 0°C with Universal Constants, for calcium carbonate pigment and latex I coatings at different pigment volume concentrations

7.1.3 Effect of Pigment Volume Concentration for Polystyrene Plastic Pigment and Latex I – Temperature Dependency

The temperature dependence of polystyrene plastic pigment and latex I coatings for varying pigment volume concentration was measured. The polystyrene plastic pigment coatings performed different form the calcium carbonate coatings in several ways. The polystyrene plastic

pigment is a polymeric material with a glass transition temperature. Therefore, for the coatings two different transition zones could be observed (latex I, Figure 39 and latex II, Figure 62). The first occurred around the glass transition temperature of the latex ("soft phase", T_g~0°C) and the second at the glass transition temperature of the polystyrene pigment ("hard phase", T_g~105°C). Below the glass transition temperature of the latex, the storage modulus of the latex (E'~2.5GPa) was actually higher then the modulus of the pure polystyrene pigment (E'~0.6GPa). Thus the addition of polystyrene pigment did not have a reinforcing effect in this temperature regime. In the temperature range above the latex glass transition temperature and below the pigment glass transition temperature, however the addition of pigment did create a reinforcing effect (1.8MPa, pure latex I, and 0.3MPa, pure latex II to 0.4GPa, pure pigment, at 110°C). As during this temperature range the polystyrene plastic pigment had a higher storage modulus then the latex I. For increasing pigment volume concentrations, a suppression of the transition zone around the latex glass transition temperature could be observed, and above the latex glass transition temperature the film response was dominated by the properties of the polystyrene pigment. Above the glass transition of the pigment (>11 5°C), differences in storage modulus of the coating films were not strongly influenced by the pigment volume concentration level. Overall the storage moduli of the pigmented polystyrene plastic pigment coatings were observed to be about one decade lower than the storage moduli measured for calcium carbonate coatings.

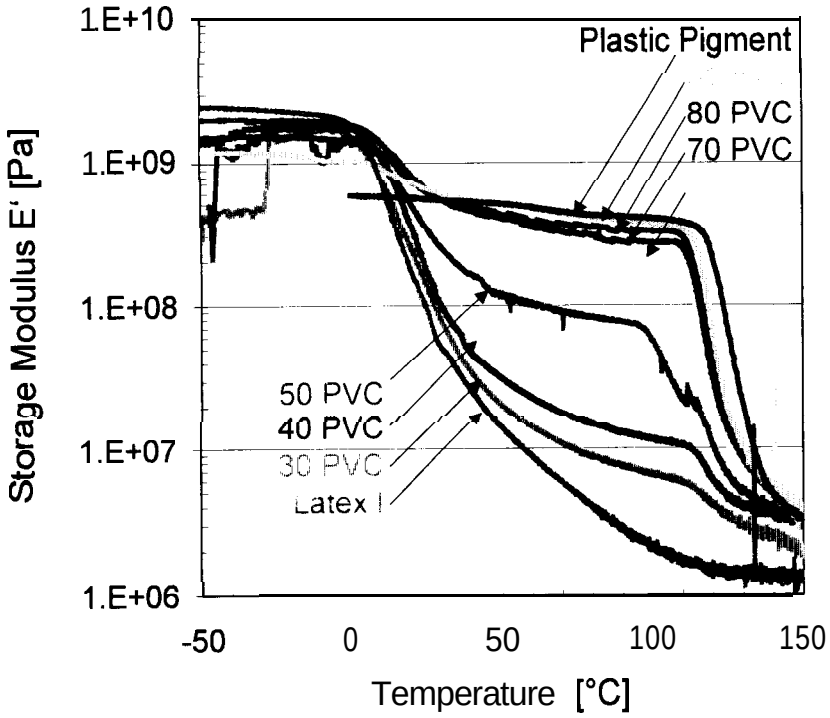

Figure 39 Storage modulus versus temperature for latex I and plastic pigment coatings at different pigment volume concentrations.

A bigger difference for the storage modulus was observed with the polystyrene plastic pigment coatings between 60% pigment volume concentration and 40% pigment volume concentration above glass transition temperatures. This was not seen with the calcium carbonate coatings and clay coatings.

The two peaks in tan Delta indicated the glass transition regions of the two components of the coating, latex and polystyrene pigment. An increase of pigmentation level resulted in a reduction of the glass transition region for polystyrene coatings. With increasing pigmentation level the maximum of the peaks in tan Delta around the binder glass transition temperature decreased, as well as the width of the peak (Figure 41).

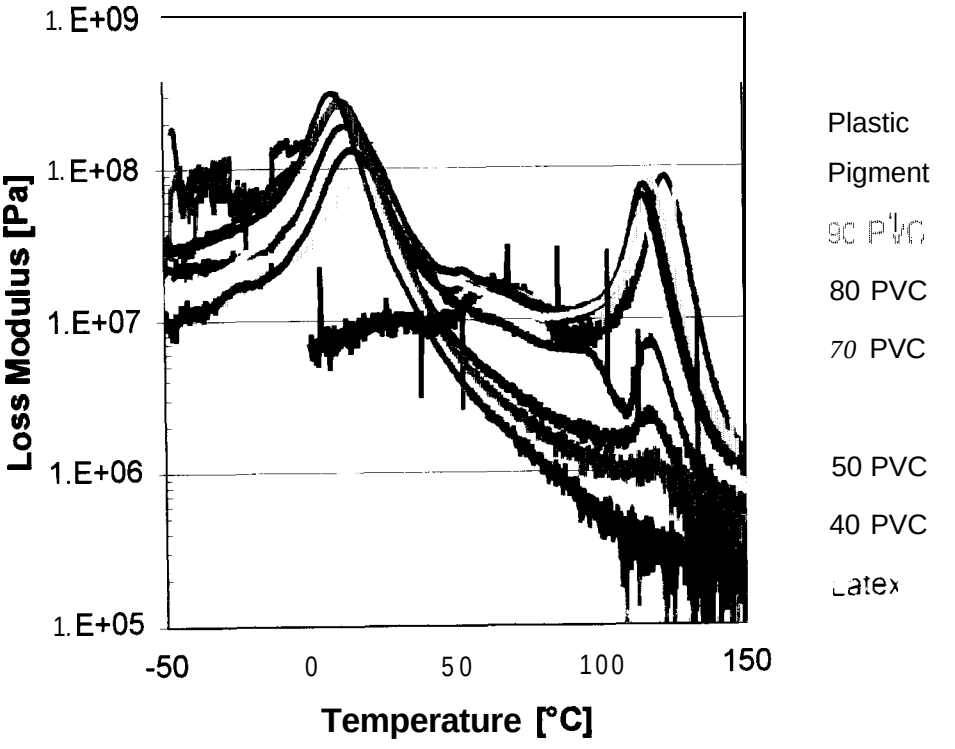

Figure 40 Loss modulus versus temperature for latex I and plastic pigment coatings at different pigment volume concentrations.

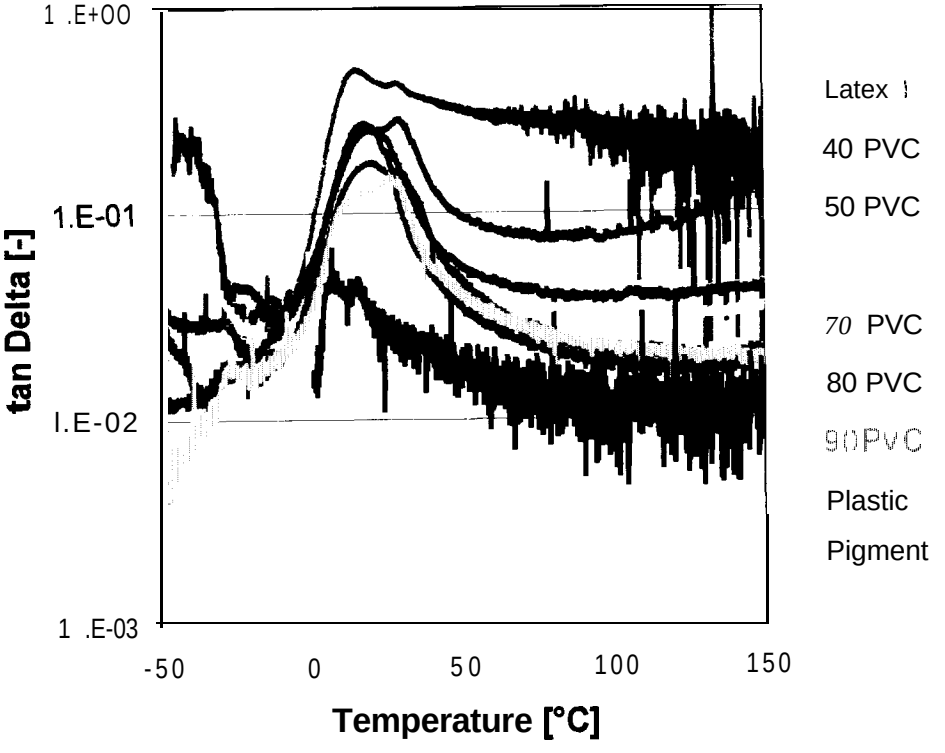

Figure 41 tan Delta versus temperature for latex I and plastic pigment coatings at different pigment volume concentrations.

The overall values of the loss moduli were reduced with increasing pigment volume concentration (Figure 40), and the peaks in loss moduli and tan Delta of the latex were shifted towards higher temperatures, suggesting an interaction between binder and pigment, Parpaillon et a/. (1985).

With increasing pigment volume concentration, the polystyrene plastic pigment coatings with latex I an increasing glass transition temperature (peak in tan Delta) for the soft phase was observed. A maximum temperature was reached at 40% pigment volume concentration (Figure 42). Whereas the glass transition temperature of the pigment phase reached its maximum for the pure pigment phase (Figure 43).

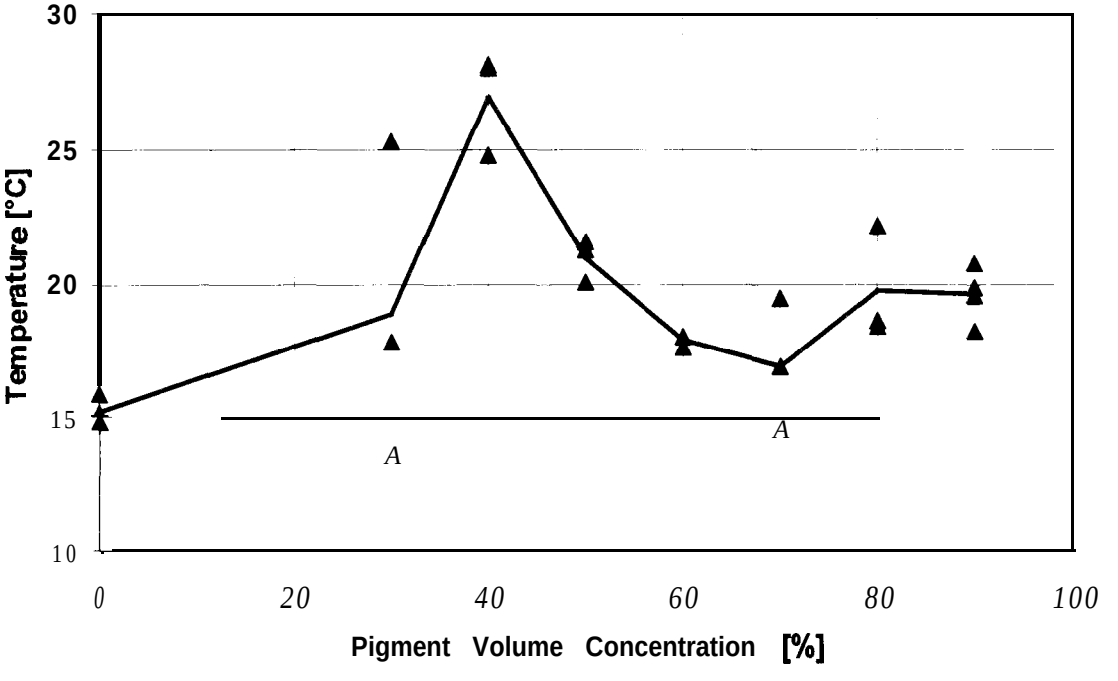

Figure 42 Temperature of tan Delta-peak (1st transition, latex) versus pigment volume concentration for latex I andplasticpigment coatings

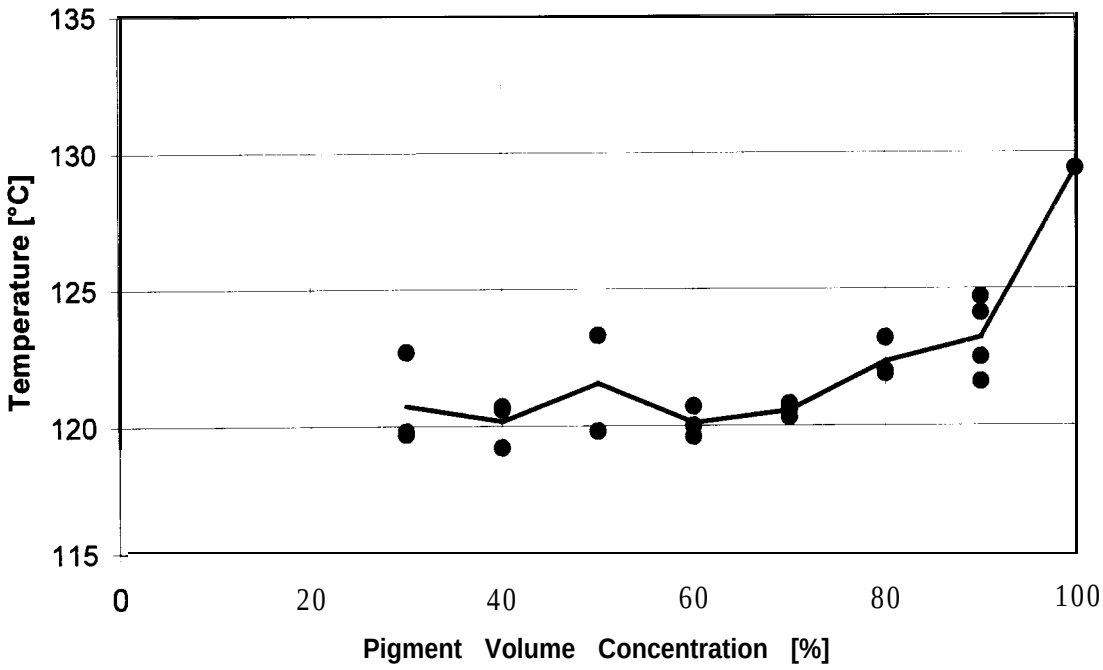

Figure 43 Temperature tan Delta-peak (2nd transition, polystyrene plastic pigment) versus pigment volume concentration for Latex I and plastic pigment coatings

Table 13 showed the development in glass transition temperature and tan Delta with increasing pigment volume concentration for polystyrene plastic pigment coatings prepared with latex I and latex II.

Table 13 Change in glass transition temperature and tan Delta for polystyrene plastic pigment coatings. prepared with the two different latices, for increasing pigmentation level determined by dynamic mechanic al thermal analysis

Peak in tan Delta (T_g[°C], tanDelta)				
	Experimental Latex I		Experimental Latex II	
	Softphase	Hard phase	Softphase	Hard phase
Latex	(16.0, 0.556) (15.3, 0.504) (14.8, 0.530)		(22.4, 1.400) (14.5, 2.064) -	
30% PVC	(17.9, 0.508) (13.6, 0.565) (25.3, 0.484)	(119.7, 0.312) (119.8, 0.316) (122.7, 0.277)		
40% PVC	(24.8, 0.420) (28.0, 0.650) (28.1, 0.643)	(119.2, 0.312) (120.7, 0.316) (120.6, 0.278)		
50% PVC	(20.1, 0.313) (21.3, 0.307) (21.6, 0.326)	(119.8, 0.594) - (123.3, 0.282)		
60% PVC	(18.1, 0.423) (18.1, 0.214) (17.7, 0.260)	(120.7, 0.8412) (120.0, 0.9052) (119.6, 0.9014)		
70% PVC	(17.0, 0.187) (19.5, 0.185) (14.5, 0.266)	(120.8, 1.015) (120.6, 1.010) (120.3, 1.020)	(21.2, 0.332) (21.7, 0.414)	(119.6, 1.573) (118.8, 1.444)
80% PVC	(18.5, 0.145) (22.2, 0.153) (18.7, 0.150)	(121.9, 1.175) (123.2, 1.180) (122.0, 1.188)	(19.2, 0.232) (17.5, 0.221)	(120.6, 1.506) (120.5, 1.479)
90% PVC	(20.8, 0.097) (19.6, 0.113) (18.3, 0.117) (19.9, 0.118)	(124.1, 1.409) (124.7, 1.292) (122.5, 1.319) (121.6, 1.298)	(19.4, 0.133) (18.8, 0.137)	(116.2, 1.521) (116.7, 1.559)
Polystyrene Pigment		(129.4, 1.435) -		(129.4, 1.435)

Hill (1987) observed that with dynamic mechanical thermal analysis, the temperature of the peaks in tan Delta were higher then the glass transition temperature determined by thermodynamic methods within a dynamic scanning calorimeter. The measurements in the dynamic mechanical thermal analyzer were influenced by the heating rate of the instrument, sample thickness of the material, and depended additionally on the frequency of oscillation. Heat flux within the sample influenced temperatures at which the peak in tan Delta occurred (Table 14). The difference in glass transition temperature observed between thermodynamic (dynamic scanning calorimetry) and mechanical measurements was about 15°C. Therefore it is recommended to use thermodynamic methods determining the glass transition temperature of a material if absolute values and high precision are necessary.

Table 14 ***Comparison of glass transition temperature determined by differential scanning calorimeter and dynamic mechanical thermal analyzer***

	Glass Transition Temperature (mid point DSC-plot)	Peak in tan Delta (DMTA) (thickness, heating rate)
Experimental Latex I	0.6 °C [a]	16.0°C (70µm, 1.0°C/min) 153°C (36µm, 1.0°C/min) 14.8°C (35µm, 1.0°C/min)
Experimental Latex II	1.0 °C [a]	235°C (165µm, 1.0°C/min) 22.4°C (26µm, 1.0°C/min) 14.5°C (21µm, 0.1°C/min)
Polystyrene Pigment	105°C [b]	129.4°C (500µm, 1.0°C/min)
Polystyrene Pigment + Latex II, 90% PVC		18.3°C 111.6°C (33µm, 0.1°C/min) 18.8°C 116.7% (34µm, 1.0°C/min) 19.4°C 116.2°C (33µm, 1.0°C/min)

a) Source: Personnel communication Dr. Peter Hayes, BASF. Charlotte, NC

b) Source: Personnel communication Dr. Terry Temperly, DOW, Midland, MI

Classical mechanics models such as the Rule of Mixtures, Halpin-Tsai equation, and Transverse Rule of Mixtures were compared with experimental measured data for the polystyrene and latex I coatings. For application of the models, the temperature at which they were applied has to be specified (-20°C, 0°C, 20°C, and 80°C). The response for the storage modulus below the latex glass transition temperature (-20°C) was in the low pigment volume concentration range slightly below the Transverse Rule of Mixture, changing at 50% pigment volume concentration to a behavior above the Rule of Mixture. The storage moduli for coatings with low pigment volume concentration (140%) were predicted well by the Transverse Rule of Mixture at 0°C and by the Rule of Mixture at 20°C. For coatings above 50% pigment volume concentrations the storage moduli were measured for both temperatures well above the Rule of Mixture. Only at 80°C Rule of Mixture and Transverse Rule of Mixture built an upper and lower boundary for the storage modulus. Storage modulus of polystyrene and latex I coatings with pigment volume concentrations above 60% were estimated by the Rule of Mixture, below 60% the Halpin-Tsai Equation gave a better estimation. At -20" and 0°C the storage modulus of the latex was larger then the storage modulus of the pigment. Between 0°C and 20°C that changes, and the storage

modulus of the pigment becomes larger then the storage modulus of the latex. This can be clearly seen by reversed curves (Figure 44).

The loss modulus at -20°C was not well predicted by the different composite theories. For 0°C the Rule of Mixture is predicting the loss modulus quite well. At 20°C the loss modulus for the pigment was still smaller then the modulus for the latex. Classical composite theories did not compare with measured response for the loss modulus at this temperature. At 80°C polystyrene pigment and latex I coatings with pigment volume concentrations below 50% were predicted well by Halpin Tsai Equation, above 60% by Rule of Mixtures (Figure 45).

The comparison of measured data of complex moduli with Rule of Mixtures, Halpin Tsai Equation and Transverse Rule of Mixtures were similar to the behavior for the storage modulus. Only at 80°C the Rule of Mixture predicted material behavior for PVC's above 60% well (Figure 46).

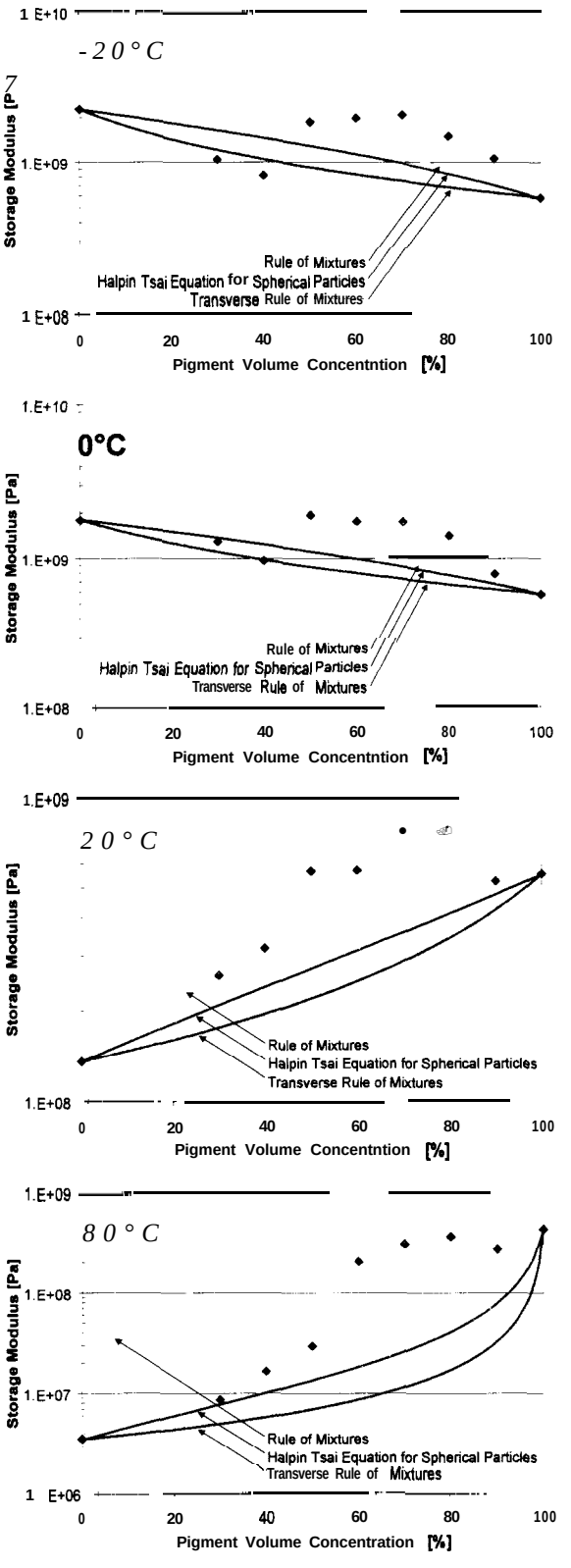

of ***Mixtures, Halpin Tsai Equation and Transverse Rule*** *of* ***Mixtures*** *for* ***storage*** *for* ***coatings with latex I and polystyrene plastic pigment at different temperature levels (0 = experimental values)***

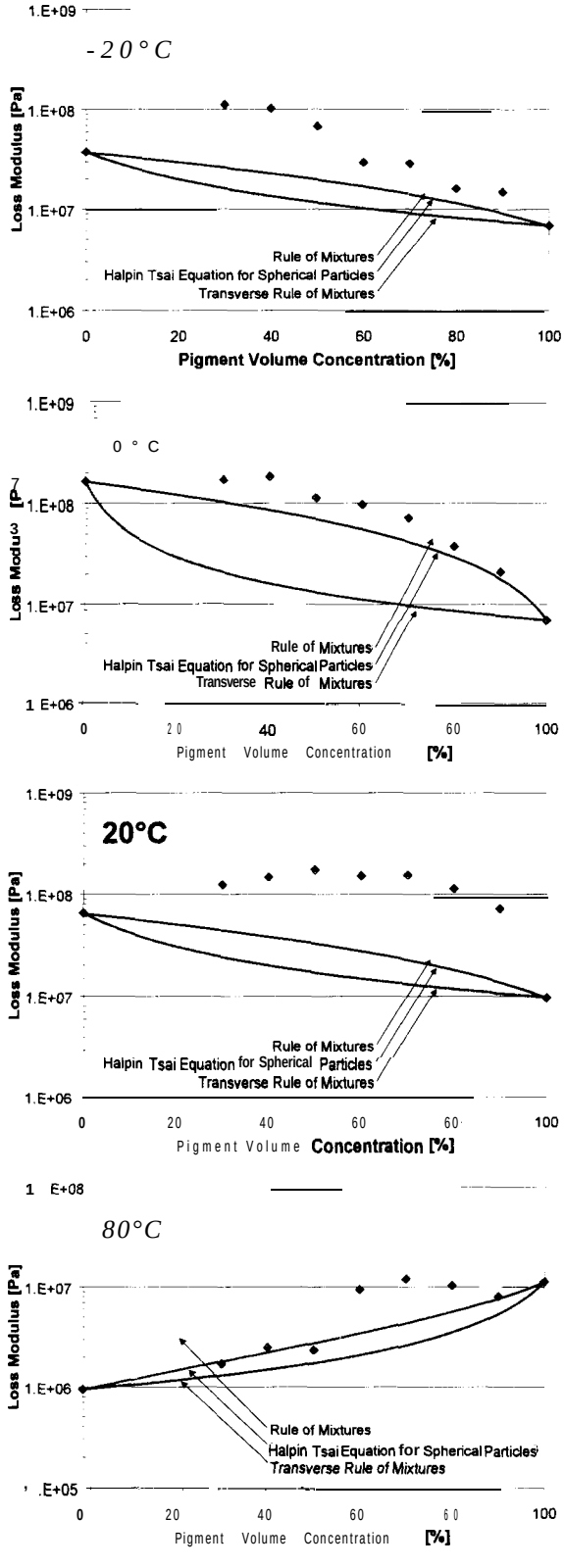

***Figure 45 Comparison Rule** of **Mixtures, Halpin Tsai Equation and Transverse Rule** of **Mixtures** for loss modulus for coatings with latex I and polystyrene plastic pigment at different temperature levels (0 = experimental values)*

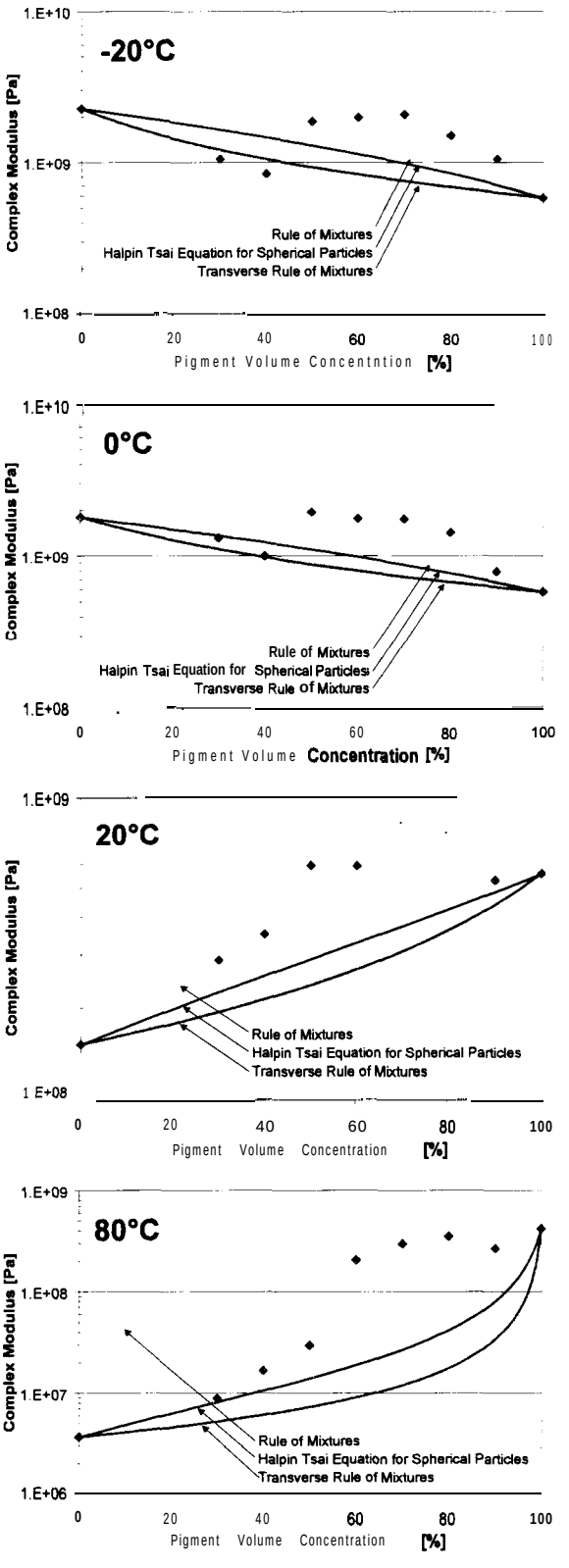

***Figure 46 Comparison Rule** of Mixtures, Halpin Tsai Equation and Transverse Rule of Mixtures for complex modulus for coatings with latex I and polystyrene plastic pigment at different temperature levels (◊ = experimental values)*

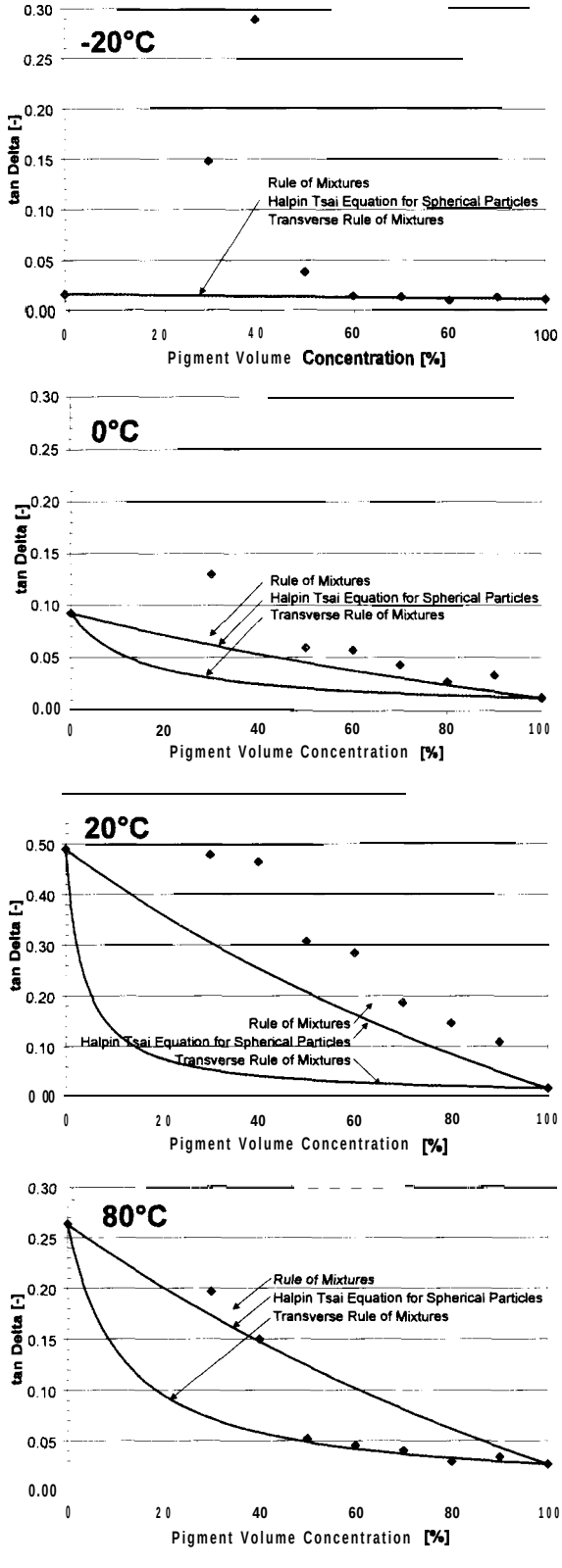

of ***Mixtures, Halpin Tsai Equation*** *for* ***spherical particles, and Transverse Rule*** *of* ***Mixtures*** *for* ***tan Delta*** *for* ***coatings with latex I and polystyrene plastic pigment at different temperature levels (0 = experimental values)***

For polystyrene pigment and latex I coatings at pigment volume concentrations above 60% the tan Delta could be predicted by different composite theories, for different temperatures. Below and around glass transition temperature (-20°C, 0°C and 20°C) the Rule of Mixtures gave a good prediction for tan Delta, above glass transition, at 80°C, the Transverse Rule of Mixture predicted very well. Figure 47.

7.1.4 Effect of Pigment Volume Concentration for Polystyrene Plastic Pigment and Latex I – Time Dependency

At frequencies above 1Hz, the storage moduli of polystyrene coatings were only slightly increased by increasing frequency (strain rates) irrespective of pigment volume concentration (Figure 48). This essentially elastic behavior showed material's storage moduli ranging from 0.8GPa (90% PVC) to 2GPa (pure latex I). The addition of pigment reduced the storage modulus of the pigmented latex films and no reinforcement took place. The major change in storage modulus occurred at frequencies of 10^{-6}Hz to 1Hz. This frequency range corresponded with the transition region observed around the glass transition temperature of the latex. Below the frequency of 10^{-4}Hz the behavior of latex changed to highly viscous. The addition of pigment reduced the rate of change in storage modulus and frequency (strain rate) dependence changed. In summary, changes in pigment volume concentration had different effects for polystyrene pigment depending on the timescale. For long-term behavior (f $< 10^{-4}$Hz) an increase in pigment volume concentration had a reinforcing effect on the coatings. For short-term behavior (f $>$ 1Hz) the storage modulus was decreased with increasing pigment volume concentration. Converting processes typically take place at frequencies about 1 0^{3}Hz to 1 0^{6}Hz. It should be emphasized that other important mechanical properties such as strength and strain to failure need not directly track with changes in moduli. Time-temperature superposition and WLF-theory were originally developed for polymeric systems. For the system polystyrene plastic pigment and latex the excellent master curves were obtained over the whole PVC range.

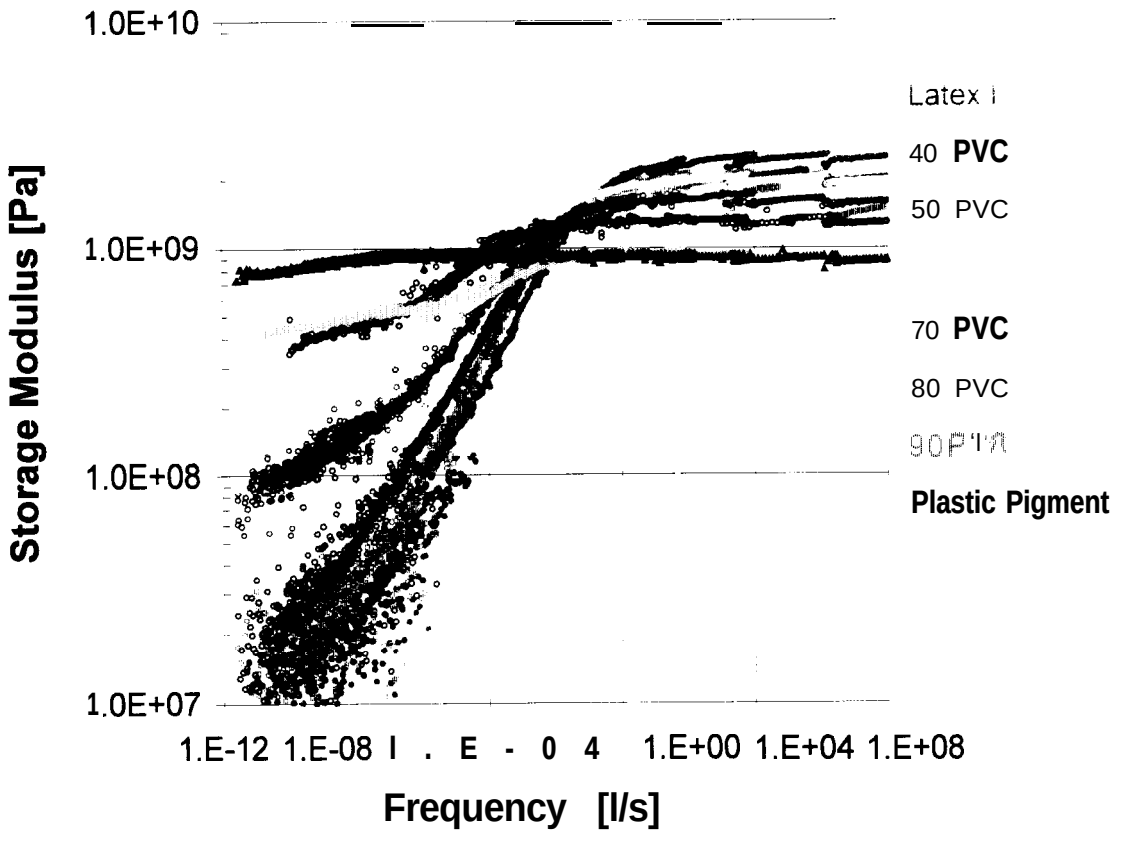

Figure 48 Master curves for latex I and polystyrene pigment calculated at 0°C.

Figure 49 showed different master curves of a polystyrene plastic pigment and latex I coating at 80% pigment volume concentration. The master curves of the storage modulus were calculated at different reference temperatures (-10°C, 0°C, 25°C). With increasing temperature, the modulus decreased, and the transition region shifted towards higher frequencies, resulting in a more viscous behavior.

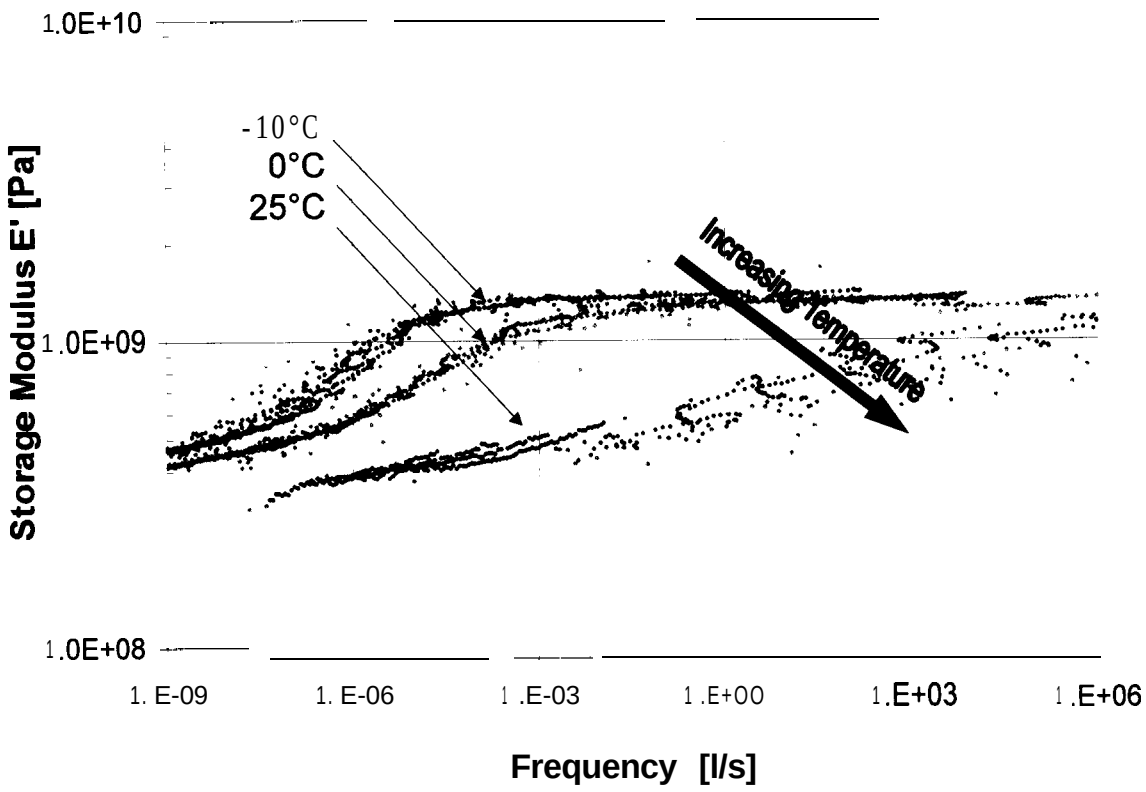

Figure 49 Master curves for latex I and polystyrene pigment at 80% pigment volume concentration, calculated at different reference temperatures: -10°C. 0°C and 25°C.

7.1.5 Effect of Pigment Volume Concentration for Clay Pigment and Latex I - Temperature Dependency

The temperature dependence of modulus of a clay pigment film was measured (Figure 50). The storage modulus exhibited a depression in the temperature range between 5°C to 25°C. Clay coating films with different pigment volume concentration levels also exhibited this depression.

Below the latex glass transition temperature, clay coatings were found very frequently to exhibit a too low storage modulus, which was then increasing to the higher value during the scans (60PVC and 70PVC, Figure 50). This was rarely observed on coatings containing other pigments. Clay

coatings with 50% pigment volume concentration showed the highest storage modulus, in this temperature range.

Above the latex glass transition region, the clay coatings exhibited storage moduli about one decade higher then calcium carbonate coatings. The higher storage modulus is due the plate-like shape of the clay particles. Pigments are orienting in plane of the coating, increasing the modulus.

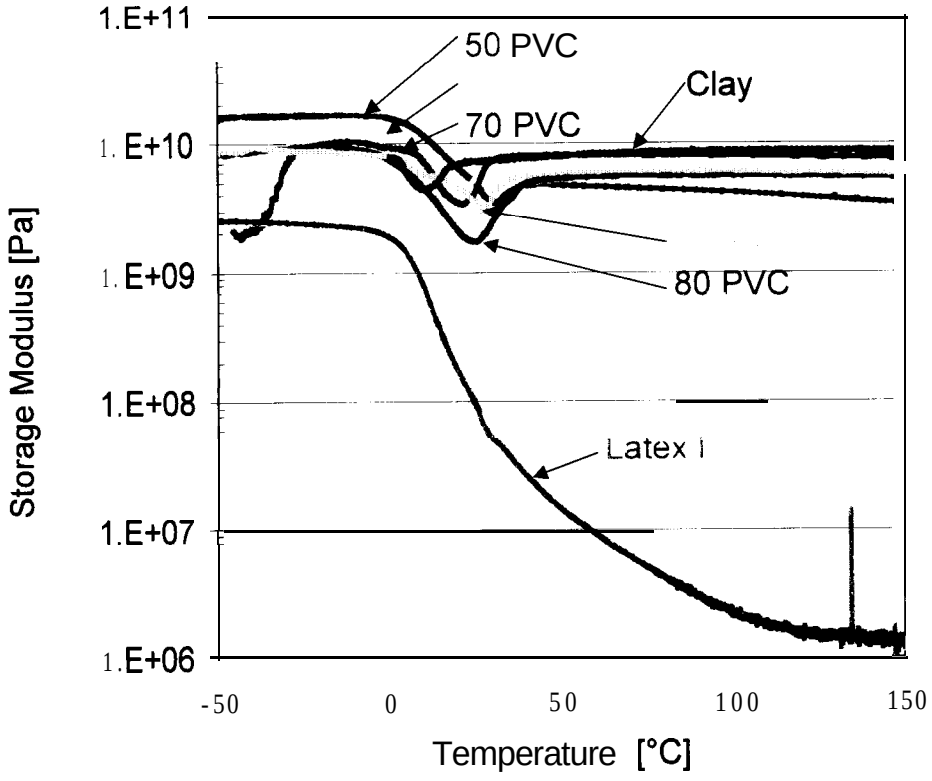

Figure 50 Storage modulus versus temperature for latex I and clay coatings at different pigment volume concentrations.

The depression in storage modulus around room temperature has been observed in experiments performed on clay/calcium carbonate coatings by Yamashita et a/. (1993) and lshikawa et a/. (1995). They described three transition regions. The first, where the storage modulus decreases until it reaches a minimum, the second, where the storage modulus increases, and the third, at

higher temperatures (around 100°C) when the storage modulus decreases again. It was suggested that the porous and discontinuous structure of the coatings caused the behavior. They suggested the first transition is due to latex glass transition region, the second due to change in packing state of the pigment, and the third due to polymer melt flow. In our experiments, pigmented coatings consisting only of clay pigments and latex did not exhibit the third transition temperatures around 100°C. A temperature scan for a 90% pigment volume concentration clay coating continuing to higher temperatures resulted in a sudden drop in storage modulus at around 170°C, similar to the drop appearing for calcium carbonate coatings around 145°C. It might be due to latex flow, or latex degradation.

Another speculation why depression was observed suggested that it was caused by the additional stress relaxation due to the measurement methods. Dynamic mechanical analysis of clay coatings performed on torsional braid analyzer did not report any depression [Zosel 1980, Parpaillon 1985, Kan et al. 1996 and 1997].

Repeating temperature scans (-50°C to +150°C) several times on one sample changed the viscoelastic behavior. For consecutive scans at 90% pigment volume concentration, the clay coatings exhibited a reversible material behavior. The depression in storage modulus above 0°C was clearly visible for three consecutive scans (Figure 20). For films at pigment volume concentration levels of 80% and less (Figure 21), subsequent temperature scans changed the curve type, i.e. only a simple transition region was observed within the second scan. The values in storage modulus of the same sample increased in each scan below the glass transition temperature. This indicated that the thermo-mechanical treatment of the scanning process deformed the structure within the clay coatings (Figure 53). For very high pigment volume concentrations, the change was more influenced by a pigment-pigment interaction.

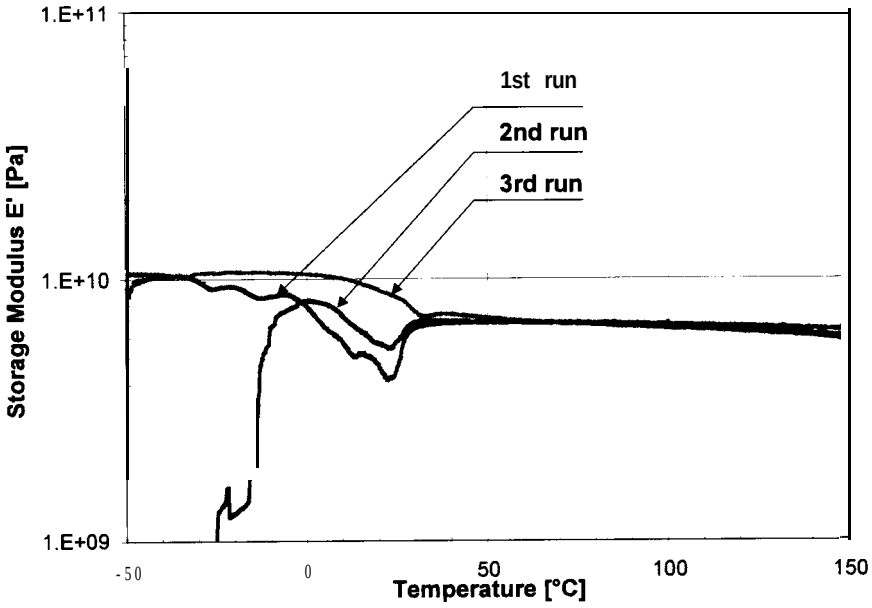

Figure 51 Three consecutive temperature scans on a clay and latex I coating sample with 90% pigment volume concentration

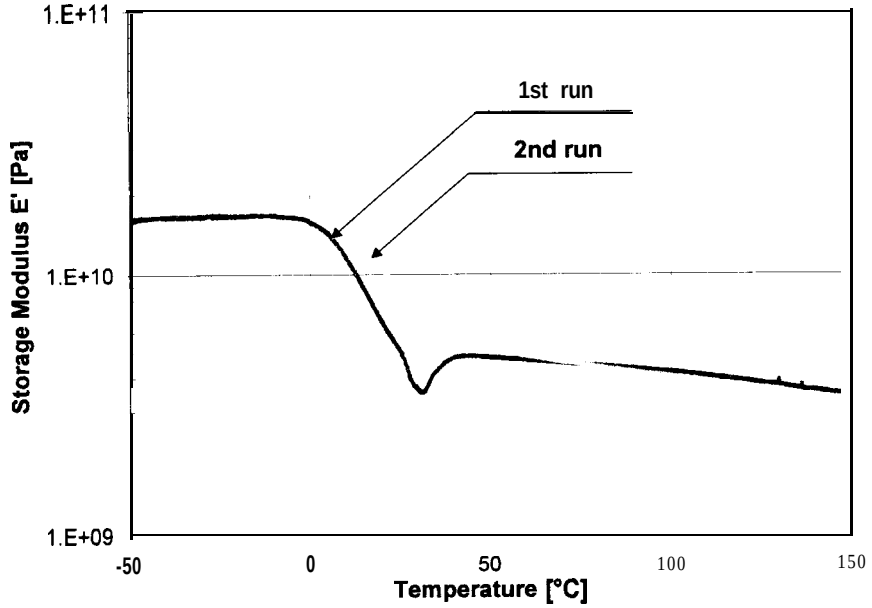

Figure 52 Two consecutive temperature scans on a clay and latex I coating sample with 50% pigment volume concentration

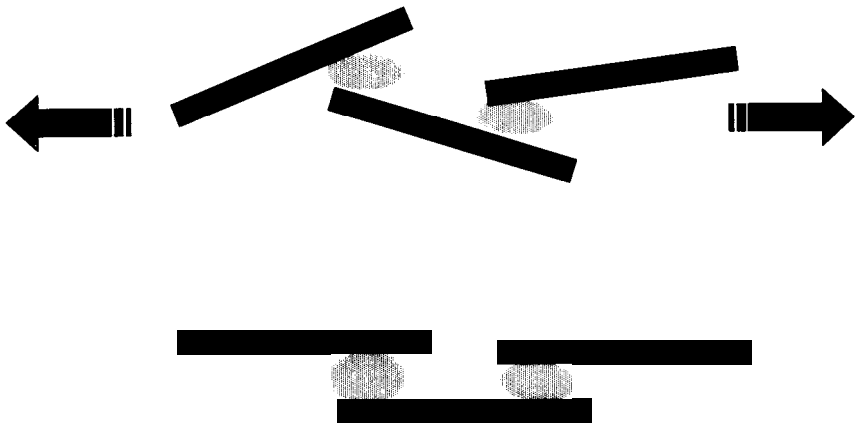

Higher orientation of the particles in plane of stress leads to an increase in modulus

For loss modulus double peaks could be observed for clay and latex I coatings at pigment volume concentrations above 60% around the glass transition region and depression region. The first peak resulted from the latex, the second is probably due to the clay pigment. 50% PVC coatings exhibited the highest loss modulus during glass transition zone, above glass transition temperature the 60% PVC coatings showed highest loss modulus (Figure 54). For tan Delta two peaks could be observed, too for coatings below 50%PVC (Figure 54).

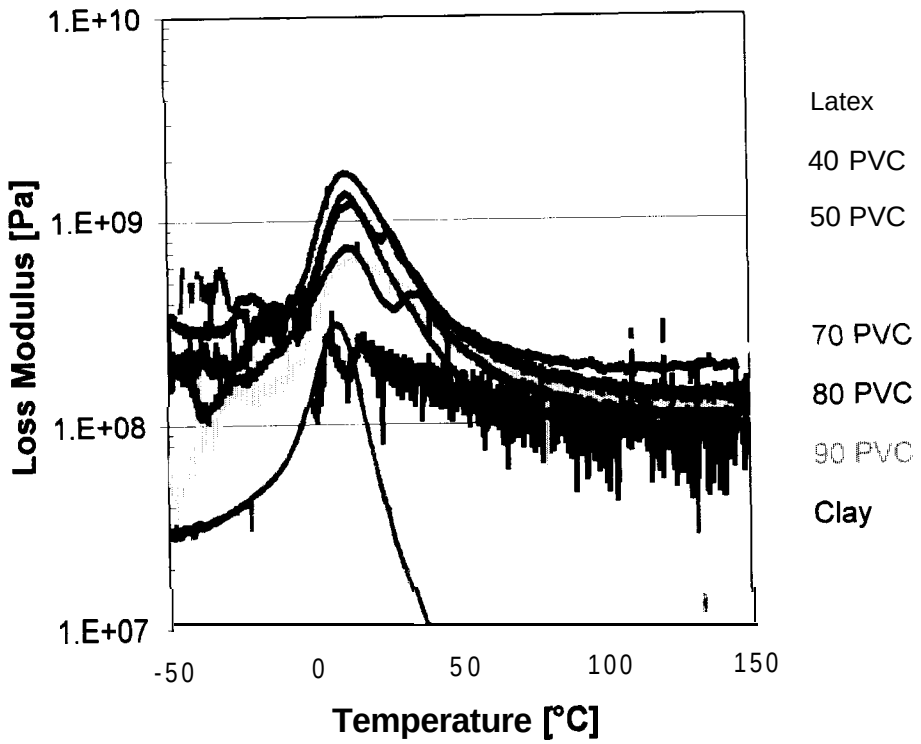

Figure 54 Loss modulus versus temperature for latex I and clay coatings at different pigment volume concentrations

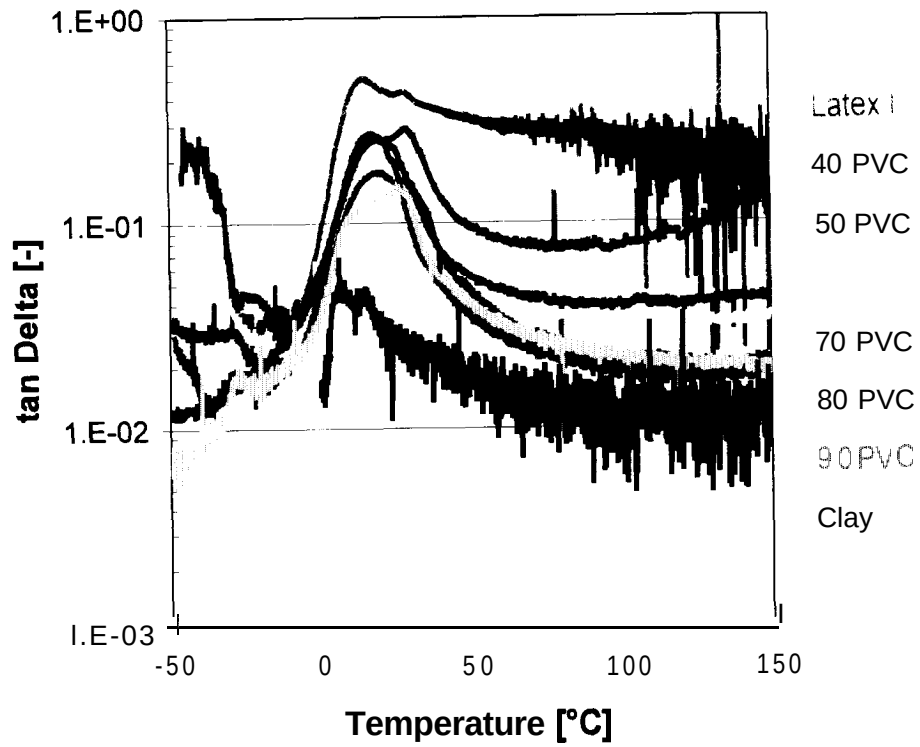

Figure 55 tan Delta versus temperature for latex I and clay coatings at different pigment volume concentrations

Rule of Mixtures, Halpin-Tsai equation, and Transverse Rule of Mixtures were compared with experimental measured data for the clay and latex I coatings at -20°C, 0°C, 20°C, and 80°C. The response for the storage modulus below the latex glass transition temperature (-20°C and 0°C) was not predicted by the different mechanical models. With increasing temperature, above the transition region at 80°C the Rule of Mixture gave an estimation for the storage modulus (Figure 56). The loss moduli were not well predicted by the different composite theories for the clay and latex I coatings for all temperatures. All measured data, exhibited loss modulus above the Rule of Mixture (Figure 57). The complex modulus performed in a similar manner as the storage modulus. At 80°C the Rule of mixture was quite well predicting the complex modulus above 50% pigment volume concentration (Figure 58). The Transverse Rule of Mixture and measured data of tan Delta for clay and latex I coatings corresponded well in the pigment volume concentration range above 60% (Figure 59).

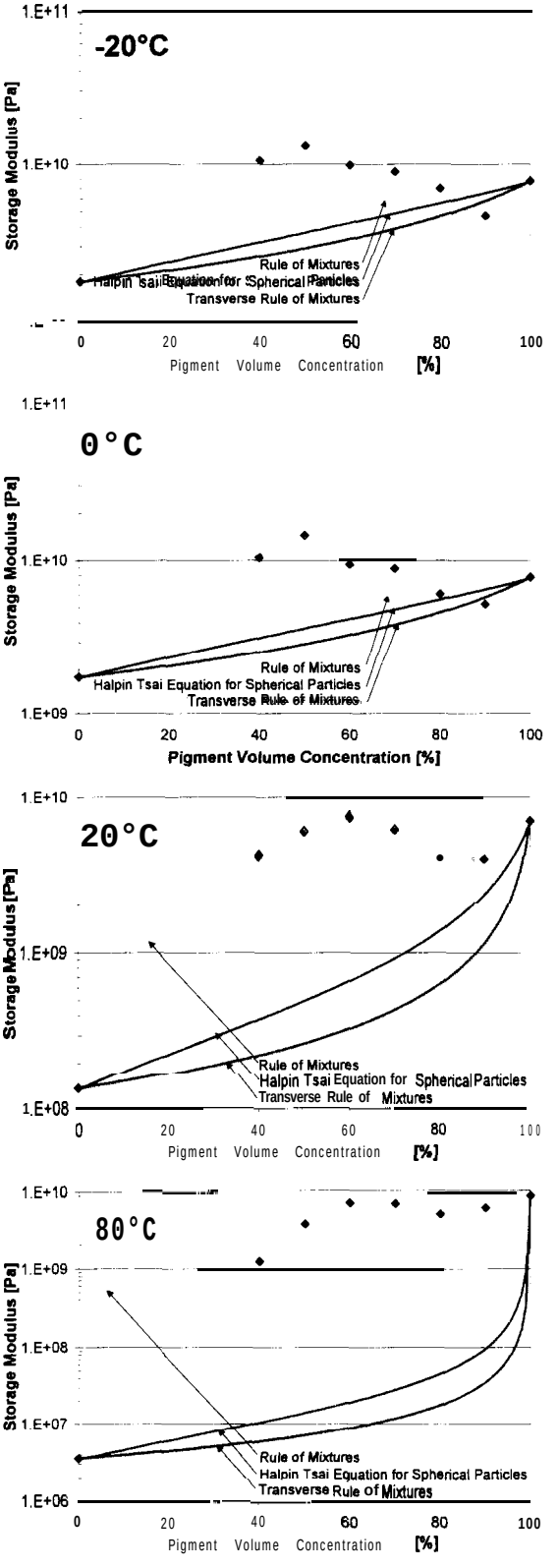

Figure 56 Comparison Rule** of **Mixtures, Halpin Tsai Equation** for **spherical particles, and Transverse Rule** of **Mixtures** for **storage modulus** for **coatings with latex I and clay pigment at different temperature levels (0 = experimental values)

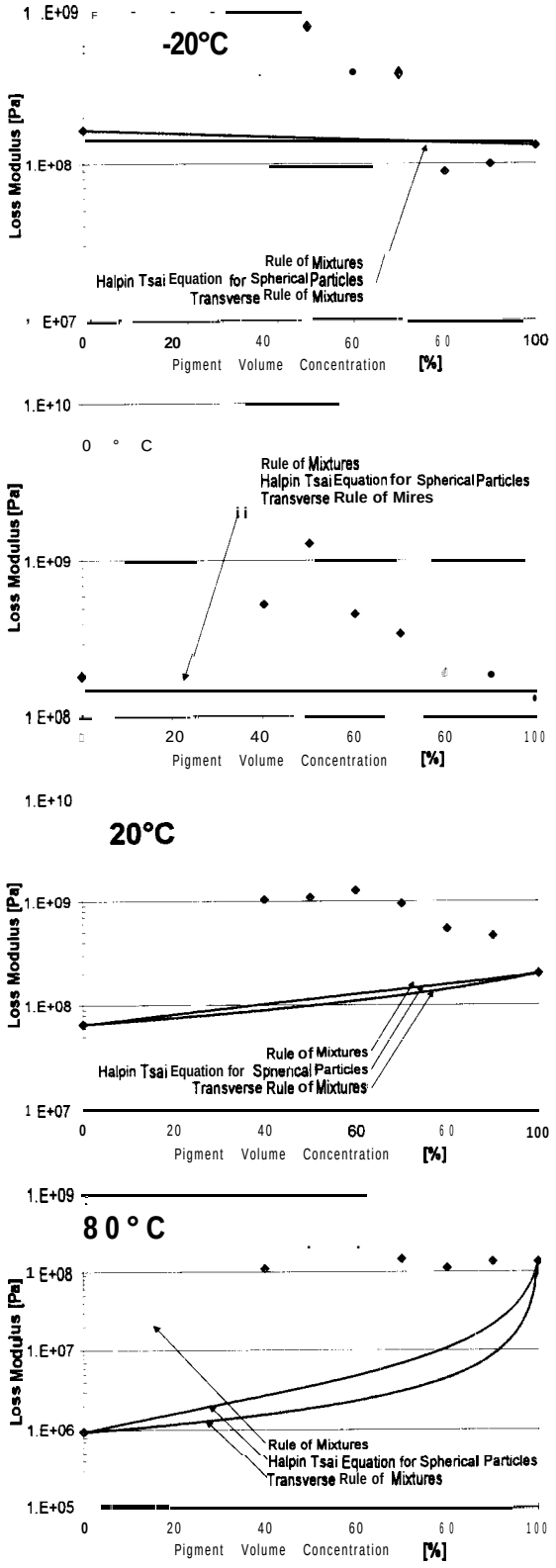

Figure 57 Comparison Rule** of Mixtures, Halpin **Tsai Equation** for **spherical particles, and Transverse Rule** of **Mixtures** for **loss modulus** for **coatings with latex I and clay pigment at** different **temperature levels (◊ = experimental values)

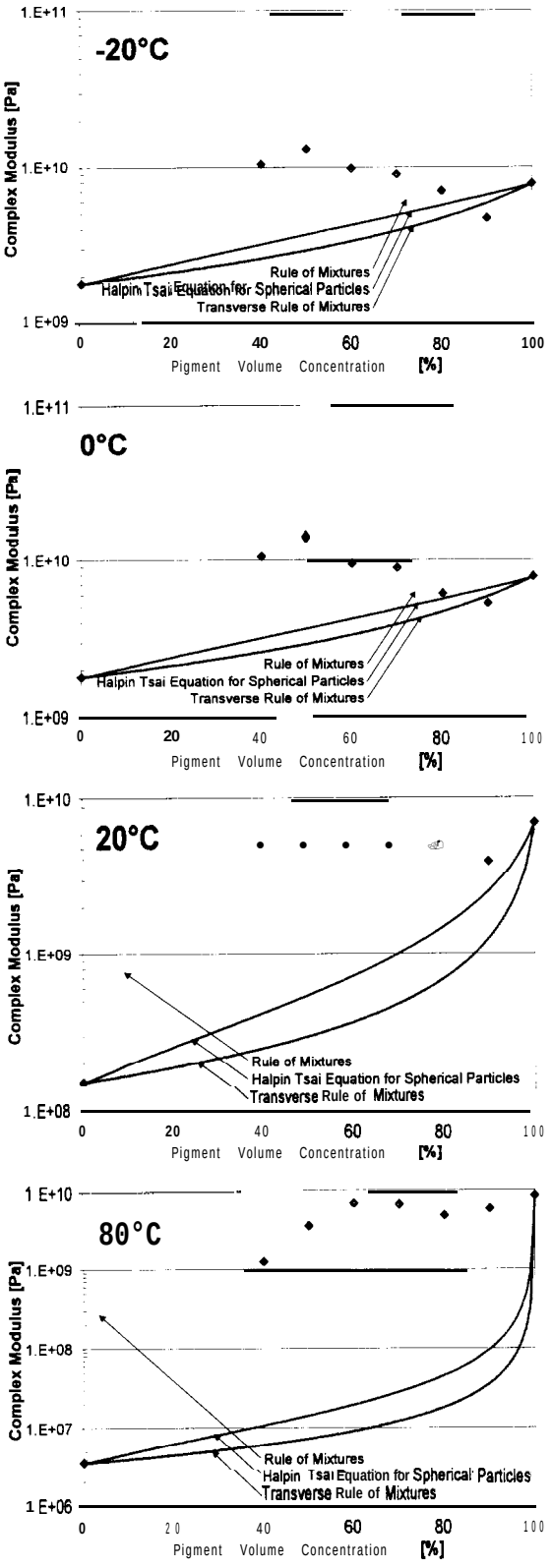

***Figure 58 Comparison Rule** of **Mixtures, Halpin Tsai Equation** for **spherical particles, and Transverse Rule** of **Mixtures for complex modulus** for **coatings with latex I and clay pigment at** different temperature levels (0 = experimental values)*

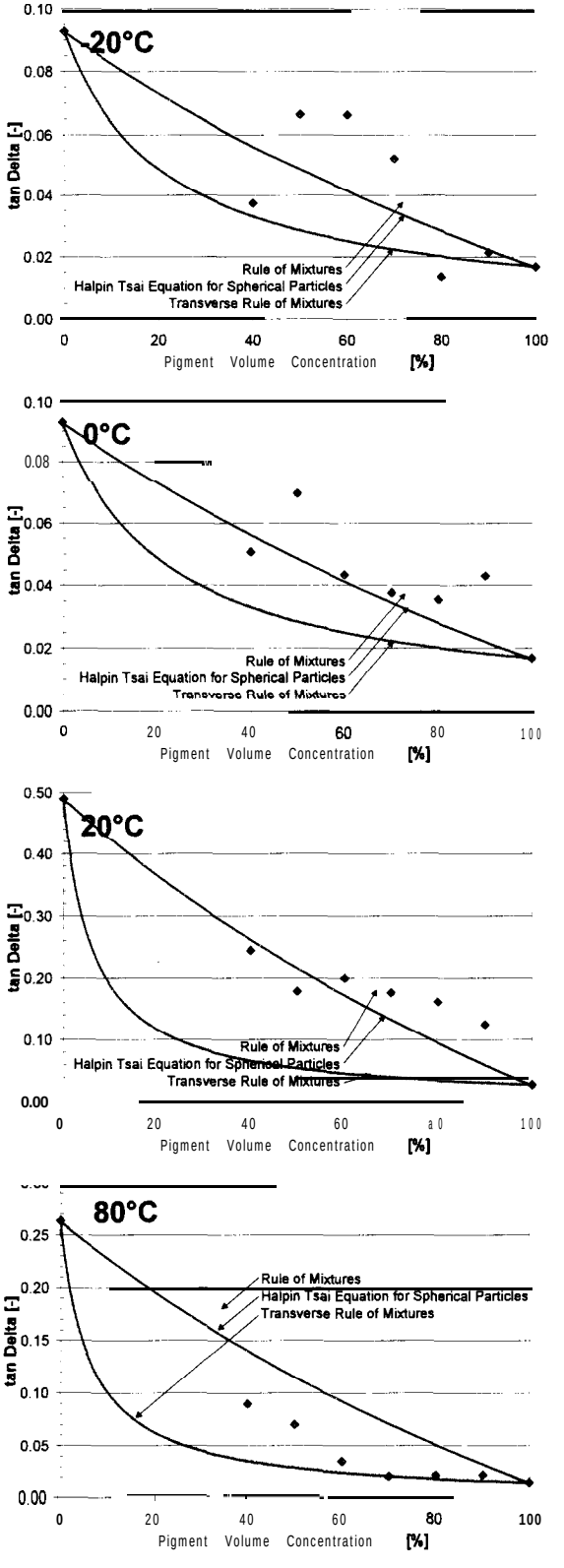

Figure 59 Comparison Rule of Mixtures, Halpin Tsai Equation for spherical particles, and Transverse Rule of Mixtures for tan Delta for coatings with latex I and clay pigment at different temperature levels (0 = experimental values)

7.1.6 Effect of Pigment Volume Concentration for Clay Pigment and Latex I – Time Dependency

The master curves in Figure 60 were calculated at 0°C, by applying time-temperature superposition and WLF-theory with Universal Constants. During each frequency scan 60 data points were recorded. Each frequency scan is represented by three points, the median of 20 measured values. For one master curve 20 frequency scans were performed, reaching from -15°C to 80°C in 5°C intervals.

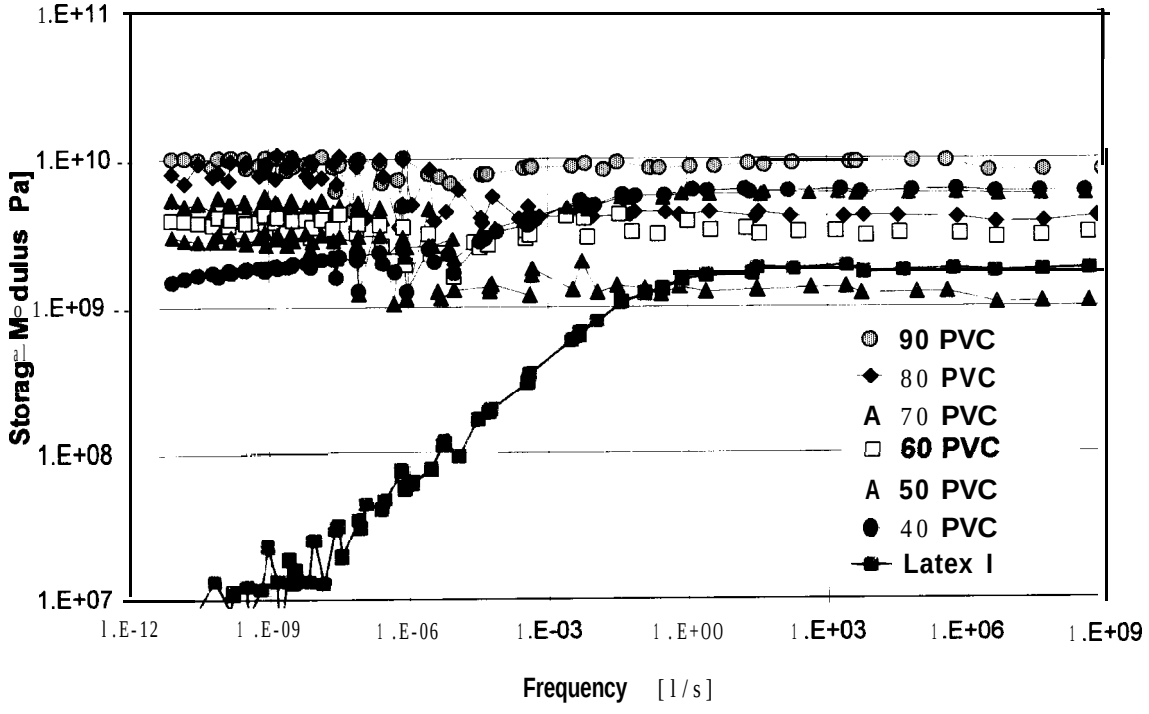

Figure 60 Master curves of storage modulus calculated at 0°C with Universal Constants, for clay pigment and latex I coatings at different pigment volume concentrations

For the clay and latex I coatings it was observed, that during the transition region (10^{-8}Hz to 10^{-3}Hz) the time-temperature superposition with WLF-theory and Universal Constants was not able to represent the storage modulus very well. The frequency scans performed at different temperatures did not complement another into a smooth master curve. The frequency region

10^{-8}Hz to 10^{-3}Hz corresponded with the temperature region around glass transition temperature where the storage modulus performed a depression. At frequencies above 1Hz, the storage moduli of clay coatings were independent of frequency (strain rates) irrespective of pigment volume concentration. This essentially elastic behavior showed material's storage moduli ranging from 1 .5GPa (pure latex I) to 9GPa (90% PVC). Below frequencies of 10^{-8}Hz the storage modulus for coatings above 50% pigment volume concentration showed less dependence on frequency. The clay and latex I coating with 40% pigment volume concentration showed a slight dependency on strain rate.

7.2 Effect of Adhesion – Carboxylation Degree of Binders

The different carboxylation degree were selected to demonstrate differences in adhesion effects. The latices distinguished in carboxylation degree (latex I: 3.5% acidic level, latex II: 0.3% acidic level, same particle size and glass transition temperature, see Table 6). It was expected that a latex with higher carboxylation degree performs with higher adhesion phenomena. The temperature and time behavior was investigated for the two different latices and for polystyrene plastic pigment and clay pigment coatings in the high pigment volume concentration range.

7.2.1 Viscoelastic Behavior with Temperature for the Two Different Latices

The investigation of storage and loss modulus with increase in temperature was shown for the two experimental latices (Figure 61). Below glass transition temperature glassy behavior dominated. The storage moduli were around 2.3GPa to 2.8GPa for both latices. The storage moduli of the two different latices were negligible affected by temperatures below the glass transition region and no appreciable difference between the latices could be observed. The loss moduli showed for both latices similar behavior below glass transition region, with a maximum of 0.4GPa to 0.3GPa during glass transition region. Within the glass transition region (0°C to 25°C) different thermal softening could be observed for the storage modulus, depending on the

carboxylation degree of the latices. The storage modulus of latex II with a lower carboxylation degree decreased more rapidly then for latex I, to a value two decades lower then latex I The stronger thermal softening was also reflected by a higher peak in tan Delta for latex II (Table 15).

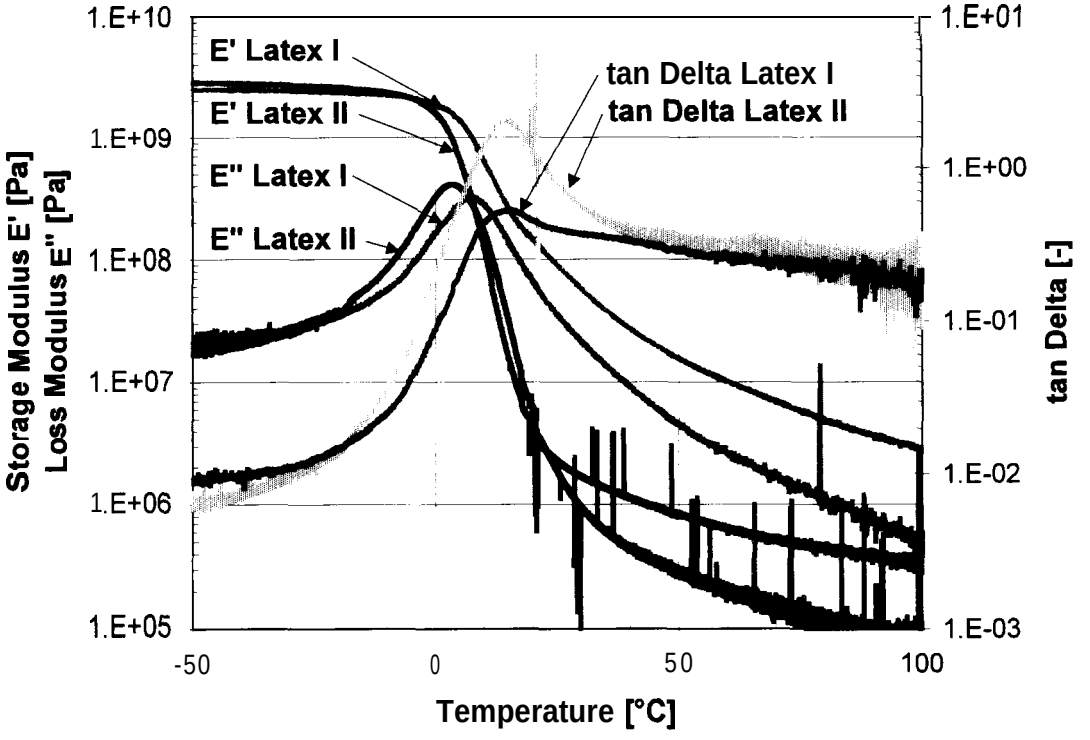

Figure 61 Influence of temperature on storage and loss modulus and tan Delta on two different styrene/butadiene latices

Above the glass transition region, latex II exhibited lower values for storage and loss modulus then latex I, whereas the relation of viscous to elastic behavior (tan Delta) for both latices below and above the glass transition region remained the same. Therefore for coatings prepared with latex II, lower values for storage and loss modulus were expected in the temperature region above latex glass transition temperature.

Table 15 ***Comparison of maximum in tan Delta for the two styrene/butadiene latices distinguishing in carboxylation degree***

	Maximum in tan Delta (Temperature)
Experimental Latex I	0.556 (16.0°C) 0.504 (153°C) 0.530 (14.8°C)
Experimental Latex II	1.400 (22.4°C) 2.064 (14.5°C)

7.2.2 Effect of Pigment Volume Concentration for Polystyrene Plastic Pigment and Latex II – Temperature and Time Dependency

Polystyrene plastic pigment coatings with latex II were only prepared in the high PVC range (Figure 62). The polystyrene plastic pigment coatings with latex I and latex II performed for pigment volume concentrations above 70% in a similar manner. For the temperature scans the coatings with latex II showed slightly lower values for storage modulus at temperatures above latex glass transition temperature as it was expected (see also Figure 66). The carboxylation degree showed only little effect on the storage moduli.

The master curves were calculated at a reference temperature of 0°C (Figure 63). As expected showed latex II for frequencies below IO" Hz a stronger strain dependency then latex I. The coating films of latex II with high pigment volume concentrations performed in the same manner then latex I with slightly lower values for storage modulus.

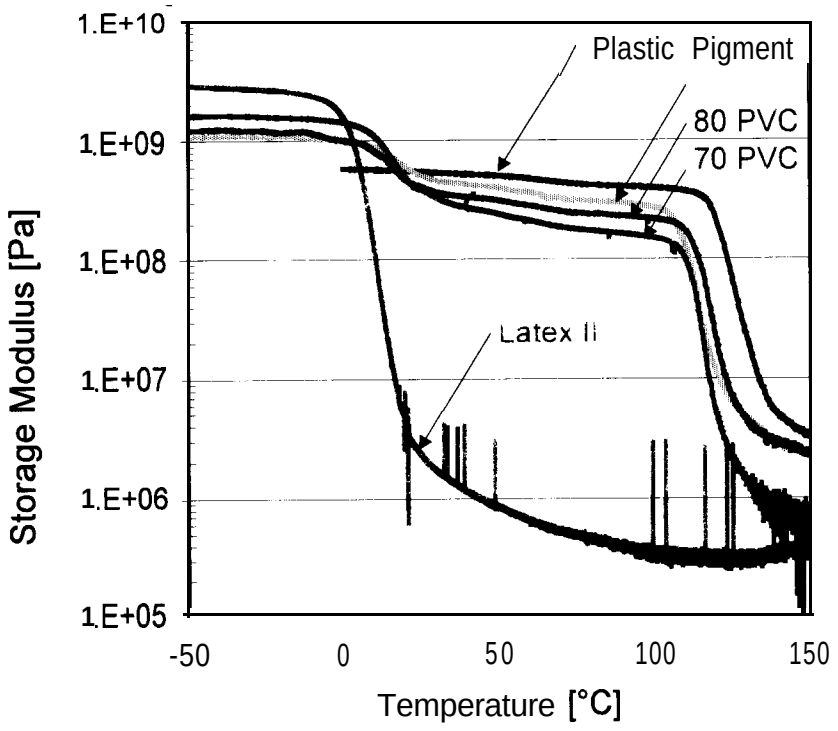

Figure 62 Storage modulus versus temperature for latex II and plastic pigment coating, at different pigment volume concentrations.

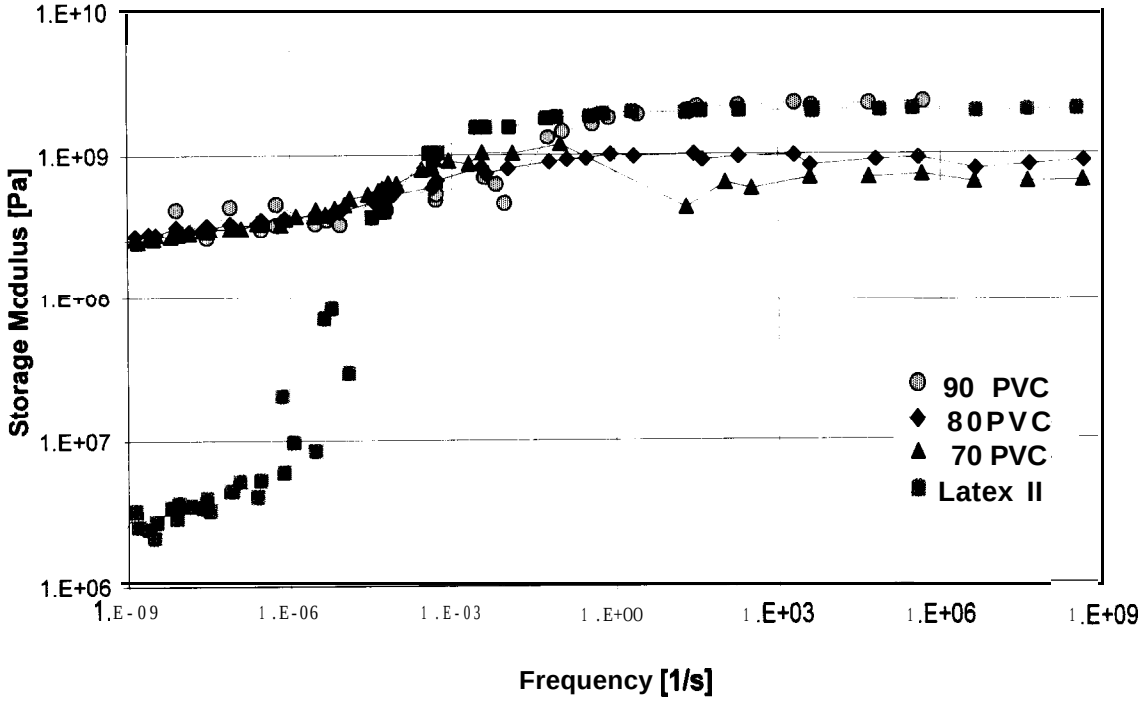

Figure 63 Master curves of storage modulus for latex II and plastic pigment coatings at different pigment volume concentrations, calculated at 0°C

7.2.3 Effect of Pigment Volume Concentration for Clay and Latex II - Temperature and Time Dependency

Clay coatings with latex II were prepared in the high PVC range (Figure 64). The with latex II performed similar as the coatings with latex I, showing a depression around the glass transition region. In the high temperature region above 40°C a lower storage modulus for the pigmented coatings was expected for latex II. The performed temperature scans showed for 90%, 80% and 70% PVC a higher value of storage modulus in this region, though (Figure 66). For clay coatings with latex II and 60% PVC the storage modulus was in the high temperature range lower compared with coatings prepared with latex I.

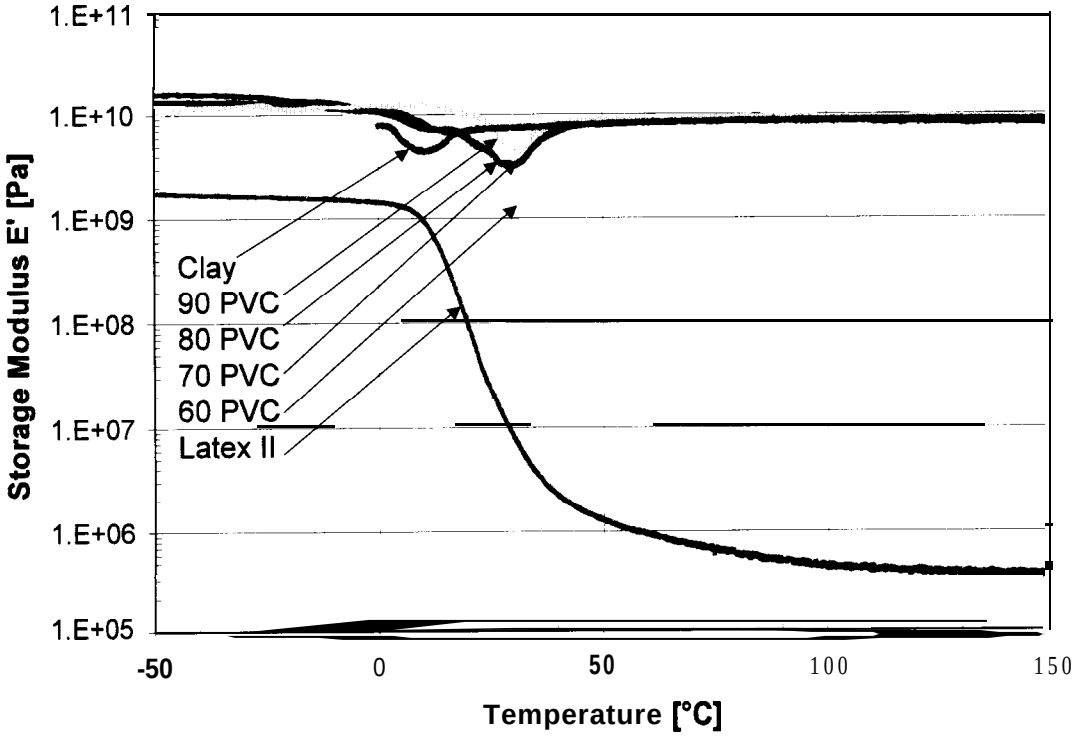

Figure 64 Storage modulus versus temperature for latex II and clay pigment coating, at different pigment volume concentrations.

The master curves were calculated at a reference temperature of 0°C (Figure 65). As expected showed latex II for frequencies below IO" Hz a stronger strain dependency then latex I. The storage modulus for the 90%, 80%, 70% and 60% PVC coatings with latex II performed with slightly higher values than for latex I over the whole frequency range.

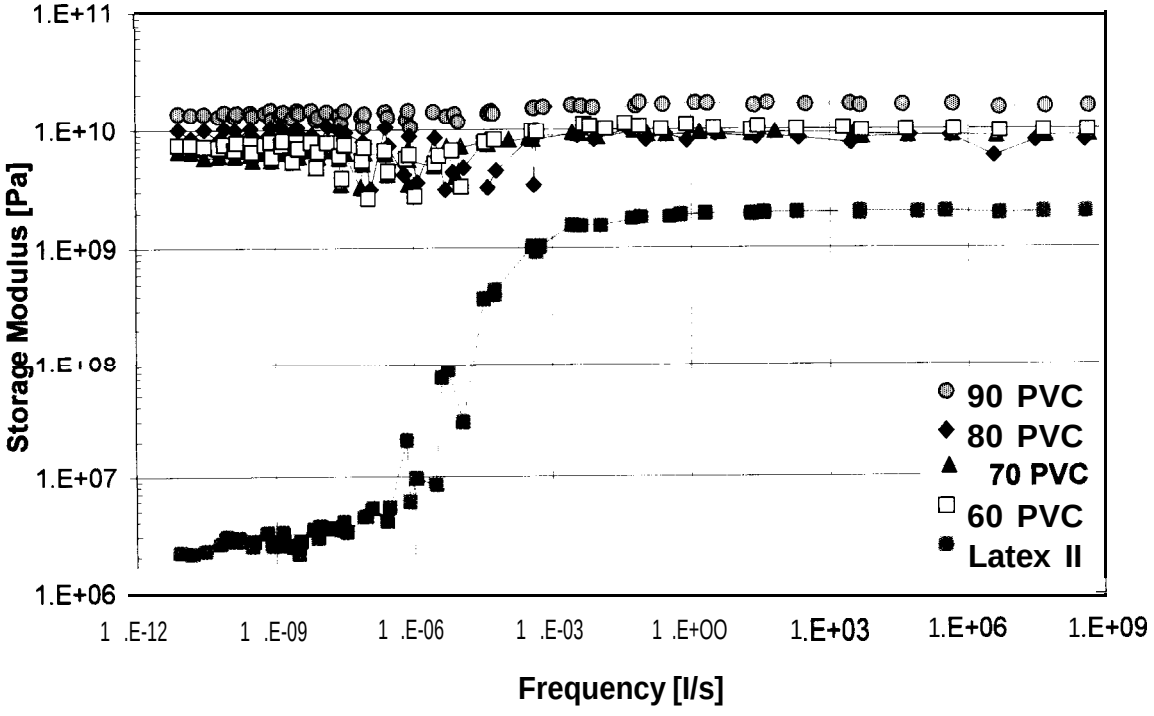

of ***storage modulus calculated at 0°C with Universal Constants,*** *for* ***clay pigment and latex II coatings at*** *different* ***pigment volume concentrations***

7.3 Comparison of Viscoelastic Behavior with Temperature for the Different Pigment Types and Latices for High Pigment Volume Concentration

The following picture demonstrates for the different pigments and latices the temperature behavior at the same pigment volume concentration. The three different types of behavior can be seen clearly.

90 PVC

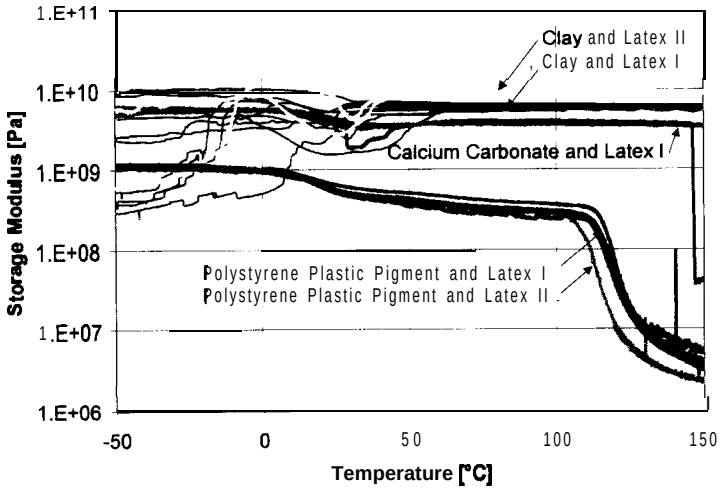

80 PVC

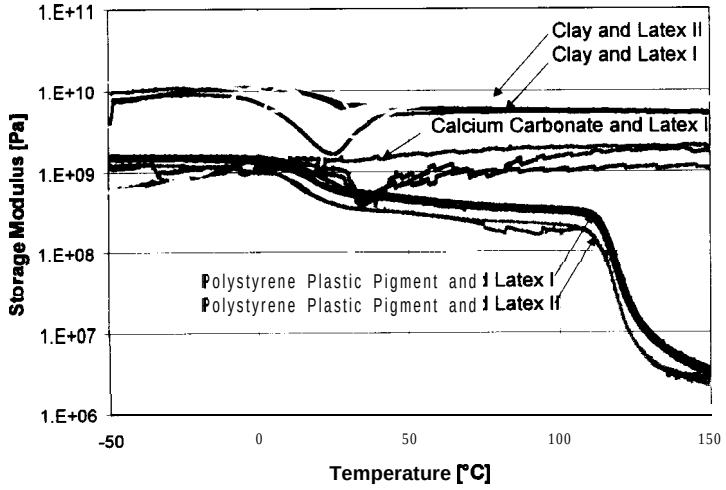

70 PVC

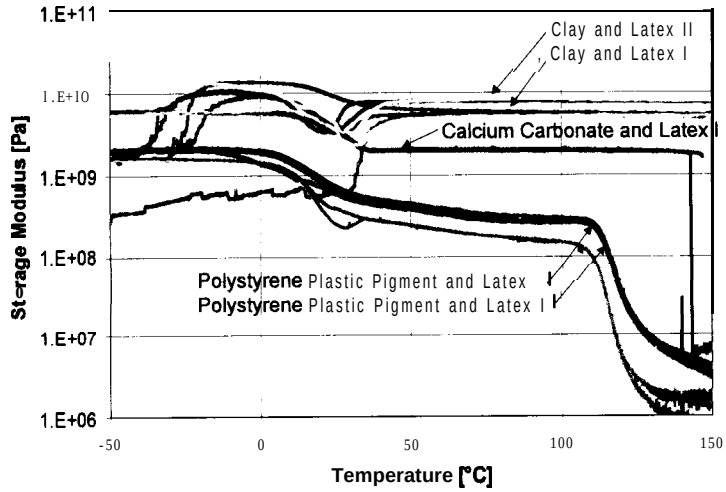

Figure 66 Storage modulus versus temperature for coatings with latex I and latex II for the different pigments at varying pigment volume concentrations

Calcium carbonate coatings showed the usual and simplest temperature behavior, with a single glass transition region. Polystyrene coatings resulted in two glass transition regions, the first one related to the transition temperature of the latex, and the second related to the glass transition temperature of the polystyrene plastic pigment. The clay coatings showed a depression behavior around the latex glass transition temperature for both latices in the high pigment volume concentration range. It also was observed, that clay coatings below the glass transition temperature did not perform very constant, repeatability was poor for low temperatures.

Clay pigments have a higher storage modulus than calcium carbonate pigments and polystyrene plastic pigments. Therefore coatings prepared with clay performed with the highest storage modulus, followed by coatings prepared with calcium carbonate and polystyrene plastic pigment coatings. The shape of the pigments additional effect the storage modulus of a composites. Plate shaped pigments (clay) show a higher modulus than prismatic shaped pigments (calcium carbonate) and spherical particles (polystyrene plastic pigment).

7.4 Burger's Model Applied on Latex I

The viscoelastic mechanical behavior can be described by mechanical models consisting of linear springs and linear dashpots. An attempt was made comparing measured data with the 4-parameter model from Burger (Figure 67). The Burger model consists of a Maxwell and a Kelvin model which are connected in series. At high frequencies Burgers model behaves like a stiff elastic solid (glassy) with an elastic modulus of E_1. For lower frequencies (below the transition region) it becomes flexible but elastic (rubbery state) with a much lower modulus than the glassy state. If the frequency is very low Newtonian flow in the Maxwell model becomes dominant, so fluid-like behavior is observed.

Figure 68 showed the master curve for latex I for the storage modulus, loss modulus and tan Delta. The master curve was obtained from measured data through time-temperature superposition. WLF-theory and Universal Constants were applied, and master curve was calculated at a reference temperature of 0°C.

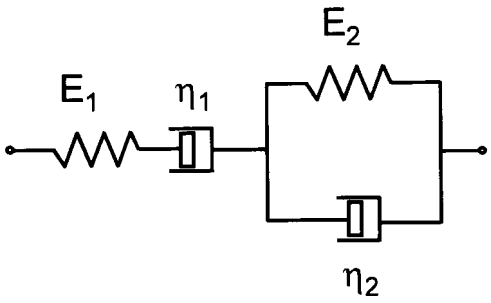

Figure 67 Burger model, consisting of a Maxwell element and Kelvin element in series

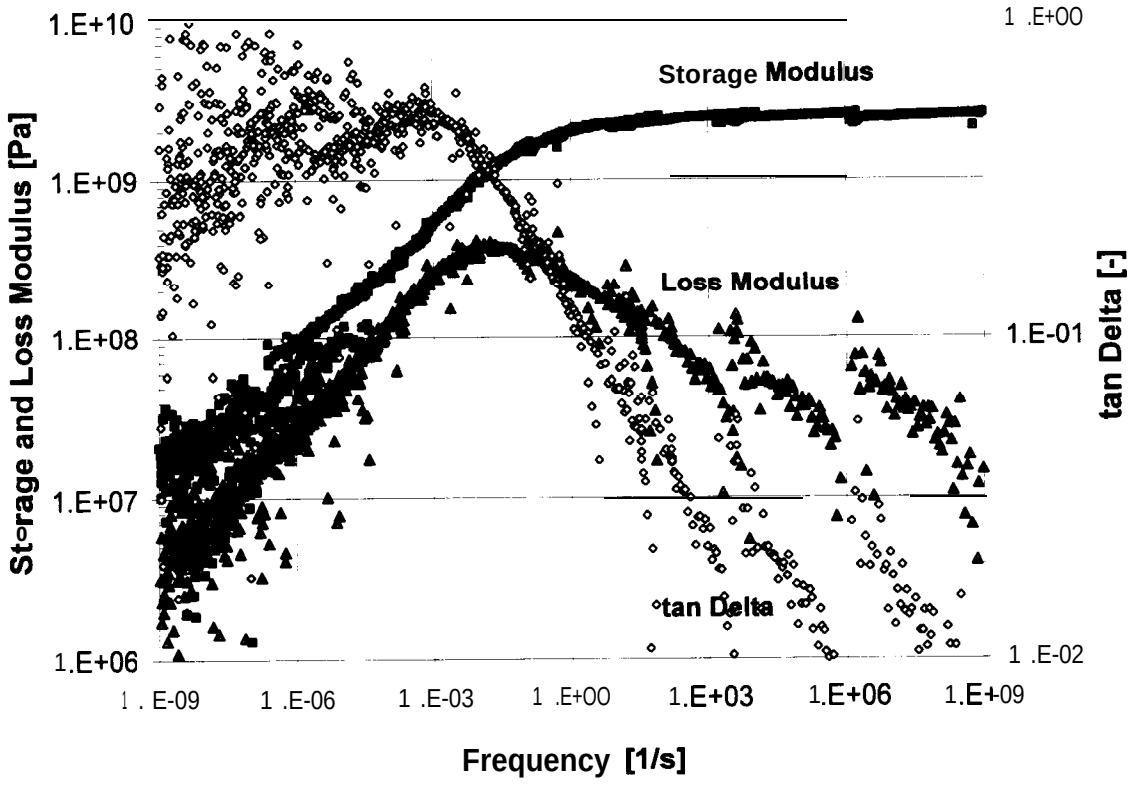

Figure 68 Master curves of storage modulus, loss modulus and tan Delta for latex I, at a reference temperature of 0°C

For calculation of the Burger model, differential equation in Table 1 was applied. The differential equation was solved for dynamic sinusoidal input in Table 2. The resulting curves are shown in Figure 69, where ω is the angular frequency. For frequencies above 1 0^2Hz, the Burger model was a good assumption for the measured data of storage modulus.

Table I6 Moduli and viscosity of spring and dashpot of Maxwell and Kelvin element

Maxwell Element		Kelvin Element	
Spring Constant $E_1 = 2.4*10^9$ Pa	Viscosity Dashpot $\eta_1 = 1*10^{10}$ Pas	Spring Constant $E_2 = 2.4*10^9$ Pa	Viscosity Dashpot $\eta_2 = 1*10^{10}$ Pas

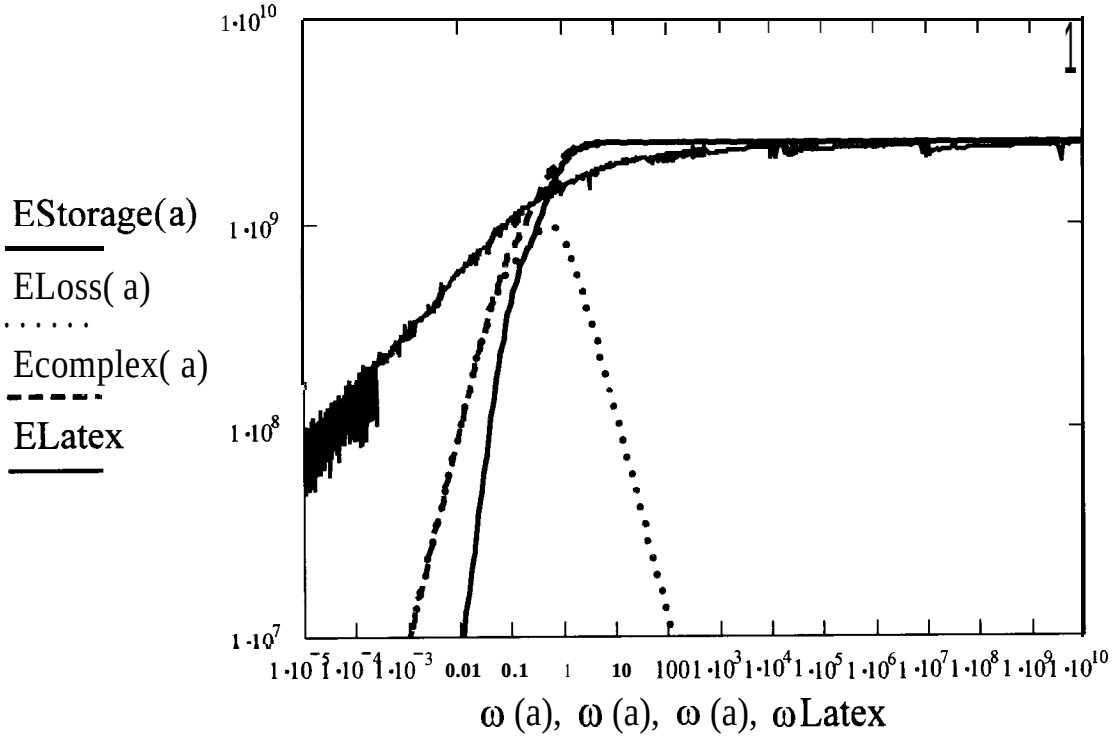

Figure 69 Comparison of storage modulus, loss modulus and complex modulus calculated by Burger model with master curve of storage modulus (—ELatex) obtained from dynamic mechanical thermal analysis

7.5 Coated Paper

Experimental studies of uncoated and coated paper have been performed in order to study the properties as a function of composition. A LWC base paper with a grammage of 41g/m² and a thickness of 70µm was coated with 90% PVC coatings of the three different pigments and experimental latex I (Figure 70 to Figure 72). The gap application resulted for the different pigments in different coat weights (Table 17). A comparison with the same coat weight would be preferable.

Table 17 Grammage and thickness of coatedpaper

	Grammage	Thickness
LWC base paper	41.0 g/m²	70 µm
LWC base paper coated with 90% PVC calcium carbonate and experimental latex I	79.8 g/m²	94 µm
LWC base paper coated with 90% PVC polystyrene plastic pigment and experimental latex I	61.8 g/m²	91 µm
LWC base paper coated with 90% PVC clay and experimental latex I	98.2 g/m²	102 µm

The LWC base paper showed a storage modulus of 4.5GPa at -50°C linearly decreasing with increasing temperature to 3.4GPa at 150°C. Loss modulus was between 0.7GPa and 1.1GPa over the temperature range. The LWC base paper did not show a transition region.

At temperatures above latex glass transition temperature the storage modulus of calcium carbonate coated paper, calcium carbonate coating (90%PVC) and LWC base paper showed the same level (Figure 70). Also for the coated paper a maximum was seen in loss modulus and tan Delta around the glass transition temperature of the experimental latex I. The transition region

was broader and showed a lower value for tan Delta than the pure calcium carbonate coating (Figure 70).

The paper coated with 90% PVC polystyrene plastic pigment and latex I resulted in a lower storage modulus than the storage modulus of the base paper. Hence the coating did not have a reinforcing effect on the paper over the whole temperature range. Around the glass transition temperatures of the experimental latex I and the polystyrene plastic pigment the loss modulus and tan Delta of the coated paper showed a maximum though less pronounced than for the pure coating sample (Figure 71).

The storage modulus of 90% PVC clay coatings was observed to be above the storage modulus of the LWC base paper. Consequently the coating showed a reinforcing effect for the coated LWC paper. For loss modulus and tan Delta the maximum values around latex glass transition temperature were below the values of the pure coating (Figure 72).

For the coated paper it was again observed that if the pure coating layer showed a higher storage modulus than the LWC base paper, the storage modulus of the coated paper increased, reinforcing the paper. If the modulus of the coating layer was lower than the modulus of the LWC base paper, the modulus of the coated paper was found to be lower than the LWC base paper, and the coating was reinforced by the paper.

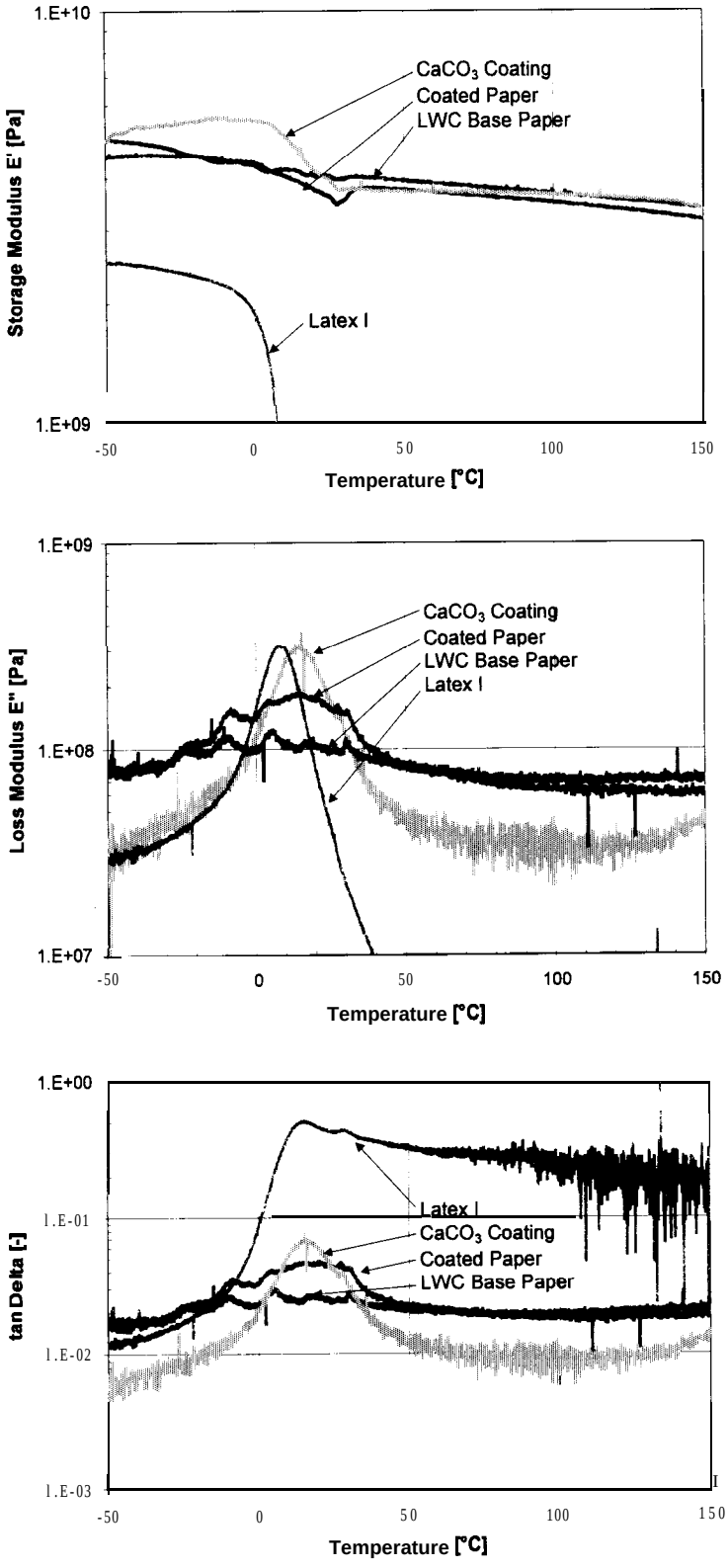

Figure 70 Storage modulus, loss modulus and tan Delta versus temperature for latex I, 90% PVC calcium carbonate coating, L WC base paper and L WC paper coated with 90% PVC coating

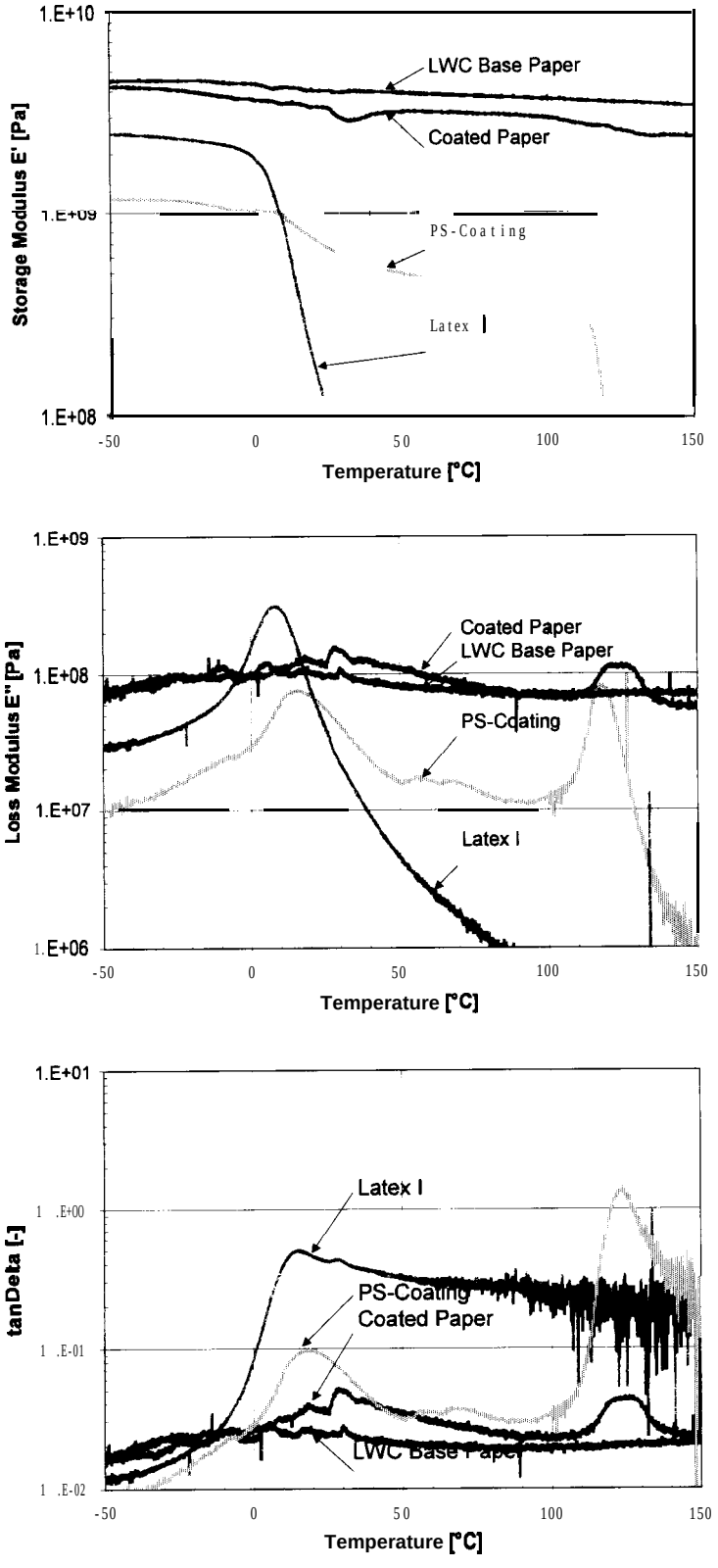

Figure 71 Storage modulus, loss modulus and tan Delta versus temperature for latex I, 90% PVC polystyrene plastic pigment coating, L WC base paper and L WC paper coated with 90% PVC coating

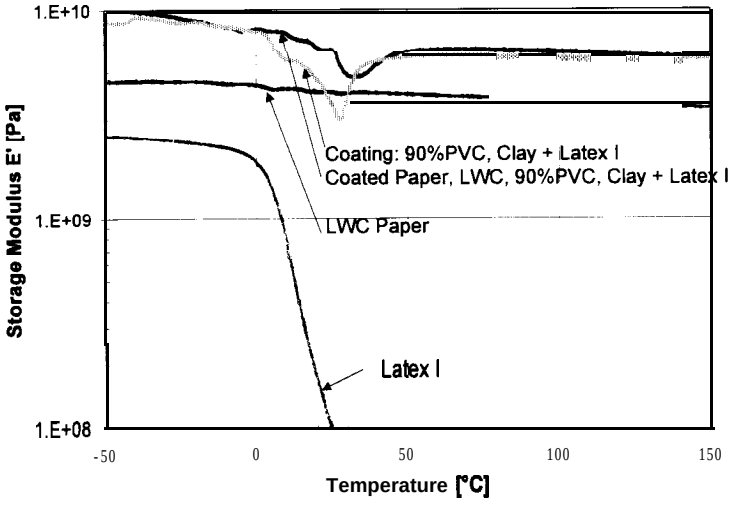

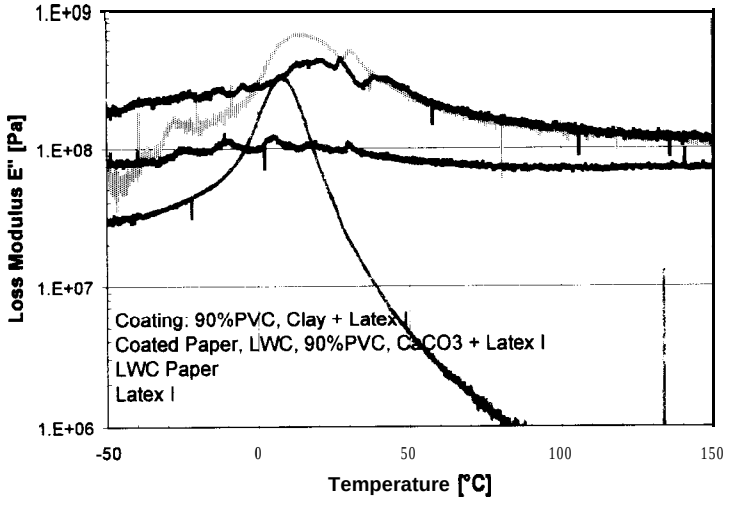

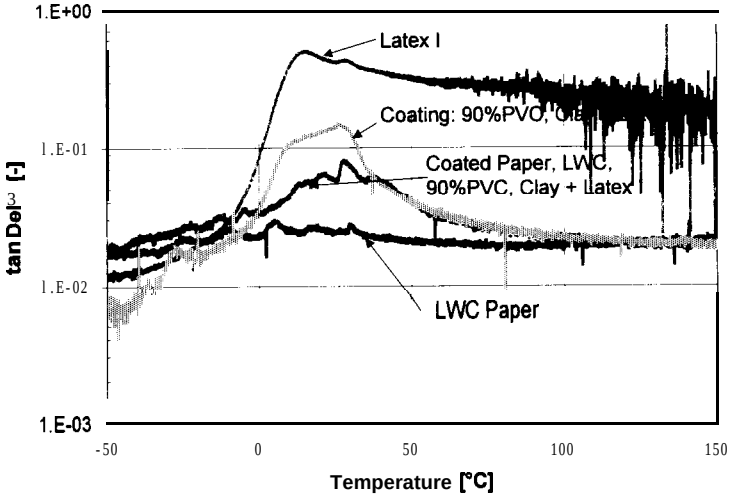

Figure 72 Storage modulus, loss modulus and tan Delta versus temperature for latex I, 90% PVC clay coating, L WC ***base*** *paper and L WC paper* ***coated*** *with 90% PVC coating*

8 Micro Structural Analysis

The sample surface morphology was investigated with an Environmental Scanning Electron Microscope. The microscopic stress-strain behavior and its relation to pigment concentration, distribution and agglomeration were evaluated by performing mechanical tensile tests within the ESEM.

8.1 Surface Analysis

Low magnifications allowed characterizing the surface structure and surface features of the coatings. Figure 73 shows two images of gold sputter coated polystyrene coatings (80% and 30% PVC) at low magnifications obtained with secondary electron detector (ESD). The particles showed few tendencies to agglomerate.

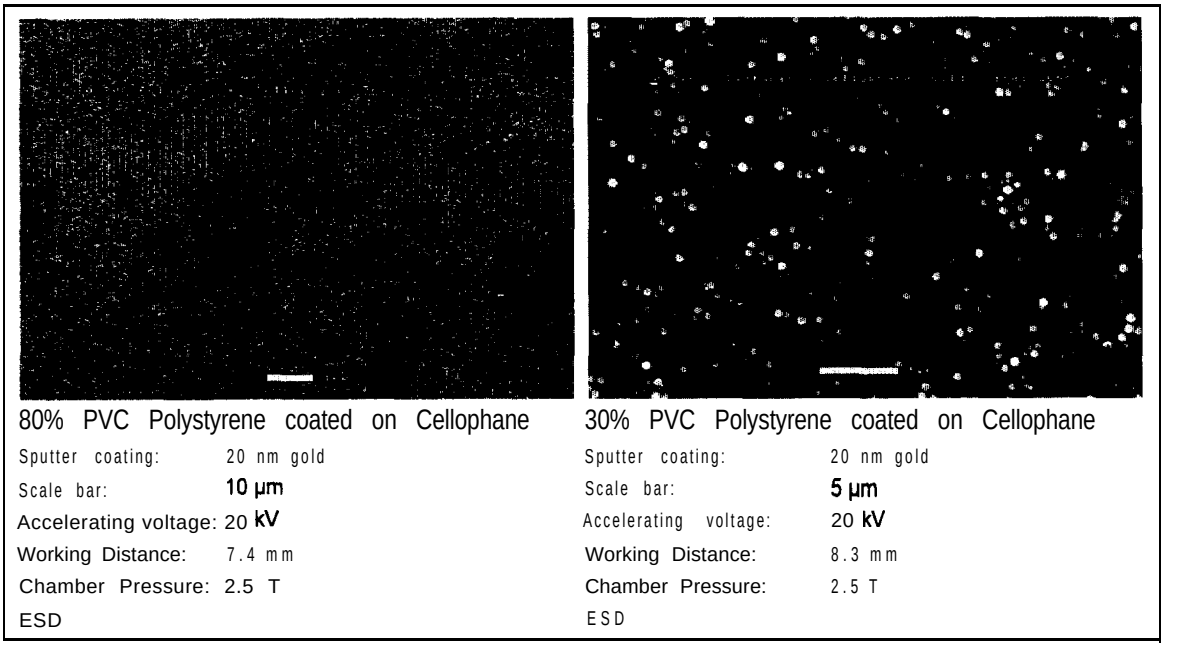

80% PVC Polystyrene coated on Cellophane		30% PVC Polystyrene coated on Cellophane	
Sputter coating:	20 nm gold	Sputter coating:	20 nm gold
Scale bar:	10 µm	Scale bar:	5 µm
Accelerating voltage:	20 kV	Accelerating voltage:	20 kV
Working Distance:	7.4 mm	Working Distance:	8.3 mm
Chamber Pressure:	2.5 T	Chamber Pressure:	2.5 T
ESD		ESD	

Figure 73 Polystyrene plastic pigment and latex I coatings with 80% and 30% pigment volume concentration at low magnifications, samples gold sputter-coated

For samples with low pigment volume concentrations it was observed that the electron beam altered the sample surface. The polymers were burnt off. This was especially observed for uncoated, non conductive surfaces.

In Figure 74 two polystyrene coatings with 80% and 70% PVC were compared at higher magnification. The latex coverage of the plastic pigments can be seen very clearly. High magnifications were necessary to clearly characterize the pigments' shape and surface character. High magnifications (>10,000X) resulted in very clear surface images (Figure 75).

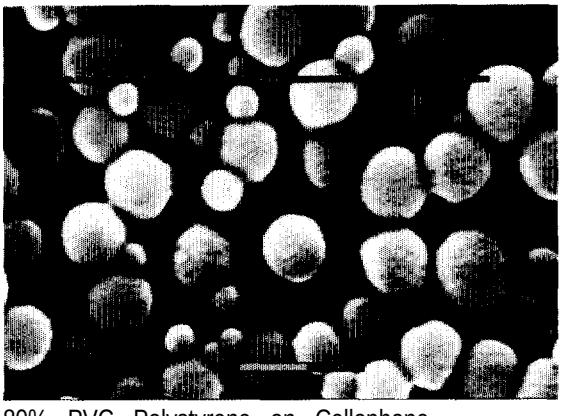

80% PVC Polystyrene on Cellophane		70% PVC Polystyrene on Cellophane	
Sputter coating:	20 nm gold	Sputter coating:	20 nm gold
Scale bar:	500 nm	Scale bar:	500 n m
Accelerating voltage:	20 kV	Accelerating voltage:	20 kV
Working distance:	7.4 mm	Working distance:	7.6 mm
Chamber pressure:	2.5 T	Chamber Pressure:	2.5 T
ESD		ESD	

Figure 74 Polystyrene plastic pigment with latex I coated on cellophane, surface with 20 nm gold sputter coated

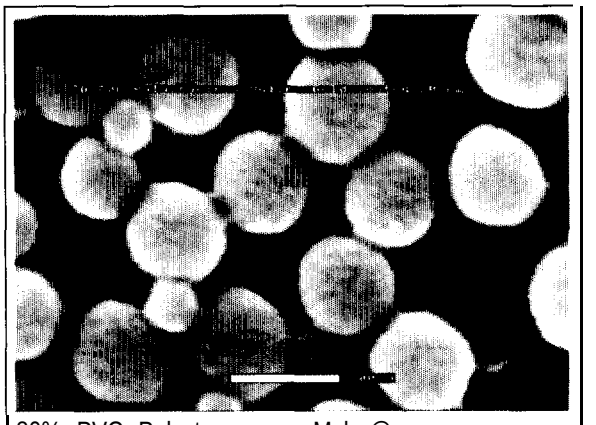

80% PVC Polystyrene on Mylar@
Sputter coating: 20 nm gold
Scale bar: 500 nm
Accelerating voltage: 20 kV
Working distance: 7.2 mm
Chamber Pressure: 2.5 T
ESD

Figure 75 80% PVC polystyrene plastic pigment and latex I coated on Mylar®, sample surface gold sputter-coated

8.2 Tensile Testing – Image Analysis

Tensile testing was performed within the ESEM. Images were taken at different elongation steps. The optimal magnification was found to be between 4000X to 8000X. At lower magnifications the pigments could not be resolved by the image analysis program. For images with too high magnifications the pictures went out of range during testing. A disadvantage of the tensile stage was that it was not possible to measure the applied force. Therefore sample breaks were not detected during testing procedure.

unstrained

sample

t = 0s

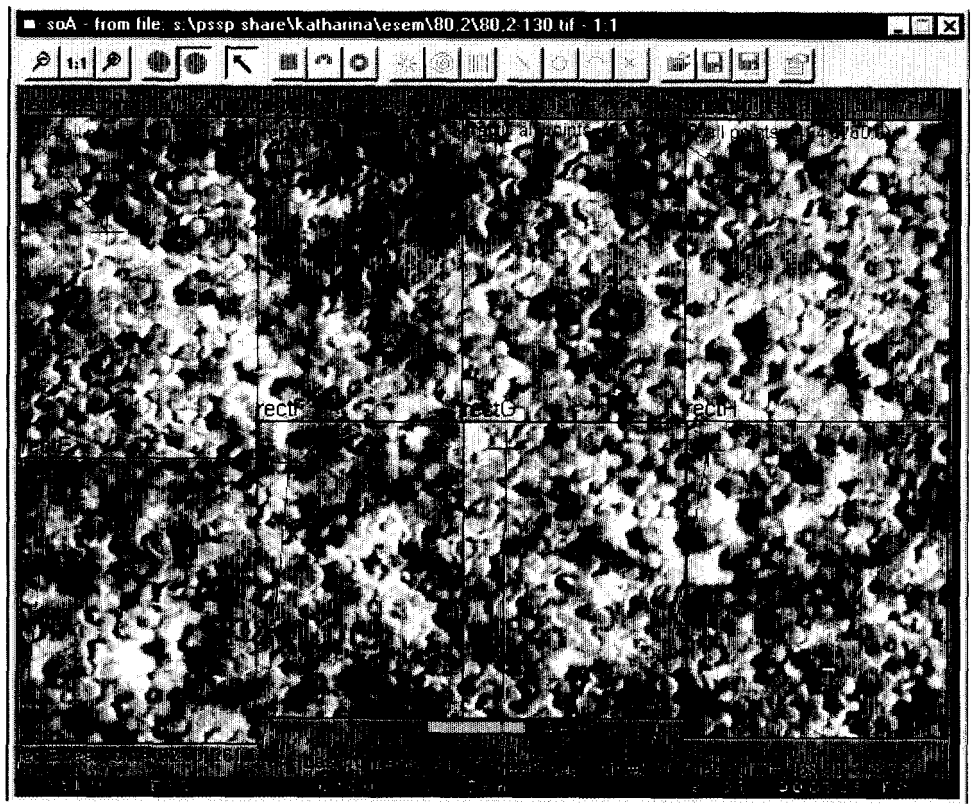

Strained

sample

after 8*10s

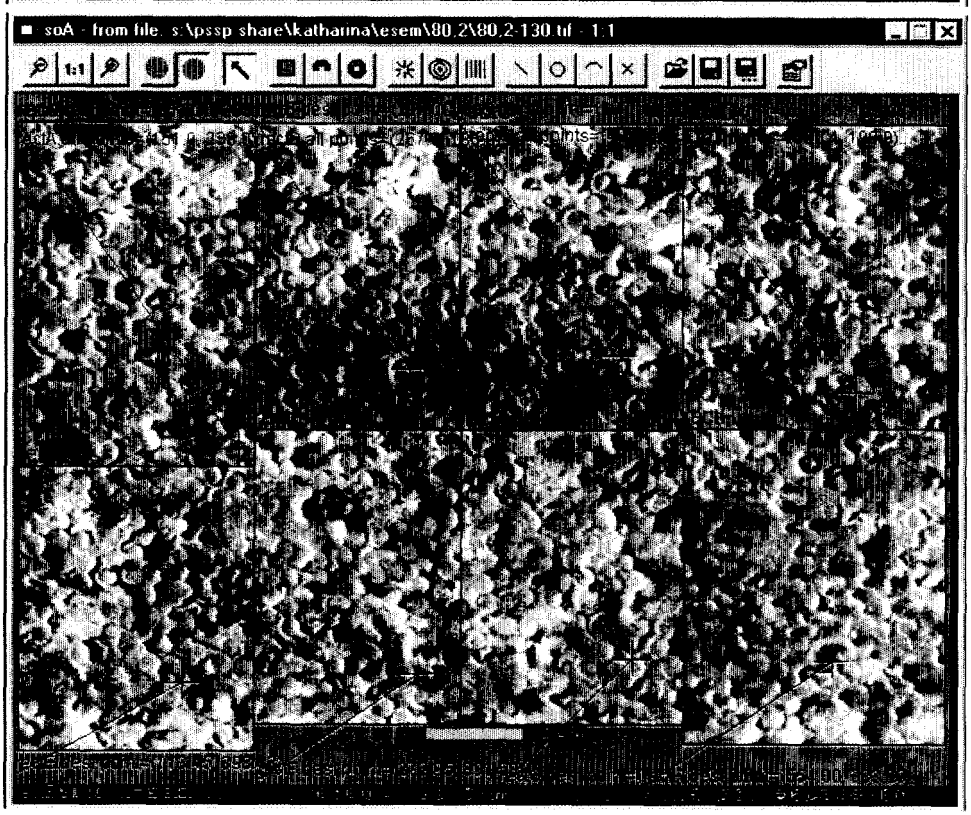

*Figure 76 80% PVC Polystyrene plastic pigment and latex I coating, before straining, and after 8 steps of strain were applied, (8*10s with 1μm/s), scale bar: 2μm*

With the image analysis program “Sherlock” the displacement of particles were traced. Figure 76 shows two images, of the unstrained sample before testing and after 8 steps of 10s of straining with a strain rate of 1µm/s applied. The matrix of absolute displacements over time is seen in Figure 77 for the marked points A to H of Figure 76. The resolution of the image analysis program depended on the magnification of the images. E.g. an image magnification of 6500X resulted in a sub-pixel resolution of 20-25nm.

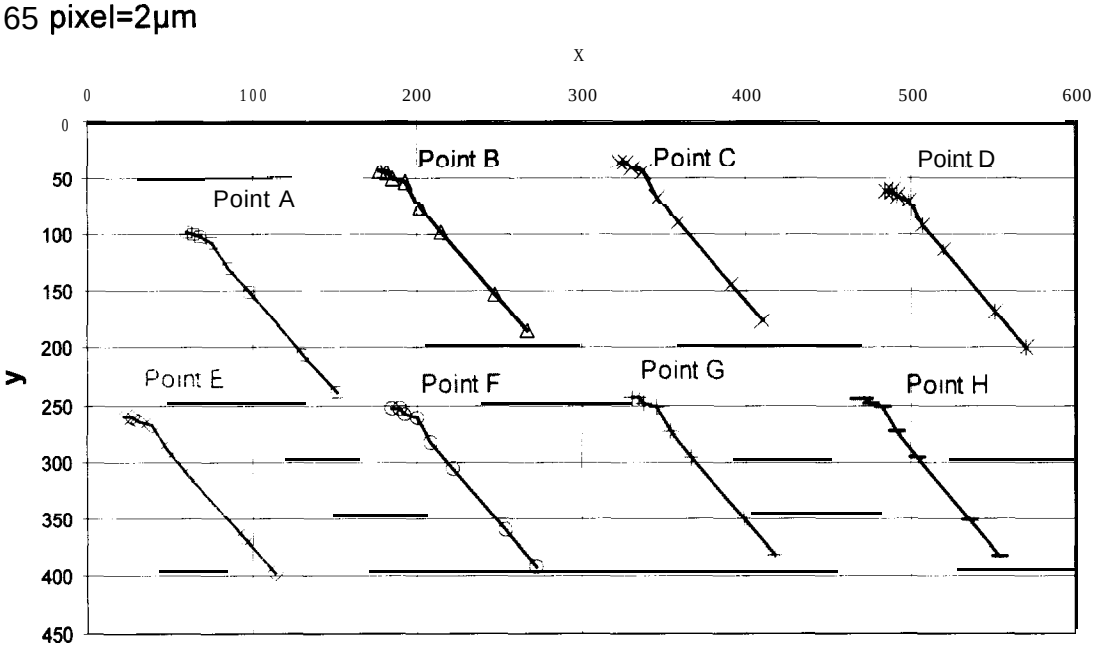

*Figure 77 80% PVC polystyrene plastic pigment and latex I coating, map **of absolute** movement **of** the 8 **different** particles in Figure 76*

The relative movements of adjacent particles are shown in Figure 78.

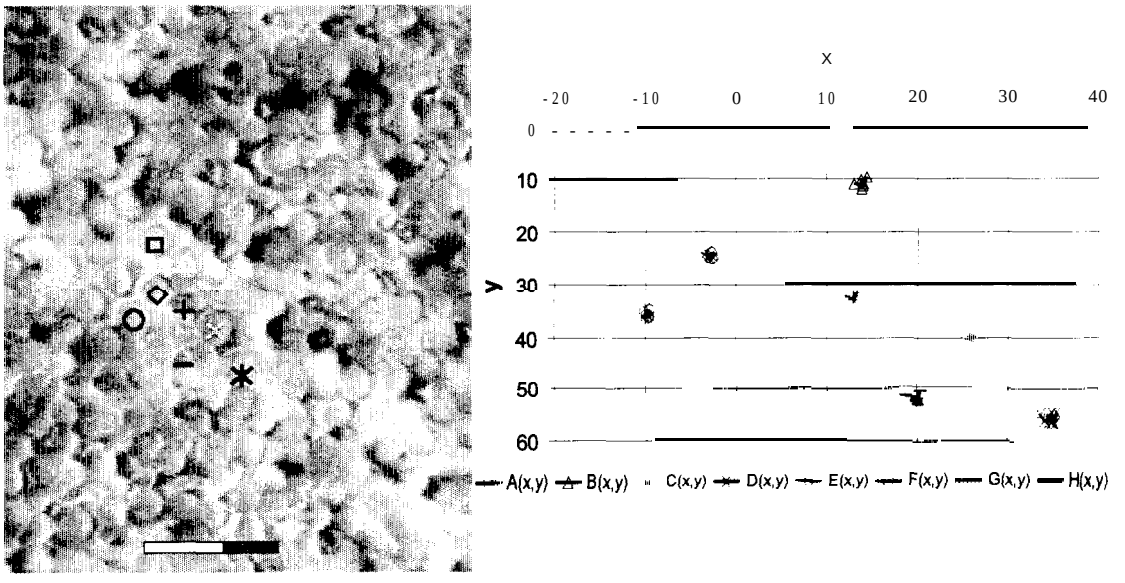

Figure 78 80% PVC polystyrene plastic pigment and latex I coating, relative movement of 8 adjacent particles, scale bar: 1μm

9 Summary and Conclusions

Coating films were prepared from model coatings with three different pigment types and two well defined latices. Mechanical tests were performed to investigate the influence of pigment type, shape, size distribution, pigmentation level and adhesion on the viscoelastic behavior of coating films.

The critical pigment volume concentration of the coatings was determined by gloss measurements. With static mechanical tests strong viscoelastic coating performance was observed. Conventional tensile testing showed for increasing pigment volume concentration that tensile strain decreased rapidly. The tensile strength was increasing with increasing pigment volume concentration, reached a maximum at the critical pigment volume concentration and dropped to a minimum above CPVC, this had been shown in previous work [Schaller 1968, Schaake 1988, Raman 1997 and 1998]. For the Young's modulus a rapid increase was observed around the CPVC, leveling off with further increase in pigment volume concentration.

By subsequent dynamic testing the viscoelastic material behavior was investigated in more detail. Behavior with temperature and time was evaluated for the three pigment types and latices with different carboxylation degree at varying pigment volume concentrations on free coating films in a tensile mode. The storage and loss modulus of the coating layers were found to be strongly related to the thermal softening of the coatings latices. At low strain levels the coatings did exhibit a linear viscoelastic behavior.

For the material systems with polystyrene plastic pigment and calcium carbonate pigment the storage moduli decreased with increasing temperature. The rate of decrease in performance was influenced by the pigment volume concentration level. The influence of pigmentation on the

modulus below the latex glass transition temperature was less pronounced then above the latex glass transition for all three pigment types. Coatings with high pigment volume concentrations exhibited little temperatures dependence above the latex glass transition temperature. This suggests, that an increasing extent of binder has reduced segmental mobility at high pigment volume concentrations (Zosel 1980).

Calcium carbonate pigment coatings showed a single transition around latex glass transition temperature. The addition of calcium carbonate pigment to latex resulted in a reinforcement effect over the entire pigment volume concentration range. Below the glass transition region a maximum storage modulus was reached, with further increase in PVC the storage modulus leveled off. Coatings prepared with polystyrene plastic pigment exhibited two transitions, the first one at the glass transition temperature of the latex, the second at the glass transition of the polystyrene pigment. Polystyrene plastic pigment actually showed below latex glass transition a lower storage modulus then the latex, hence the addition of plastic pigment did not lead to reinforcement. Above the latex glass transition temperature and below the pigment glass transition had the addition of pigment a reinforcing effect. For clay coatings a different behavior was observed. Pure clay samples exhibited a depression reaction at temperatures from 5" to 25°C. This depression was also observed for coatings at the different PVC levels. Below latex glass transition temperature, storage modulus increased with increasing pigment volume concentration. Around the critical pigment volume concentration the highest storage modulus was reached, further increase of resulted in a decrease in storage modulus. For the depression behavior was observed that it was partly reversible for very high pigment volume concentrations. Below 80% pigment volume concentration the depression behavior was irreversible and resulted in a common transition for subsequent reruns.

Pigmented coatings containing pigments with orientation axis resulted in a higher storage modulus. Therefore clay coatings performed with the highest storage modulus, followed by calcium carbonate coatings and polystyrene plastic pigment coatings. The plate-like clay

pigments are building a composite with particle orientation in plane of coating. Calcium carbonate coatings exhibit an orientation of the anisometric particles, too. Although it has to be considered, that the effect of pigment geometry and shape are combined with other pigment properties, e.g. different surface chemistry.

The glass transition temperatures determined by peak of tan Delta with dynamic mechanical thermal analysis were found to be higher then when measured with dynamic scanning calorimetry. With increase in pigment volume concentration coating glass transition temperature increased to a maximum.

Table 18 Summary of CPVC and mechanical behavior with increase in PVC level

	CPVC by TAPPI gloss	Typical viscoelastic behavior with temperature	Storage Modulus below T_g with increase in PVC	Storage Modulus above T_g with increase in PVC	T_g with increase in PVC
Calcium Carbonate	50%	single transition	⇑ leveled off at 70% PVC	⇑	Maximum at 70% PVC
Polystyrene plastic pigment	70%	two transitions	⇓	⇑	$T_{g\ -\ latex}$ Maximum at 40% PVC $T_{g\ -\ polystyrene}$ ⇑
Clay	60%	depression	Maximum at 50% PVC	⇑	

Classical composites theories (Rule of Mixture, Transverse Rule of Mixture and Halpin-Tsai Equation) were compared with experimental obtained data. It was seen that those models were in general not capable to predict the moduli over the temperature and pigment volume concentration range. Although for certain temperature levels, and pigments as well as pigment volume concentrations a good agreement was found.

Time-temperature superposition and WLF-theory with Universal Constants were used to construct master curves of the viscoelastic response of coatings at different pigment volume concentration levels. Compared with the temperature behavior the master curves resulted in similar curves, where low temperature corresponds to high frequency (short time behavior) and high temperature corresponds with low frequency (long time behavior). The transition regions occurred during a frequency range of 10^{-6}Hz to 1 Hz (corresponding with 0°C to 25°C). Time-temperature superposition was developed for polymeric systems. It was observed, that for the polystyrene plastic pigment coatings better master curves resulted.

The effect of adhesion was tried to be determined by evaluating two latices with different carboxylation degree. The decrease of storage and loss modulus in glass transition region was more rapid for the latex with lower carboxylation degree, exhibiting lower values above the glass transition region and for low frequencies. The effect of adhesion could not be determined by dynamic mechanical thermal analysis. The measurements were performed at low strains, in the linear viscoelastic region [Harding and Berg 1997].

Information about surface morphology of the pigments and coatings was obtained by surface observation in the scanning electron microscope. With tensile tests in the images at increasing elongation levels were obtained. Image analysis was used to trace particle movements.

Recommendations for future work:

To determine the influence of the shape on mechanical properties a different geometry within the same pigment type should be used.

Blends with different pigment types could be prepared, and verified if the mechanical response can be predicted from the single pigment phases.

The depression observed with clay coatings coincided with the latex glass transition temperature. Determine how the response would look like, if the latex glass transition temperature is well below of above this temperature range.

Effect of calendering or mechanical conditioning on the presence of clay depression should be investigated, to compare with the effect seen in DMTA through successive scans of the same specimen.

10 References

Agarwal, B.D. and Broutman L.J. (1980) Analysis and Performance of Fiber Composites, John Wiley & Sons, New York, ISBN O-471-05928-5, 355p.

Aklonis, J.J. and MacKnight, W.J. (1983) Introduction to Polymer Viscoelasticity, John Wiley & Sons Inc., ISBN O-471-86729-2, 295p.

Al-Turaif, H. and Lepoutre, P. (2000) Evolution of surface structure and chemistry of pigmented coatings during drying, Progress in Organic Coatings, 38: 43-52.

Anwari, F., Carlouo, B.J., Chokshi, K., DiLorenzo, M., Heble, M., Knauss, C.J., McCarthy, J., Patterson, R., Rozik, P., Slifko P.M., Stipkovich, W., Weaver, J.C., and Wolfe, M. (1991) Changes in hiding during latex film formation: Part IV. Effect of toning and film thickness, Journal of Coatings Technology, 65(816): 89-102.

Asbeck, W.K. and van Loo, M. (1949) Critical pigment volume relationships, Industrial and Engineering Chemistry, 41(7): 1470-1475.

ASTM D 2354-68 (1993) Standard Test Method for Minimum Film Formation Temperature (MFT) of Emulsion Vehicles, American Society for Testing Materials, Philadelphia, PA.

Barnes, H.A., Hutton, J.F. and Walters, K. (1989) An Introduction to Rheology, Elsevier Science Publishers B.V., ISBN O-444-87469-0, 199p.

Benabdi, M. and Roche, A.A. (1997) Mechanical properties of thin and thick coatings applied to various substrates. Part II. Young's modulus determination of coating materials, Journal of Adhesion Science Technology, 11(3): 373-391.

Berg, J.C. (1993) Wettability, Surfactant Science Series, Vol. 49, Marcel Dekker, INC., New York, ISBN O-8247-9046-4, 531 p.

Bierwagen, G.P. (1972) CPVC Calculations, Journal of Paint Technology, 44(574): 46-55.

Bierwagen, G.P. (1992) Critical pigment volume concentration (CPVC) as a transition point in the properties of coatings, Journal of Coating Technology, 64(806): 71-75.

Bierwagen, G.P. and Hay, T.K. (1975) The reduced pigment volume concentration as an important parameter in interpreting and predicting the properties of organic coatings, Progress in Organic Coatings, 3: 281-303.

Bierwagen, G.P. and Rich, D.C. (1983) The critical pigment volume concentration in latex coatings, Progress in Organic Coatings, 11: 339-352.

Braun, J.H. (1993) Introduction to Pigments, Federation of Societies for Coating Technology, Blue Bell, PA, 19422 USA.

Cox, **H.L.** (1952) The elasticity and strength of paper and other fibrous materials, British Journal of Applied Physics, 3: 72-79.

Danilatos, G.D. (1980) Mechanisms of detection and imaging in the ESEM, J. Microscopy, 160(1): 9.

del Rio, G. and Rudin, A. (1996) Latex particle size and CPVC, Progress in Organic Coatings, 28: 259-270.

Dickson, R. (1997) Adhesion and cohesion in coated paper, Ph.D. Dissertation, University of Maine.

Engström, G. and Lind, M. (1995) Biegesteifigkeit pigmentgestrichener Papiere, Wochenblatt fur Papierfabrikation, 123(7): 290-294.

Engström, G. and Rigdahl, M. (1992) Binder migration – Effect on printability and print quality, Nordic Pulp and Paper Research Journal, No. 2: 55-74.

Evanoff, P.C., Gerlach, W., and Lyne, M.B. (1983) Surface strength terminology, TAPPI Press, Atlanta. GA.

Ferry, J.D. (1980) Viscoelastic Properties of Polymers, 3rd edition, John Wiley & Sons Inc., ISBN o-471-04894-1, 641 p.

Findley, W.N., Lai, J.S., and Onaran K. (1989) Creep and relaxation of nonlinear viscoelastic materials: with an introduction to linear viscoelasticity, Dover Publications Inc., 31 East 2nd Street, Mineola, N.Y. 11501, ISBN O-486-66016-8, 371p.

Floyd, F.L. and Holsworth, R.M. (1992) CPVC as point of phase inversion in latex paints, Journal of Coatings Technology, 64(806): 65-69.

Flügge, W. (1967) Viscoelasticity, Blaisdell Publishing Company, Waltham, Massachusetts, 127p.

Fried, J.R. (1995) Polymer Science and Technology, Prentice Hall, New Jersey, ISBN 0-13-685561 -X, 509p.

Hagemeyer, R.W. (1997) Pigments for Paper, TAPPI Press.

Hagen, R., Salmen, L., and de Ruvo, A. (1993) Dynamic mechanical studies of a highly filled composite structure: A lightweight coated paper, Journal of Applied Polymer Science, 48: 603-610.

Hagen, T., Salmén, L., Lavebratt, H., and Stenberg, B. (1994) Comparison of dynamic mechanical measurements and T_g determinations with two different instruments, Polymer Testing, 13: 113-128.

Halpin, J.C. and Tsai, S.W. (1969) Effects of environmental factors on composite materials, AFML-TR 67-423. June 1969.

Hammer, C.O. and Maurer, F.H.J. (1998) Barium sulfate-filled blends of polypropylene and polystyrene: Microstructure control and dynamic mechanical properties, Polymer Composites, 19(2): 116-125.

Harding, P.H. and Berg, J.C. (1997) The role of adhesion in the mechanical properties of filled polymer composites, J. Adhesion Sci. Technol., 1 l(4): 471493.

Harper, C.A. (1996) Handbook of Plastics, Elastomers, and Composites, 3rd edition, McGraw Hill.

Hill, L.W. (1987) Mechanical Properties of Coatings, Federation Series on Coating Technology, 1315 Walnut ST., Philadelphia, PA 19107 USA.

Inoue, M. and Lepoutre, P. (1992) Influence of structure and surface chemistry on the cohesion of paper coatings, Journal of Adhesion Science Technology, 6(7): 851-857.

Ishikawa, O., Yamashita, T., and Tsuji, A. (1995) Characterizing mechanical properties of latex film and coating layer in paper coating using dynamic mechanical thermal analyzer. In Surface Phenomena and Latexes in Waterborne Coatings and Printing Technologies, Plenum Press New York, p. 91-105.

Joyce, M., Hagen R., and de R uvo, A. (1997) Mechanical consequences of coating penetration, Journal of Coatings Technology, 69(869): 53-58.

Kan, C.S., Kim, L.H., Lee, D.I., and van Gilder, R.L. (1996) Viscoelastic properties of paper coatings: Structure/property relationship to end use performance", TAPPI Coating Conference Proceedings, pp. 49-60.

Kan, C.S., Kim, L.H., Lee, D.I., and van Gilder, R.L. (1997) Viscoelastic properties of paper coatings: Relationship between coating structure-viscoelasticity and end-use performance, TAPPI Journal, 80(5): 191-201.

Keddie, J.L. (1997) Film formation of latex, Materials Science and Engineering, 21 :101-1 70.

Lepoutre, P. (1989) The structure of paper coatings: An update, Progress in Organic Coatings, 17: 98-106.

Lepoutre, P. (1994) Adhesion and cohesion of coated papers, Polymer News, Vol.19: 334-339.

Lepoutre, P. and Alince, B. (1981) Dry sintering of latex particles in pigmented coating. I. Influence on coating structure and properties, Journal of Applied Polymer Science, 26: 791-798.

Lepoutre, P. and Hiraharu, T. (1989) On the cohesion of clay and $CaCO_3$ coatings, Journal of Applied Polymer Science, 37: 2077-2084.

Lepoutre, P. and Rezanowich, A. (1977) Optical properties and structure of clay-latex coatings, TAPPI, 60(11): 86-91.

Lundqvist, Á. (1996) Surface energy characterization of cellulosic fibres and pigment coatings by inverse gas chromatography (IGC), Licentiate Thesis, Kungl Tekniska Högskolan, Institutionen for Pappers- och Massateknik, Avdelningen for Pappersteknik, Stockholm, Sweden.

Mark, J.E. (1993) Physical Properties of Polymers, 2nd edition, ACS Professional Reference Book, Washington, DC.

Mark, J.E. (1996) Physical Properties of Polymers Handbook, AIP Press, Woodbury, New York, ISBN l-56396-295-0, 723p.

Nakamura, Y., Fukuoka, Y., and Ilda T. (1998) Tensile test of poly(vinyl chloride) filled with ground calcium carbonate particles, Journal of Applied Polymer Science, 70: 311-316.

Nolan, G.T. and Kavanagh, P.E. (1995) Computer simlation of particle packing in acrylic latex paints, Journal of Coatings Technology, 67(850): 37-43.

Nolan, G.T. and Kavanagh, P.E. (1995) Octahedral configurations in random close packing, Powder Technology, 83: 253-258.

Nolan, G.T. and Kavanagh, P.E. (1995) Random packing of nonspherical particles, Powder Technology, 84: 199-205.

Okomori, K., Enomae, T., and Onabe, F. (1999) Evaluation and control of coated paper stiffness, TAPPI Advanced Coating Fundamentals Symposium, p. 121-132.

Parpaillon, M., Engström, G., Pettersson, I., Fineman, I., Svanson, S.E., Dellenfalk, B., and Rigdahl M. (1985) Mechanical properties of clay coating films containing styrene-butadiene copolymers, Journal of Applied Polymer Science, 30: 581-592.

Perkins, R.W. (1990) Micromechanical models for predicting the elastic and strength behavior of paper materials, in "Materials Interactions Relevant to the Pulp, Paper, and Wood Industries", Material Research Society, Pittsburgh, Pennsylvania, p. 99-l 18.

Raman, K. (1997) Micromechanical properties of coated paper, M.S. Thesis, Dept. of Chemical Engineering, University of Maine.

Rigdahl, M., Lason, L., Hagen, R., Karlsson, O., and Wesslén, B. (1997) Heterogeneous latices as binders in porous particle structures, Journal of Applied Polymer Science, 63: 661-670.

Schaake, R.C.F., v.d. Heikant, J.A.M., and Huisman, H.F. (1988) CPVC relationships III. The real CPVC and its relationship to Young's modulus, magnetic moment, abrasive wear and gloss, Progress in Organic Coatings, 16: 265-276.

Schaller, E.J. (1968) Critical pigment volume concentration of emulsion based paints, Journal of Coatings Technology, 40(525): 433.

Shaler, S.M., Groom, L.H., and Mott, L. (1995) Microscopic analysis of woodfibers using ESEM and confocal microscopy, Proc. of 3rd Wood fiber / polymer composites conferences 1995.

Sjörgen, B.A. and Berglund, L.A. (1997) Failure mechanisms in polypropylene with glass beads, Polymer Composites, 18(1): l-8.

Stieg, F.B. (1973) The influence of PVC on paint properties, Progress in Organic Coatings, 1: 351-373.

Suhling, J.C. (1990) Continuum models for the mechanical response of paper and paper composites: past, present, and future, in "Materials Interactions Relevant to the Pulp, Paper, and Wood Industries", Material Research Society, Pittsburgh, Pennsylvania, p. 245-255.

TAPPI Test Methods, (1998-1999) Technical Association of the Pulp and Paper Industry Test Methods, TAPPI Press, Atlanta.

Thimoshenko, S.P. and Goodie, J.N. (1970) Theory of Elasticity, 3rd ed., McGraw-Hill Book Company, New York, 567p.

Toussaint, A. (1973/74) Influence of pigmentation on the mechanical properties of paint films, Progress in Organic Coatings, 2: 237-267.

Tsai, S.W. and Hahn, H.T. (1980) Introduction to Composite Materials, Technomic Pub.Co., Lancaster PA.

Wu, S. (1982) Polymer Interface and Adhesion, Marcel Dekker, INC., ISBN 0-8247-1533-O.

Yamaguchi, Y., Ishikawa, O., Yamashita, T., and Tsuji. A. (1993) A study of viscoelastic properties of coated layer in paper coating, TAPPI Advanced Coating Fundamentals, p. 51-58.

Yaseen, M. and Ashton, H.E. (1977) Effect of free film preparation method on physical properties of organic coatings, Journal of Coatings Technology, 49(629): 50-58.

Zosel, A. (1980) Mechanical behavior of coating films, Progress in Organic Coatings, 8: 47-79.

BIOGRAPHY OF THE AUTHOR

Katharina M. Prall was born in Gmunden, Austria on June 13, 1968. She was raised in Laakirchen, Austria and graduated from Technical High School Vocklabruck, Austria in Mechanical and Technical Engineering in June 1982. She then attended the University of Technology Graz, Austria studying Process Engineering with specialization in Pulp and Paper Technology. She graduated in 1996 as Enchartered Engineer (Dipl.-Ing.). In 1997 she came to the States and joined the Paper Surface Science Program of the Chemical Engineering Department at the University of Maine.

Katharina M. Prall is a candidate for the Doctor of Philosophy degree in Chemical Engineering from The University of Maine in December, 2000.